ÉTUDE DE MICELLES DE COPOLYMÈRES À BLOCS RÉPONDANTS À DEUX STIMULI

par

Juan Xuan

Thèse en cotutelle

présentée au Département de chimie en vue

de l'obtention du grade de docteur ès sciences (Ph.D.)

FACULTÉ DES SCIENCES

UNIVERSITÉ DE SHERBROOKE

présentée au State Key Laboratory of Polymer Materials Engineering en vue

l'obtention du grade de Docteur

FACULTÉ DES SCIENCES

SICHUAN UNIVERSITY

Février 2014

le jury a accepté la thèse de Madame Juan Xuan
dans sa version finale.

Membres du jury

Professeur Yue Zhao
Directeur de recherche
Département de chimie

Professeur Hesheng Xia
Codirecteur de recherche
Université de Sichuan

Pr Carmel Jolicoeur
Membre interne
Département de chimie

Professeur Yves Dory
Membre interne
Département de chimie

Professeur Jean-François Morin
Membre externe Université
Laval

Professeur Armand soldera
Président-rapporteur
Département de chimie

SOMMAIRE

Les copolymères à blocs sensibles aux stimuli (SR-BCPs) et leurs assemblages, tels que les micelles, les vésicules et les hydrogels, peuvent subir des changements physiques ou chimiques en réponse à l'évolution des conditions environnementales. Pour un excellent SR-BCP, habituellement, de légères modifications de l'environnement sont suffisantes pour induire des modifications relativement drastiques dans la conformation, la structure ou les propriétés du polymère. Ces polymères sont aussi appelés polymères stimuli-réactifs ou polymères intelligents et ils ont un grand potentiel d'application dans de nombreux domaines. Au cours des deux dernières décennies, un intérêt de recherche et développement particulier a été porté sur l'exploitation des SR-BCPs pour utilisation comme systèmes de relargage de médicaments. Dans de nombreux cas, les changements induits par des stimuli dans la structure ou la morphologie des assemblages de BCPs peuvent entraîner la libération de l'espèce encapsulée, parfois d'une manière contrôlable spatialement et temporellement par le choix d'un stimulus approprié et en ajustant les paramètres de la méthode de stimulation utilisée. De façon générale, le fait d'avoir un certain type de groupements réactifs à un stimulus donné dans la structure permet aux SR-BCPs de reconnaître et réagir à ce stimulus.

Malgré les énormes progrès réalisés sur les SR-BCPs, un certain nombre de questions fondamentales restent à résoudre afin de leur permettre de se trouver dans des applications pratiques. Pour y arriver, la clé ou le défi réside dans l'amélioration du niveau et de la complexité de contrôle sur les SR-BCPs ainsi que la sensibilité avec laquelle ces polymères réagissent à des stimuli. Généralement, il est souhaitable d'obtenir une réaction rapide sous l'action d'une stimulation modérée. A cette fin, il est nécessaire d'effectuer des recherches fondamentales sur la conception rationnelle de nouveaux SR-BCPs ainsi que sur le développement de méthodes de stimulation qui peuvent amplifier l'effet d'un stimulus. Les travaux de recherche présentés dans cette thèse s'inscrivent dans ce domaine de recherche. Plus spécifiquement, nous avons étudié des micelles de BCPs qui répondent à deux types de stimuli. D'une part, nous avons étudié un mécanisme d'amplification basé sur l'effet des ultrasons combiné à la thermosensibilité de BCPs. D'autre part, nous avons développé une nouvelle conception de BCPs qui permet aux micelles

d’être détruites soit de manière photochimique, soit par des réactions d'oxydo-réduction, tout en ayant le nombre minimum des groupes stimuli-réactifs dans la structure du polymère. Notre recherche a généré de nouvelles connaissances dans ce domaine et suggère de nouveaux moyens sur la façon dont les questions de sensibilité et de contrôle complexe des micelles SR-BCPs peuvent être abordées, contribuant ainsi à l'avancement des connaissances fondamentales.

Le cœur de cette thèse est composé de trois publications résultant des projets réalisés. Dans le premier projet, afin de coupler la sensibilité aux ultrasons et la thermosensibilité, nous avons mené une étude ayant pour but de trouver des structures possibles de polymères qui sont susceptibles d'être affectées par les ultrasons. Nous avons effectué une étude comparative sur la destruction des micelles formées par divers BCPs et la libération concomitante d'un colorant hydrophobe encapsulé (rouge du Nil) par les ultrasons focalisés de haute intensité (HIFU). Nous avons constaté que toutes les micelles formées par les quatre copolymères diblocs synthétisés, étant constitués d'un même bloc du polyoxyde d'éthylène (PEO) hydrophile et d’un bloc de polyméthacrylate hydrophobe différent, peuvent être perturbées par les ultrasons. Toutefois, l'ampleur de la perturbation et la libération du colorant encapsulé dans la micelle est influencée par la structure chimique du block hydrophobe. En particulier, les micelles du PEO-*b*-PIBMA (poly(1-isobutoxyméthacrylate d'éthyle)) et du PEO-*b*-PTHPMA (poly(méthacrylate de 2-tétrahydropyrannyle)), qui possèdent une unité acétal labile dans le groupe latéral, subissent des perturbations plus importantes en raison, probablement, d’une réaction d’hydrolyse de l’ester induite par les ultrasons, donnant lieu à une libération plus rapide du colorant. En revanche, les micelles du PEO-*b*-PMMA (poly(méthacrylate de méthyle)), dont le bloc polyméthacrylate est plus stable, sont plus résistantes aux ultrasons et présentent une cinétique de libération du colorant plus lente que les autres micelles. De plus, l’analyse des spectres infrarouges des solutions micellaires, enregistrés avant et après l’exposition aux ultrasons, suggère une réaction d’hydrolyses pour le PEO-*b*-PIBMA et le PEO-*b*-PTHPMA, mais montre l'absence d’une quelconque réaction chimique pour le PEO-*b*-PMMA. L'effet de la structure de copolymère à blocs sur la réactivité des micelles à l'irradiation HIFU à hautes fréquences permet de mieux comprendre comment des micelles de BCPs sensibles aux ultrasons peuvent être conçues.

Sur la base du premier projet, dans le deuxième projet, nous avons démontré une nouvelle approche pouvant amplifier l'effet de HIFU sur la destruction des micelles de BCPs en solution aqueuse. L'idée est d'introduire une petite quantité des unités comonomères sensibles aux ultrasons dans le bloc thermosensible et initialement hydrophobe. On peut alors former une micelle dont le noyau est composé du polymère sensible aux ultrasons. Si la réaction induite par les ultrasons sur le noyau permet d'augmenter la température de solution critique inférieure (LCST) du polymère thermosensible au-dessus de la température de la solution micellaire, la micelle doit être dissolue car tout le BCP est devenu soluble dans l'eau. Pour tester la validité de ce nouveau mécanisme, nous avons synthétisé et étudié un copolymère dibloc de PEO-*b*-P(MEO_2MA-*co*-THPMA) (MEO_2MA représente 2-(2-méthoxyéthoxy) méthacrylate d'éthyle), dans lequel le bloc thermosensible P(MEO_2MA-*co*-THPMA) est hydrophobe à T>LCST. Le THPMA a été choisi en raison de sa plus grande réactivité vis-à-vis des faisceaux HIFU que les autres monomères étudiés dans le premier projet. Les résultats montrent que les HIFU peuvent effectivement augmenter la LCST du bloc P(MEO_2MA-*co*-THPMA) et, par conséquent, induire la dissociation des micelles à une température constante de la solution. Une analyse spectrale en RMN ^{13}C a fourni des preuves montrant que l'hydrolyse des groupes THPMA se produit sous l'irradiation HIFU et que la destruction des micelles provient d'une augmentation de la LCST en raison de la conversion des motifs hydrophobes THPMA en motifs acides méthacryliques (MAA) hydrophiles. Cette méthode de modifier la LCST par une irradiation des ultrasons est générale et peut être appliquée aux autres groupements sensibles aux ultrasons dans la conception de ce type de SR-BCPs. Cette étude a ainsi démontré un nouveau mécanisme d'amplification et de contrôle des micelles de BCPs via la modification induite par les ultrasons de la température de transition de phase (LCST) du bloc constituant le noyau micellaire.

Le troisième projet présenté dans cette thèse portait sur une conception rationnelle de BCPs ayant un but précis: permettre aux micelles d'être perturbées par deux types de stimuli en utilisant le nombre minimal des unités sensibles à des stimuli dans la structure de BCPs. Pour ce faire, nous avons conçu et synthétisé un nouveau copolymère tribloc amphiphile de type ABC, soit le poly(oxyde d'éthylène) - *disulfure* – polystyrene - *o-nitrobenzyle* - poly(2-(diméthylamino) éthylméthacrylate) (PEO-*S*-*S*-PS-*ONB*-PDMAEMA). Il dispose d'une liaison disulfure

redox-clivable entre les blocs PEO et PS ainsi que d'un groupe *o*-nitrobenzyle (ONB) photoclivable à la jonction des blocs PS et PDMAEMA. Nous avons montré que ce modèle est une stratégie utile pour permettre aux micelles de BCPs de répondre soit à un agent réducteur comme le dithiothréitol (DTT) dans une solution, soit à l'exposition à la lumière UV, tout en ayant le nombre minimum des groups stimuli-réactifs dans la structure du copolymère (deux unités par chaîne). Nos investigations ont révélé que les micelles de ce copolymère tribloc peuvent être perturbées de différentes façons. Lorsqu'un seul stimulus est appliqué, l'enlèvement d'un type des chaînes de polymère hydrophile à partir de la couronne de micelles, soit le PEO par clivage par oxydo-réduction ou le PDMAEMA par photoclivage, entraîne un effet limité de déstabilisation sur la dispersion des micelles. L'agglomération de quelques micelles apparaît mais la dispersion reste essentiellement stable. En revanche, en cas d'utilisation combinée des deux stimuli qui clivent à la fois le PEO et le PDMAEMA, une agrégation importante du polymère se produit à la suite de l'élimination de l'amphiphilicité du polymère.

Mots clés : copolymères à blocs sensibles aux stimuli; micelles; systèmes d'administration de médicaments; ultrasons focalisés de haute intensité; la température de solution critique inférieure; polymères redox-sensibles; polymères photosensibles.

ABSTRACT

Stimuli-responsive block copolymers (SR-BCPs) and their assemblies, such as micelles, vesicles and hydrogels, can undergo physical or chemical changes in response to changing environmental conditions. For an excellent SR-BCP, usually, slight changes in the environment are sufficient to induce relatively drastic changes in either the conformation or structure or properties of the polymer. Stimuli-reactive polymers are often referred to as smart polymers and they have great application potential in many fields. Over the past two decades, particular research and development interest has been focused on exploiting SR-BCP assemblies as drug delivery systems (DDSs). In many cases, stimuli-induced changes in the structure or morphology of BCP assemblies (drug carriers) can result in the release of loaded species, sometimes in a spatially and temporally controllable manner by choosing an appropriate stimulus and adjusting the parameters of the used stimulating method. Generally speaking, by having a certain type of stimuli-reactive moieties in the structure, SR-BCP assemblies have an ability to recognize a specific stimulus and react to its presence accordingly.

Despite the tremendous progress achieved on SR-BCPs, a number of fundamental issues remain to be addressed in order to enable real-life applications of these smart polymers. Of them, an increasing level and complexity of control on SR-BCPs as well as the sensitivity with which these polymers react to stimuli are key and challenging. It is highly desirable to obtain a fast reaction under the action of a modest stimulation. To this end, fundamental research is necessary on rational and creative BCP structural design as well as on development of stimulation methods that can amplify the effect of a stimulus. The research work presented in this thesis falls into this important topic. More specifically, we studied BCP micelles that are responsive to two types of stimuli. On the one hand, we investigated an amplification mechanism based on coupling the ultrasound reactivity with the thermosensitivity of BCPs. On the other hand, we developed a BCP structural design that allows micelles to be disrupted by either light or redox agents while having the minimum number of stimuli-reactive moieties in the polymer structure. Our research provided new insights into and suggested new means on how the issues of sensitivity and complex control of SR-BCP micelles can be tackled, thus contributing to the advancement of fundamental

knowledge.

The core of this thesis is comprised of three publications resulting from the projects realized in our research work. In order to couple the ultrasound sensitivity and thermosensitivity, in the first project, we carried out studies to find possible polymer structures that are susceptible to be affected by ultrasound. We conducted a comparative study on the disruption of the micelles formed by various BCPs and the concomitant release of an encapsulated hydrophobic dye (Nile Red) by high-intensity focused ultrasound (HIFU). It was found that all micelles formed by the four synthesized diblock copolymers, being composed of a hydrophilic poly(ethylene oxide) (PEO) block and a different polymethacrylate hydrophobic block, could be disrupted by ultrasound. However, the extent of the micellar disruption and dye release was found to be influenced by the chemical structure of the micelle-core-forming hydrophobic polymethacrylate. In particular, micelles of PEO-*b*-PIBMA (poly(1-(isobutoxy)ethyl methacrylate)) and PEO-*b*-PTHPMA (poly(2-tetrahydropyranyl methacrylate)), whose hydrophobic blocks have a labile acetal unit in the side group and are more likely to undergo ester hydrolysis, could be disrupted more severely by ultrasound, giving rise to a faster release of Nile Red. By contrast, micelles of PEO-*b*-PMMA (poly(methyl methacrylate)), whose polymethacrylate block is more stable, appear to be more resistant to ultrasound irradiation and exhibit a slower rate of dye release than other BCPs. Moreover, infrared spectra recorded with micelles before and after ultrasound irradiation of the aqueous solution of the micelles give evidence for the occurrence of chemical reactions, most likely hydrolysis, for PEO-*b*-PIBMA and PEO-*b*-PTHPMA, but absence of chemical reactions for PEO-*b*-PMMA. The effect of BCP chemical structure on the reaction of micelles to high-frequency HIFU irradiation shows the perspective of designing and developing ultrasound-sensitive BCP micelles for ultrasound-based delivery applications.

On the basis of the first project, in the second project, we demonstrated a new approach that could amplify the effect of HIFU on the disassembly of BCP micelles in aqueous solution. By introducing a small amount of ultrasound-labile comonomer units into the micelle core-forming thermosensitive polymer, the ultrasound-induced reaction of the comonomer could increase the lower critical solution temperature (LCST) of the thermosensitive polymer due to a polarity change, which renders the BCP soluble in water without changing the solution temperature and, consequently, results in disassembly of BCP micelles. To prove the validity of this new mechanism, we synthesized and investigated a diblock copolymer of PEO-*b*-P(MEO_2MA-*co*-THPMA) (MEO_2MA stands for 2-(2-methoxyethoxy)ethyl methacrylate).

In the thermosensitive random copolymer block P(MEO_2MA-*co*-THPMA), which is hydrophobic at T>LCST, THPMA was chosen due to its greater reactivity under HIFU than other monomer structures investigated in the first project. We found that HIFU could indeed increase the LCST of the P(MEO_2MA-*co*-THPMA) block and, as a result, dissociate the BCP micelles at a constant temperature. A ^{13}C NMR spectral analysis provided critical evidence that hydrolysis of the THPMA groups occurs under HIFU irradiation and the micellar disassembly originates from an increase in the LCST due to the ultrasound-induced conversion of hydrophobic comonomer units of THPMA onto hydrophilic methacrylic acid (MAA). This ultrasound-changeable-LCST approach is general and can be applied by exploring other ultrasound-labile moieties in the BCP design. By transducing an ultrasound-induced effect into a changing thermosensitivity of the micelle core-forming block, this study demonstrated a new amplification and control mechanism for SR-BCP micelles.

The third project presented in this thesis dealt with a rational BCP design that had a specific purpose: allowing BCP micelles to be disrupted by two types of stimuli while using the minimum number of stimuli-reactive moieties in the BCP structure. The unveiling of such BCP structures provides insight into how to make BCP micelles sensitive to stimuli. To do this, we designed and synthesized a new amphiphilic ABC-type triblock copolymer, namely, poly(ethylene oxide)-*disulfide*-polystyrene-*o-nitrobenzyl*-poly(2-(dimethylamino)ethylmethacrylate) (PEO-*S*-*S*-PS-*ONB*-PDMAEMA), which features a redox-cleavable disulfide linkage between the PEO and PS blocks as well as a photocleavable ONB group as the junction of the PS and PDMAEMA blocks. We demonstrated that this design is a useful strategy to allow BCP micelles to respond to both a reducing agent like dithiothreitol (DTT) in solution and exposure to UV light while having the minimum number of stimuli-reactive moieties in the block copolymer structure (two units per chain). Our investigations found that the micelles of this triblock copolymer could be disrupted in different ways. When only one stimulus is applied, the removal of one type of hydrophilic polymer chains from the micelle corona, either PEO by redox-cleavage or PDMAEMA by photocleavage, results in a limited destabilization effect on the dispersion of the micelles. The agglomeration between a few micelles appears but the dispersion remains essentially stable. By contrast, under combined use of the two stimuli that cleaves both PEO and PDMAEMA, severe polymer aggregation occurs as a result of elimination of the polymer amphiphilicity. Moreover, by loading the hydrophobic Nile Red in the micelles, the fluorescence quenching of the dye by aqueous medium under the different uses of the two stimuli appears to correlate with the different extents of the micellar disruption.

Keywords : Stimuli-responsive block copolymers; micelles; drug delivery systems; high-intensity focused ultrasound; lower critical solution temperature; redox-sensitive polymers; photosensitive polymers.

摘要

刺激响应嵌段共聚物（SR-BCPs）和它们的自组装体（例如胶束、囊泡和水凝胶）可以对环境的改变做出物理或者化学变化的响应。对于优良的 SR-BCP，在通常情况下，环境中的微小变化都足以诱导无论是在聚合物构象或者结构或者性能上相对很大的变化。刺激-反应性聚合物通常被称为智能聚合物，它们在许多领域具有很大的应用潜力。在过去的二十年中，专业的研究和新产品的开发一直聚焦在利用 SR-BCP 自组装体作为载药体系（DDSs）。在许多情况下，刺激诱导 BCP 自组装体（药物载体）结构或者形貌的改变都可以导致加载药物的释放。通过选择适当的刺激和调节用于刺激方法的参数，可以实现加载药物在空间和时间上的可控释放。一般来说，通过具有特定类型的刺激-反应性结构部分，SR-BCP 自组装体就具有了识别特定刺激并做出相应反应的能力。

尽管 SR-BCPs 已经取得了巨大的发展，但是使这些智能聚合物能够在现实生活中得到应用，一些根本性的问题仍然需要加以解决。其中的关键和挑战是增加对 SR-BCPs 控制的深度和复杂性，以及对刺激响应的敏感度。使 SR-BCPs 能够在适度的刺激作用下做出快速的反应是人们梦寐以求的。为此，对于合理地创造性地设计 BCP 结构以及发展可以放大刺激效应的刺激方法的基础研究是非常有必要的。在本论文中提出的研究工作属于这一重要课题。具体来说，我们研究了双重刺激响应 BCP 胶束。一方面，基于 BCPs 的超声温度双重敏感性，我们研究了一种放大机制。另一方面，我们开发设计了一种在聚合物结构中只含有最少数目刺激-反应单元的 BCP 结构，可以让胶束被光或者还原剂破坏。我们的研究对于如何解决 SR-BCP 胶束的敏感性和复杂可控性提出了新的见解和方法，从而有利于基础知识的进步。

本论文的核心是由三篇已经发表的研究工作组成。为了实现超声和温度双重敏感性，在第一个研究课题中，我们对于容易受超声影响的聚合物结构进行了研究。我们比较了由不同 BCPs 组成的胶束结构在高强度聚焦超声（HIFU）作用下的破坏情况以及伴随着的包覆疏水染料（尼罗红）的释放情况。实验结果显示，四种以聚环氧乙烷为亲水端，不同的聚甲基丙烯酸酯为疏水端的两嵌段聚合物胶束都可以被超声扰动。然而，形成胶束疏水内核的聚甲基丙烯酸酯的化学结构影响胶束破坏和染料释放的程度。特别是，PEO-*b*-PIBMA（聚（ 1-（异丁氧基）乙基甲基丙烯酸酯） ）和 PEO-*b*-PTHPMA（聚（2-四氢吡喃基甲基丙烯酸酯） ）的疏水端具有不稳定的酯键侧基，因此在超声作用下更容易酯键水解。他们的胶束也更容易

被超声扰动，从而更快的释放尼罗红。相比之下，PEO-*b*-PMMA（聚甲基丙烯酸甲酯）的聚甲基丙烯酸酯链段比较稳定。因此相对于其他胶束，PEO-*b*-PMMA 胶束在超声下更稳定，释放染料的速度也相对较慢。根据超声辐照前后胶束水溶液的红外光谱显示，PEO-*b*-PIBMA 和 PEO-*b*-PTHPMA 在超声辐照下发生了水解反应，但是 PEO-*b*-PMMA 没有发生化学反应。在高频率 HIFU 辐照下，BCP 的化学结构对胶束反应的影响展现了设计和发展应用超声-敏感 BCP 胶束的新视角。

在第一个研究课题的基础上，在第二个研究课题中，我们展示了一种可以放大 HIFU 在水溶液中对 BCP 胶束破坏效果的新方法。通过在形成胶束内核的温敏性聚合物中引入少量的超声不稳定共聚单体，由于超声诱导共聚体极性的变化从而增加温敏性聚合物的最低临界溶液温度（LCST）。这使得在没有改变溶液温度的情况下，BCP 溶于水，并进一步导致 BCP 胶束的瓦解。为了证明这种新机制的可行性，我们合成并研究了二嵌段共聚物 PEO-*b*-P(MEO$_2$MA-*co*-THPMA)（MEO$_2$MA 代表 2-(2-甲氧基乙氧基)乙基甲基丙烯酸酯）。当 T > LCST 时，无规的热敏嵌段共聚物 P(MEO$_2$MA-*co*-THPMA)是疏水的。选择 THPMA 是因为在第一个研究课题里，相比于其他结构的单体，它对于 HIFU 的辐照更敏感，具有更大的反应活性。我们发现， 通过 HIFU 的辐照确实可以增加 P(MEO$_2$MA-*co*-THPMA)链段的 LCST，导致 BCP 胶束在温度不变的情况下瓦解。^{13}C NMR 提供了关于超声诱导 THPMA 基团水解和由于超声诱导使疏水的 THPMA 共聚单元转变成亲水的 MAA 从而使 LCST 增加进一步导致胶束瓦解的关键证据。这种超声改变 LCST 的方法具有普遍意义，可以被用来探索在 BCP 设计中其他的超声不稳定基团。通过把超声诱导效应转换成胶束内核的温敏性变化，这项研究展示了一种全新的 SR-BCP 胶束的放大和控制机制。

在这篇论文中所展示的第三个研究课题是设计一个具有特定目的的合理的 BCP 结构。即允许在使用最少的刺激响应官能团的情况下，BCP 胶束可以在两种刺激下瓦解。这种 BCP 结构的展示可以使我们更深入的了解如何使 BCP 胶束对刺激敏感。为此，我们设计并合成了新的两亲性 ABC 型三嵌段共聚物，即聚（环氧乙烷） - *二硫化物* - 聚苯乙烯 - *邻* - *硝基苄基* - 聚（2 - （二甲基氨基）乙基甲基丙烯酸酯） (PEO-*S*-*S*-PS-*ONB*-PDMAEMA)。它在 PEO 和 PS 嵌段之间具有可还原裂解的二硫键，在 PS 和 PDMAEMA 嵌段之间具有可光裂解的 ONB 基团。我们证实，对于使具有最少数量的刺激-反应官能团（每条分子链上仅有两个）的 BCP 胶束可以同时在还原剂二硫苏糖醇

（DDT）水溶液中和紫外光照下发生响应，此设计是一种行之有效的策略。我们研究发现，这种三嵌段共聚物胶束可以以不同的方式被破坏。当只施加一种刺激时，无论是还原裂解 PEO 链段，或是光裂解 PDMAEMA 链段，都只有一种亲水链从胶束外壳被移走，这都只能导致胶束分散有限的不稳定。虽然一些胶束之间发生了团聚，但是分散体系总体上基本保持稳定。与之相对的，在两种刺激同时作用的情况下，PEO 和 PDMAEMA 链段的同时断裂使聚合物的两亲性消失，从而导致聚合物严重的聚集。此外， 在两种刺激不同的施加情况下，通过在胶束中装载疏水尼罗红的方式，结果显示染料的荧光在水中的淬灭与胶束被破坏的不同程度有关。

关键词 ：刺激响应嵌段共聚物；胶束；药物载体；高强度聚焦超声；最低临界溶液温度；氧化还原敏感性聚合物；光敏聚合物。

ACKNOWLEDGEMENT

First of all, I would like to thank my supervisor Prof. Yue Zhao for giving me this opportunity to study in his laboratory at the Université de Sherbrooke and for his continuous guidance in my research and in my pursuit of my Ph.D degree. Without his vision and guidance, none of the achievements presented in my thesis would have been possible. I am eternally grateful to what he has taught me during my years in Sherbrooke. I also would like to thank my co-supervisor Prof. Hesheng Xia for his guidance, suggestions and discussions during my years in Sichuan University.

I am grateful to Prof. Jean-Francois Morin (Université Laval), Profs. Armand Soldera, Carmel Jolicoeur and Yves Dory (Université de Sherbrooke) for being part of the jury of my thesis. I also would like to thank all the professors and staff in the Department of Chemistry for their help during my study.

I would like to thank all group members, both present and past, in the Polymers and Liquid Crystals Laboratory, including Mrs. Xia Tong, Dr. Dehui Han, Mr. Olivier Boissière, Dr. Yi Zhao, Dr. Bin Yan, Dr. Yan Qiang, Mr. Hongji Zhang, Mr. Shangyi Fu, Mr. Hu Zhang, Mr. Damien Habault, Mr. Jun Xiang, Mr. Guo Li, Mr. Weizheng Fan, Mrs. Marlène Gnéragbé, Mrs. Aurélie Lespes, Dr. Maxime Pelletier, Dr. Surjith Kumar, Dr. Bo He, Dr. Donghua Li, Dr. Feng Shi and Mr. Jean-François Wehrung for the joyful working atmosphere and countless help and discussions. Especially, I thank Mrs. Xia Tong for the great help in all characterization works and assistance in starting all my measurements in the lab.

I also acknowledge Dr. Maxime Pelletier for his synthesis of the block copolymer used in the first project, Dr. Yi Zhao and Dr. Bin Yan for their synthesis of the block copolymer used in the second project, Mr. Olivier Boissière, Dr. Luc Tremblay and Prof. Serge Lacelle for their NMR characterization and analysis in the second project, Dr. Dehui Han for his synthesis of the block copolymer used in the third project, and Mr. Jeff Sharman for his help and assistance in characterizing some of my samples. I thank my other friends in and outside of Sherbrooke for the generous help and encouragement that made my entire study enjoyable and memorable.

My sincere thanks go to all members of the Dynamic Polymeric and Composite Materials Laboratory of Sichuan University for their kindness and help during my stay at Sichuan University,

especially Mrs. Guoxia Fei, Mr. Yongwen Li, Mr. Rui Tong and Mrs. Jie Wang.

I acknowledge the Chinese Scholarship Council for awarding me a scholarship that made my study in Sherbrooke possible. I would like to thank all the members of the Education Office of the Chinese Embassy in Canada, especially Mr. Shaohua Liu and Mr. Jianjun Zhai for all their help during my stay in Canada.

I would like to thank my family for all the love and support throughout the years, especially my parents and my husband Xing Chen. Without your endless encouragement and support, none of this would have been possible.

Finally, I am grateful to the financial support from Natural Sciences and Engineering Research Council of Canada (NSERC), le Fonds de recherche du Québec: Nature et technologies (FRQNT) and the Université de Sherbrooke. Their funding awarded to Prof. Zhao allowed me to conduct my research work.

TABLE OF CONTENT

LIST OF ABBREVIATIONS

SR-BCPs: stimuli-responsive block copolymers

DDS: drug delivery system

PEO: poly(ethylene oxide)

PEG: poly(ethylene glycol)

PTHPMA: poly(2-tetrahydropyranyl methacrylate)

PIBMA: poly(1-(isobutoxy)ethyl methacrylate)

PTHFEMA: poly((2-tetrahydrofuranyloxy)ethyl methacrylate)

PMMA: poly(methyl methacrylate)

MAA: methacrylic acid

PAA: poly(acrylic acid)

NR: Nile Red

PLA: poly(lactic acid)

P4VP: poly(4-vinylpyridine hydrochloride)

D_H: hydrodynamic diameter

LCST: lower critical solution temperature

UCST: upper critical solution temperature

ATRP: atom transfer radical polymerization

PCM: phase-change material

PNIPAM: poly(N-isopropyl acrylamide)

THP: tetrahydropyran

$PMEO_2MA$: poly(2-(2-methoxyethoxy)ethyl methacrylate)

PEGMA: poly(ethylene glycol) methyl ether methacrylate

PS: polystyrene

THF: tetrahydrofuran

PDMAEMA: poly(*N,N'*,-dimethylaminoethyl methacrylate)

ONB: *o*-nitrobenzyl

PMDETA: *N, N, N′, N′, N″*-pentamethyldiethylenetriamine

HEMA: 2-hydroxyethyl methacrylate

UCNP: upconverting nanoparticle

AuNP: gold nanoparticle

CMA: 4-methyl-[7-(methacryloyl)oxyethyloxy] coumarin]

DMA: *N, N*-dimethylacrylamide

DTT: dithiothreitol

GSH: glutathione

ABP: amphiphilic block copolymer

TEA: triethylamine

DCM: dichloromethane

DMF: *N, N*-dimethylforamide

DCC: *N, N'*-dicyclohexylcarbodiimide

DMAP: 4-(dimethylamino)pyridine

MPEG: poly(ethylene glycol) methyl ether

PNB: 5-propargylether-2-nitrobenzyl bromoisobutyrate

SP: spiropyran

MC: merocyanine

NIR: near-infrared

DOX: doxorubicin

PPS: poly(propylene sulfide)

PPO: poly(propylene oxide)

PCL: poly(caprolactone)

PAzoMA: poly(azobenzene methacrylate)

OEGMA: oligo-(ethylene glycol) methacrylate

HIFU: high-intensity focused ultrasound

PDI: polydispersity

UV : ultraviolet

AFM: atomic force microscopy

SEM: scanning electron microscope

TEM: transmission electron microscopy

FTIR: fourier transform infrared

^{13}C NMR: carbon nuclear magnetic resonance

SEC: size exclusion chromatograph

GPC: gel permeation chromatography

DLS: dynamic light scattering

^{1}H NMR: proton nuclear magnetic resonance

LIST OF SCHEMES

CHAPTER 3

LIST OF FIGURES

INTRODUCTION

CHAPTER 1

CHAPTER 2

CHAPTER 3

CHAPTER 4

INTRODUCTION

Polymers capable of responding to external or internal stimuli can be considered as one of the most exciting research areas and have been actively investigated for commercial applications (1-3). Although Mother Nature provides inspiration for designing and developing new materials, creating polymers that can react to stimuli in a controllable and predictable manner still remains as a significant challenge. Generally, this type of polymers is defined as stimuli-responsive polymers that can undergo relatively large and abrupt, physical or chemical changes in response to small external stimuli. They are smart polymers that can adjust their properties according to the environment stimuli such as changes in temperature, pH and ion concentration, or exposure to light, electrical field and mechanical force. Their responses are typically changes in one or more of the many properties including color, transparency, water solubility, electrical conductivity, shape, surface characteristics and so on (4-6). Usually, slight changes in the environment are sufficient to induce a large property variation of these polymers. In short, stimuli-responsive polymers are among the most interesting and versatile materials, and a considerable amount of efforts have been devoted to this research area (7-10).

These polymers have an ability to recognize a specific stimulus and make a desired response, owning to the presence of certain stimulus-responsive groups or moieties in the polymer structure. Using ultrasound-responsive polymers as an example: upon exposure to ultrasound, those ultrasound-sensitive groups in the polymer are first activated and display some sort of response such as a change in polarity or structural modification, which in turn is translated and amplified into macroscopic changes. Basically, the sensitivity of a polymer to a stimulus is determined by the reaction kinetics of the response groups in the polymer chain, which leads the co-operative interactions the material in and controls the outcome at the macroscopic level. These phenomena can happen on different time or spatial scales. Normally, polymer materials at the micro- and nano-scale are more sensitive than their bulk counterparts because of faster reactions to the stimuli.

Recently, much interest on stimuli-responsive polymers has been focused into the biomedical

fields, including diagnostics, drug delivery, tissue or cell engineering (regenerative medicine), as well as thermoresponsive surface systems (11-15). In particular, self-assembled and nanostructured aggregates of stimuli-responsive block copolymers (SR-BCPs), such as micelles or vesicles, have been extensively studies for their great potential as controlled drug delivery systems (DDSs) (16-20). In such BCPs, one or more blocks bear moieties that are reactive to certain types of stimuli. Under application of a stimulus, the nano-aggregates of BCPs can be disrupted, resulting in release of loaded guest molecules (drug, imaging agent, etc.). To obtain a good DDS, a number of factors have to be taken into account, ranging from ease of delivery to effectiveness of the drugs. During the past decades, formulations that control the rate and period of drug delivery and target specific areas of the body for treatment have been rapidly developed (21-25). However, the current methods of DDSs still exhibit specific and serious problems that need scientists to resolve. For example, the potencies and therapeutic effects of many drugs are limited or reduced because of the partial degradation of the DDSs that occurs before they reach a desired target in the body. To tackle this problem, stable DDSs that can protect the loaded drug and ensures long circulation time in the blood are required. Therefore, the goal of all advanced DDSs is to deploy medications intact to specifically targeted parts of the body through a medium that can control the therapeutic administration by means of either a physiological or chemical trigger. It is in this context that BCP micelles and vesicles have been attracting more and more interest during the last decade or so. In many published research works, they have been shown to be effective in enhancing drug targeting specificity, lowering systemic drug toxicity, improving treatment absorption rates, and providing protection for pharmaceuticals against biochemical degradation.

To form stable micelles or vesicles in aqueous solution, BCPs need to be amphiphilic, containing hydrophilic and hydrophobic portions. Generally, they can self-assemble into core-shell structures when the hydrophobic blocks are driven to agglomerate forming an interior core while the hydrophilic blocks are turned outward facing toward the water to form the outer shell. BCP micelles can be used as DDSs because the hydrophobic interior has the capacity solubilize and hold drugs poorly soluble in aqueous solution. In most cases, BCP micelles are only tens of nanometers in diameter. This magnitude of dimension is excellent for enclosing drug molecules. Moreover, their hydrophilic outer shells help protect the cores and their contents from chemical

attack by the aqueous medium in which they must travel. Finally, since the used BCPs are stimuli-responsive, drug release from the micelles can be triggered by stimuli as a result of structural or morphological disruption. One major topic in this area is to develop BCP micelles that allow for the fine-tuning of the release kinetics of the loaded drug in a target-specific and timely way. To date, most BCP micelle-based delivery systems are formed with a hydrophilic poly(ethylene oxide) (PEO) or poly(ethylene glycol) (PEG) block (26). This polymer has a good solubility in physiological media and prevents the adsorption of plasma proteins, which can trigger immune response (27,28).

Due to the particularity of BCP micelle-based DDSs, the stimulus should be physiological friendly and should not introduce any contaminants into the body. It is also necessary for the micelles to travel a long distance and possess good control of chemical or physical reactions at specific location and time (i.e., remote, spatial and temporal control). Consequently, many kinds of stimuli-responsive BCP DDSs have been developed in response to a variety of stimuli such as pH (29,30), temperature (31,32), light (33,34) and enzyme (35,36), to name a few. In recent years, particularly, there has been growing interest in utilizing ultrasound as a stimulus to induce the disruption of BCP micelles and trigger the release of their payloads (37-39). As compared to other external stimulation, ultrasound has special advantages in allowing for remote control of the disruption process of BCP micelles. It can penetrate deep into the body in a noninvasive way and be applied locally with focused beams. Because of these intrinsic advantages of focused ultrasound, it has been developed as an interesting trigger for the release of substances from BCP micelles (40-42) and other types of nanocarriers (43-46).

In what follows, we will focus our attention on the relevant literature about the various stimuli used in our research, namely, ultrasound irradiation, temperature change, redox reaction and exposure to light. A description of each stimulus will be given in the first part of the Introduction Since most of the work reported in this thesis is about these stimuli triggered disruption and release from BCP micelles, representative examples of stimuli-reactive BCP micelles in the literature will also be discussed showing the most recent achievements. In the second part, different approaches of making dual-stimuli-responsive BCP micelles, which is the main topic of

this thesis, will be introduced to set the background of our research. The Introduction will be closed with a statement of the objectives of the thesis work.

1. Stimuli and the Use for Block Copolymer Micelles

1.1. Ultrasound

Ultrasound, or sound of high frequency above 20 kHz, is inaudible to the human ear. When a medium is exposed to ultrasound, it undergoes changes due to two major mechanisms: thermal effect and acoustic cavitation (nonthermal). When a medium is under ultrasound treatment, it experiences periodic pressure oscillations at a frequency and amplitude determined by the ultrasound source (47). Compared with the simple pressure oscillations, the secondary effects of pressure oscillations are often more significant and capable of producing thermal effects. Owing to absorption of part of the sound waves, the medium will have its temperature elevated immediately. Increasing temperature of the medium is not the main activating effect of ultrasound, but it could form an important part. The most significant secondary effect is a phenomenon referred to as acoustic cavitation involving rapid growth and collapse of bubbles (inertial cavitation) or sustained oscillatory motion of bubbles (stable cavitation) (48). Since the bubble collapse is a phenomenon induced throughout the liquid by ultrasound and can generate many chemical and mechanical effects, the inertial cavitation is considered a major mechanism for causing alterations to medium (49). There is a distinction between two types of cavitation. In inertial cavitation, bubbles oscillate in an unstable manner about their equilibrium, expanding to 2 or 3 times their resonant size before collapsing violently during a single compression half cycle. By contrast, in stable cavitation, bubbles exist for a considerable number of acoustic cycles, while the radius of each bubble varies about an equilibrium value (50). The acoustic cavitation can concentrate acoustic energy in small volumes resulting in temperatures of thousands of kelvin, pressures of GPa, local accelerations 12 orders of magnitude higher than gravity, shockwaves, and photon emission. In short, it converts acoustics into extreme physics and create a vigorous environment.

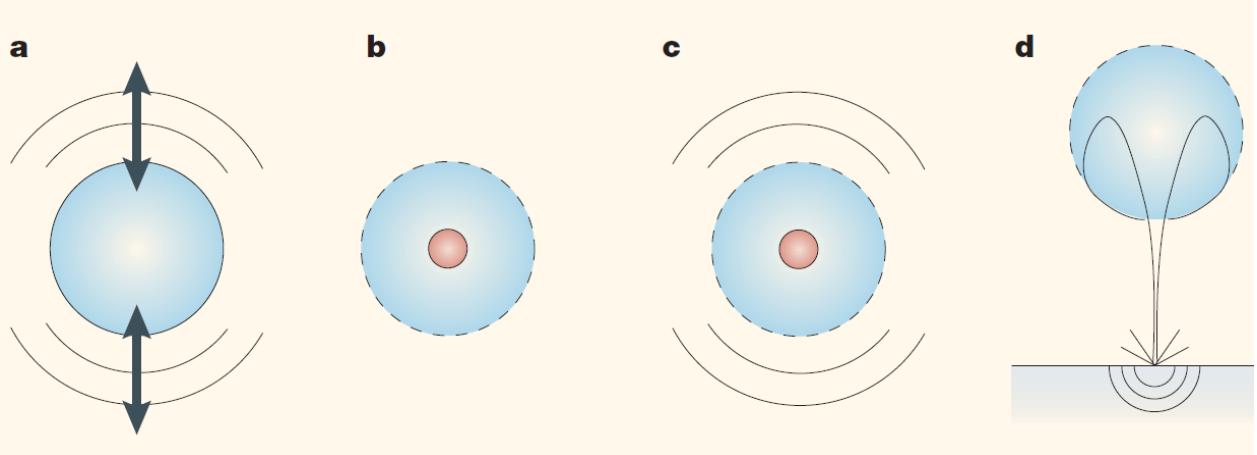

Figure 1. Mechanisms of ultrasound cavitation. (a) Acoustic streaming: cavitation bubbles can oscillate around their resonant size and generate velocities inducing shear stresses. (b) Sonochemistry: sudden collapse of bubbles generates momentary high temperatures in the bubble core. The hot bubble can induce chemical changes in the surrounding medium, including free-radical generation. (c) Shock waves: sudden collapse of cavitation bubbles leads to the formation of shock waves. (d) Liquid microjets: collapsing bubbles near a surface experience non-uniformities in their surroundings that results in the formation of high-velocity microjets. [47]

The severity of the ultrasound effects is governed by several parameters, primarily the frequency and amplitude (power or intensity) of the ultrasound. Due to the crucial importance of frequency for ultrasound effects, the ultrasound technology can be classified into two groups of low frequency ultrasound and high frequency diagnostic ultrasound. For the low frequency ultrasound, the ultrasound with a long wavelength is difficult to focus; thus when low frequency ultrasound is introduced into human body, the ultrasonic cavitation can destroy the vivo structures. This drawback restricts practical clinical use of low frequency ultrasound. For high frequency ultrasound, the ultrasonic wave can be focused, meaning that the intensity is quite high only in the focal spot, while in other areas, the intensity can be low to be acceptable by human body.

Thanks to the discovery of the piezoelectric effect by Jacques and Pierre Curie, Paul Langevin and colleagues built the first ultrasound transducer as submarine sonar in the early 1900s. Several

years later, ultrasound was first introduced into therapy by Wood and Loomis, and they reported the physical and biologic effects of high-frequency and high-intensity ultrasound in 1927 (51). High intensity focused ultrasound (HIFU) refers to a high frequency focused ultrasound of which ultrasound beams are emitted from a high-powered transducer. A typical HIFU system consists of a signal generator, a power amplifier and an acoustic lens transducer. The signal generator controls the frequency and initial amplitude of the input signal, which is amplified using the power amplifier. The amplified signals are transmitted to the HIFU transducer to generate the desired ultrasound beam. HIFU transducers can be spherical-shaped transducers or phased arrays. They are constructed to make ultrasound beams converged and deposit maximum acoustic energy into the focal millimeter-sized volume. The acoustic lens transducer can determine the focal dimensions by the geometry of the transducer (aperture and focal length) and its operating frequency. The first report of application of HIFU to humans was in 1960 (52), but this technique did not gain significant clinical acceptance until the 1990s, despite successful ophthalmological treatments before this date. In recent years, HIFU treatment has been increasingly used as a non-contact and remote control approach in medical treatment.

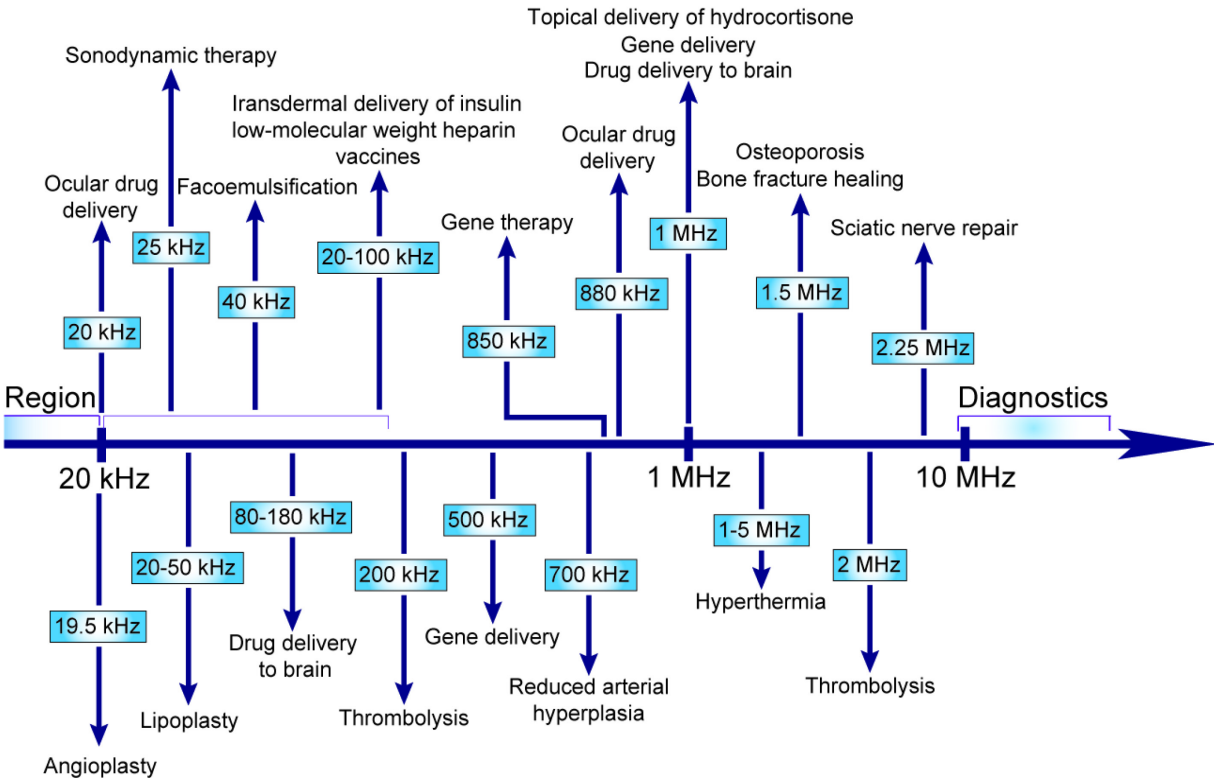

Figure 2. A partial summary of ultrasound frequencies used for medical applications. Each item in

the figure corresponds to one or more literature reports. The figure provides an overview of the conditions used for medical ultrasound applications and does not necessarily depict optimal or recommended conditions. For many applications, more than one condition has been used. A significant clustering of applications is found around a frequency of 1 MHz. [47]

Compared with other techniques such as cryotherapy, laser, microwave, and radiofrequency, HIFU has some distinct advantages (53). It is noninvasive and nonionizing, which means it can be repeated for many times because it has no long-term cumulative effects. Because human tissues have viscoelastic characteristics, the acoustic energy is lost and converted to heat. HIFU treatment can raise the tissue temperature in the focal area in seconds and to maintain this temperature for 1 s or longer (54). Ultrasonic energy absorption within the focal volume inducing high temperatures can also be focused precisely on tissue volumes as small as several cubic millimeters, with temperatures outside this region being kept at levels that are not cytotoxic. This important feature of HIFU lesions makes the damage spatially confined without damaging the intervening or surrounding tissue. Since the focal dimensions can be determined by the acoustic lens transducer, the desired size and shape of a larger HIFU target can be achieved by multiple sonications combining individual lesions in a matrix format.

In recent years, ultrasound has been employed as a stimulus to trigger and control the release of drugs from liposomes (55), polyelectrolyte microcontainers (56), multilayered capsules (57), microemulsions (58), and BCP micelles (59). However, the use of ultrasound as a rational means to control the disruption of BCP micelles remains largely unexplored. Rapoport and coworkers first studied ultrasound triggered drug release using doxorubicin-loaded Pluronic micelles and showed that ultrasound can effectively penetrate deep into the body in a noninvasive way (60). However, the weak cavitation effects of high frequency ultrasound do not help to achieve micellar disruption and drug release. For instance, they reported a very slow release for Pluronic P105 micelle under 1 MHz high frequency ultrasound (37). Therefore, a focused ultrasound mode was used to improve the release efficiency for high frequency ultrasound. To enable the use of HIFU as an effective trigger for controlled drug release, it is of fundamental interest to develop BCP

micelles that can be rapidly and efficiently disrupted by high-frequency ultrasound, that is, under a relatively weak cavitation effect.

Some reported studies aimed at investigating the effects of HIFU on BCP micelles and tried to identify BCP structures that are more susceptible to be disrupted by the ultrasound. Zhang et al. studied the use of HIFU to affect the micelles of PEG-*b*-PLA, where PLA stands for poly(lactic acid). They reported that by adjusting the HIFU irradiation time, intensity and location, the release of a loaded hydrophobic dye, Nile Red (NR), from the BCP micelles could be tuned. In contrast to previous reports (41), it was found that no reversible encapsulation of the dye occurred after the HIFU was turned off. This irreversible release from the PEG-*b*-PLA micelle was attributed to a chemically breaking process of micelle structure due to the degradation of the copolymer chains resulting from the transient cavitation in the HIFU focal spot (Figure 3)

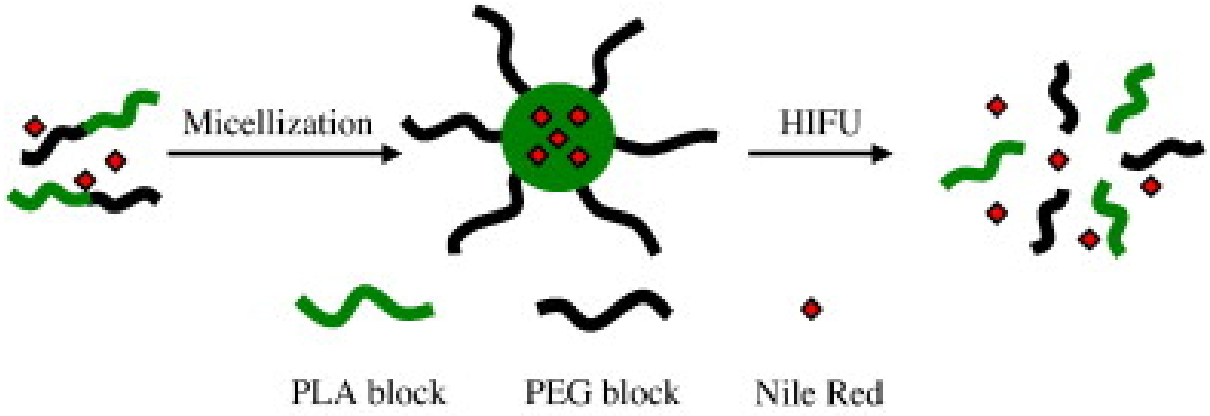

Figure 3. Schematic illustration of the HIFU responsive release of encapsulated dye molecules (NR) from the PEG-*b*-PLA micelle. [41]

Later, Wang et al. reported on the finding that micelles formed by the amphiphilic diblock copolymer PEO-*b*-PTHPMA, where PTHPMA stands for poly(2-tetrahydropyranyl methacrylate) are sensitive to HIFU (1.1 MHz) (61). More interestingly, the spectral characterization results suggest the occurrence of hydrolysis of THPMA side groups induced upon exposure to HIFU beams. The concept of rational design for ultrasound sensitive BCPs was introduced in this study. The hydrophobic PTHPMA block possesses labile chemical linkages in the structure that are

likely to react to the effect of HIFU and create a shift of the hydrophilic-hydrophobic balance toward the destabilization of the micelles.

Those recent studies show the potential to develop ultrasound-sensitive BCP micelles by having labile chemical bonds in the copolymer structure, and to use the high-frequency HIFU to trigger a chemical reaction for the disruption of micelles. Since HIFU can act deep in an aqueous solution, it is an attractive remote and noninvasive stimulus for controlled drug delivery applications. With HIFU-sensitive polymer micelles, ultrasound offers the desired temporal and spatial control over the disruption of drug carriers and the resulting release. More studies are needed to disclose BCP chemical structures that can react more sensitively to HIFU beams in a controlled way.

1.2. Temperature Change

For very long time, thermo-sensitive polymers have been among the most studied stimuli responsive materials due to their ability to change solubility, conformation and shape and so on upon a simple temperature variation. This feature has been the basis for a wide range of biomedical and nanotechnology applications (62-66). Also, the use of temperature change as a stimulus is potentially cheap and convenient. Water is easily available, environmentally friendly and can be the solvent for a wide range of materials or products, which is preferable to organic solvents. Therefore, thermosensitive water-soluble polymers displaying hydrophilic-hydrophobic phase transitions upon cooling or heating of the solution are of great interest for researchers. Thermosensitive polymers can be utilized as part of copolymer architectures, which makes it possible to use the temperature change to promote the formation, transformation or deformation of self-assembled BCP aggregates in aqueous solution. For amphiphilic water-soluble BCPs, their ability to self-assemble into micelles, lamellar aggregate, vesicles or hydrogels is one of the most interesting solution properties. The self-assembly process can be reversible for thermosensitive BCPs.

When polymers are dissolved in organic solvents, generally they become more soluble when heated. For water-soluble polymers, however, they often exhibit better solubility in cold water and become phase separated (or precipitated) upon heating. This type of thermosensitivity is

characterized a lower critical solution temperature (LCST), below which the polymer is soluble and above which it is insoluble (11). It is largely dependent on the hydrogen bonding capabilities of the constituent monomer units. Thus, polymers can exhibit LCST behavior in strongly interacting solvents such as water. After phase separation (being insoluble) on heating, those polymers can generally be redissolved on subsequent cooling. Moreover, the phase separation temperature of a given polymer can be changed by incorporating either relatively hydrophobic co-monomer units (LCST decreases) or hydrophilic co-monomer units (LCST increases). There is a balance between hydrophobic, hydrophilic and H-bond-mediated interactions, which determines the solubility of the LCST polymers in water (Figure 4). The key parameter defining the ‘‘responsive’’ or the ‘‘smart’’ behavior of the polymers is a nonlinear response to an external signal. For LCST polymers, this means a clear solubility-insolubility transition occurring over a narrow temperature range. As in nature, the bulk response of the thermosensitive polymers is usually due to multiple cooperative interactions such as loss of H-binding, which, although individually weak, ultimately evokes a large structural change in the material when summed up over the whole polymer.

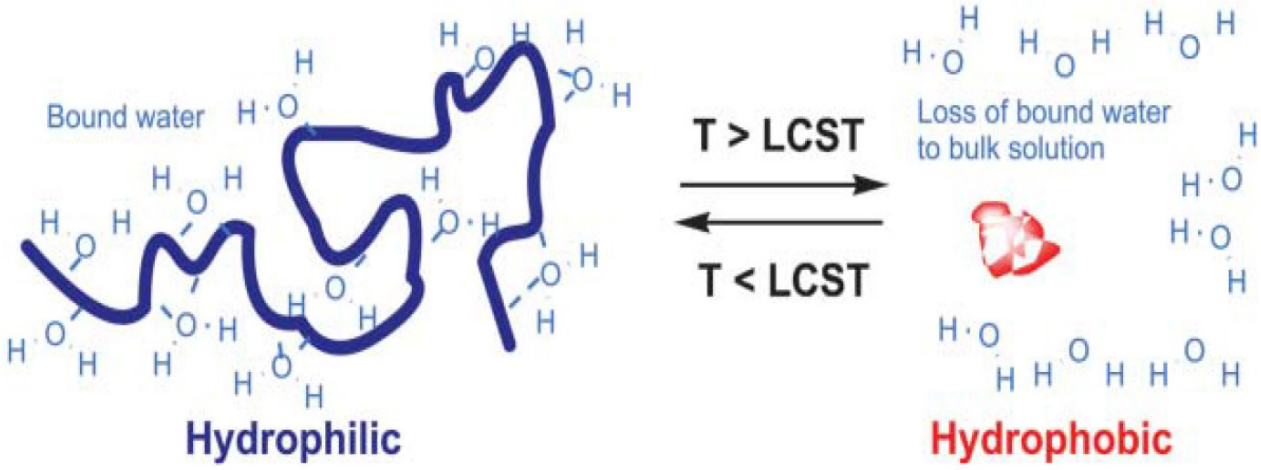

Figure 4. Schematic of ‘smart’ polymer response with temperature. [11]

Normally, it is preferable to work with LCST polymers that display a very short phase transition time and, generally, the transition from the soluble to insoluble regime on heating can be

monitored by measuring the cloud-point temperature, at which the optical transmittance of the polymer solution drops due to light scattering caused by the separated polymer phase. In the soluble state below LCST, the coiled structure is favored as this allows for the maximum interaction between the polymer and water molecules. In systems where strong hydrogen bonding is possible, such interactions make the polymer easier to dissolve in aqueous solution. At higher temperatures, the hydrogen-bonding effect weakens; concomitantly the 'hydrophobic effect', the tendency of the system to minimize the contact between water and hydrophobic surfaces increases; hence, the transition from coiled to a denser globule structure for the polymer occurs.

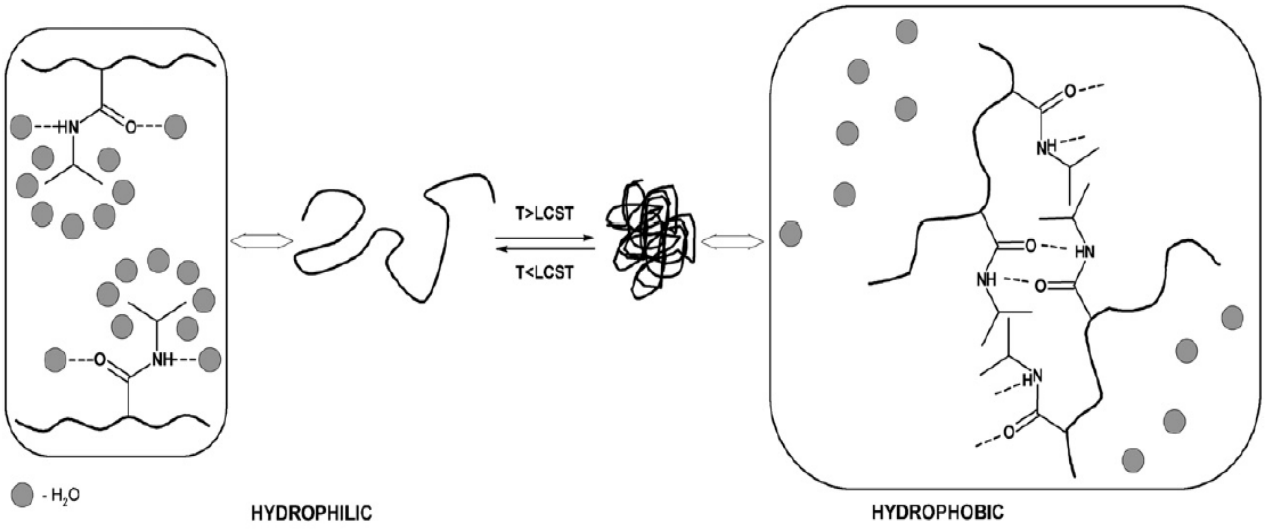

Figure 5. Illustration of temperature induced PNIPAM phase transition. [67]

Polymers bearing the amide functionality form the largest group of thermosensitive polymers. These polymers are biocompatible and display temperature-dependent phase behavior in aqueous solution, which makes them attractive for drug delivery and tissue engineering. The most studied thermosensitive polymer, not only among this group but overall, is arguably poly(N-isopropyl acrylamide) (PNIPAM). It has a LCST around 32 °C in water (67), close to the body temperature. Below its LCST, the polymeric chains hydrate and exist as an expanded coil state forming hydrogen bonds with water molecules; while upon heating above its LCST, it becomes more hydrophobic and undergoes a sharp and reversible coil-to-globule transition (Figure 5). Although PNIPAM exhibits a very sharp transition when heated, a broad hysteresis can be observed in the

cooling process. This behavior was previously observed by Wu et al. with PNIPAM of narrow molecular weight distribution, and assigned to an irreversible coil-to-globule transition involving four distinct thermodynamically stable states (68). Furthermore, the LCST of PNIPAM is relatively insensitive to environmental conditions, which is an advantage for applications. Indeed, slight variations of pH, polymer concentration, or chemical environment generally affect the LCST of PNIPAM by only a few degrees (69).

Owning to possible concerns on the toxicity of N-isopropylacrylamide monomer, Lutz and co-workers prepared a series of biocompatible polymers that exhibited similar thermoresponsive behaviors as PNIPAM (70,71). They possess two oligo (ethylene glycol) units of different chain-lengths as side groups, which have similar chemical nature but different hydrophilicity. This leads to the formation of thermosensitive polymers with diverse LCSTs. For instance, the polymer of 2-(2-methoxyethoxy)ethyl methacrylate (MEO_2MA) bearing only two ethylene oxide units as side groups, is soluble in water at room temperature and exhibits a LCST around 26 °C (72). Fortunately, because the LCSTs and solubility of the polymers strongly dependent on the length of oligo(ethylene glycol) side chain units, polymers with longer ethylene oxide side chains can exhibit much higher LCSTs in water (typically around 90 °C for poly(ethylene glycol) methyl ether methacrylate (PEGMA) with side chains of 8-9 ethylene oxide units) (73). More interestingly, the LCST of the random copolymer P(MEO_2MA-*co*-PEGMA) can be precisely adjusted to between 26 and 90 °C by varying the composition of the two co-monomers (74). For example, LCSTs of 32, 37 and 39 °C were obtained with copolymers containing 5, 8 and 10% of PEGMA units in the copolymer, respectively. These novel thermosensitive macromolecules are very promising for biomedical applications since they are principally composed of biocompatible oligo(ethylene glycol) segments. Linear PEG is a cheap, neutral, water-soluble, nontoxic, biocompatible polymer and probably the most widely applied synthetic polymer in biotechnology and medicine (26). As mentioned above, it is also the most used polymer for the hydrophilic corona of BCP micelles. Furthermore, nonlinear PEG analogues (i.e., macromolecules constructed from oligo(ethylene glycol) macromonomers) have been shown to be as biocompatible as their linear counterparts (75-77). In this context, thermosensitive PEG analogues could become in a near future extremely popular materials for biotechnology applications.

Poly(*N,N*-dimethylaminoethyl methacrylate) (PDMAEMA) is a representative example of the third most investigated group of thermosensitive polymers. It is a polymethacrylate that bears the tertiary amine functionality in the side group. Owing to this structure, the polymer has not only LCST but also is sensitive to change in pH. It is wildly exploited for drug delivery and biotechnology due to its water solubility and the weak polybasic nature, meaning that it can be partially protonated in the physiological environment. PDMAEMA has shown a LCST around 40 °C in water (78-81). The dimethylamino group in DMAEMA is known to be a powerful hydrogen bond acceptor (82,83), so the LCST can be adjusted by tuning the interactions between polymer and water (84-86). By copolymerization of DMAEMA with some hydrogen bond donor units or basification of the polymer solution, the LCST will shift to lower temperatures, due to the formation of hydrogen bonds between polymer groups. When the polymer solution is acidified or incorporating some hydrogen bond acceptor units into PDMAEMA, the LCST will shift to the high temperatures due to the formation of hydrogen bonds between polymer and water. For instance, at pH 4, DMAEMA are fully ionized and the increased electrostatic repulsive force is developed between charged sites on DMAEMA, which interferes with the hydrophobic interactions between the DMAEMA groups and thus making the LCST unobservable on heating the aqueous solution (87).

Polymers exhibiting LCST behavior have been used to construct a variety of thermosensitive architectures including BCPs. There are numerous reviews in the literature (62,88-92). Some examples of application demonstrated by our group are outlined below. In one case (89), in order to make thermosensitive gold nanoparticles (AuNPs), they were coated with diblock copolymers that display either a LCST or an opposite UCST (upper critical solution temperature) in aqueous solution in response to temperature change without aggregation of the nanoparticles. This was achieved by using a diblock copolymer PEO-*b*-PDMAEMA with the PDMAEMA block tethered to the surface of AuNPs. With such design, even with polymer chains on AuNPs becoming dehydrated at T>LCST or T<UCST, the use of water-soluble PEO as the outer block allowed the colloidal stability of AuNPs to be retained (Figure 6). In another case, BCPs containing one LCST block were utilized to obtained polymer nonogels with photo-tunable sizes (90). A series of coumarin-containing double-hydrophilic block copolymers of

P(NIPAM-*co*-CMA)-*b*-P(DMA-*co*-CMA), where DMA stands for *N,N*-dimethylacrylamide and CMA for 4-methyl-[7-(methacryloyl)oxyethyloxy]coumarin], were synthesized. Such a copolymer can be dissolved in cold water at T<LCST of the P(NIPAM-*co*-CMA) block; on heating the solution to T>LCST, micelles are formed with the P(NIPAM-*co*-CMA) core and the P(DMA-*co*-CMA) shell. At this point, irradiation with UV light at λ >310 nm can induce photodimerization of coumarin side groups resulting in both core- and shell-cross-linking. Subsequently, when the micellar solution is cooled to T<LCST of the P(NIPAM-*co*-CMA) block, the crosslinking prevents the polymer dissolution from occurring, which leads to the formation of nanogel (cross-linked water-soluble polymers in the form of nanoparticles). The photochangeable size of the nanogel comes from the fact that the coumarin dimerization is reversible. When the coumarin dimers are photo-cleaved under UV light at λ < 260 nm, the crosslinking density can be controlled, which determines the swelling degree of the nanogel particles. With this BCP design, the photo-induced size change was found to be more important than nanogels with only cross-linked core or only cross-linked shell.

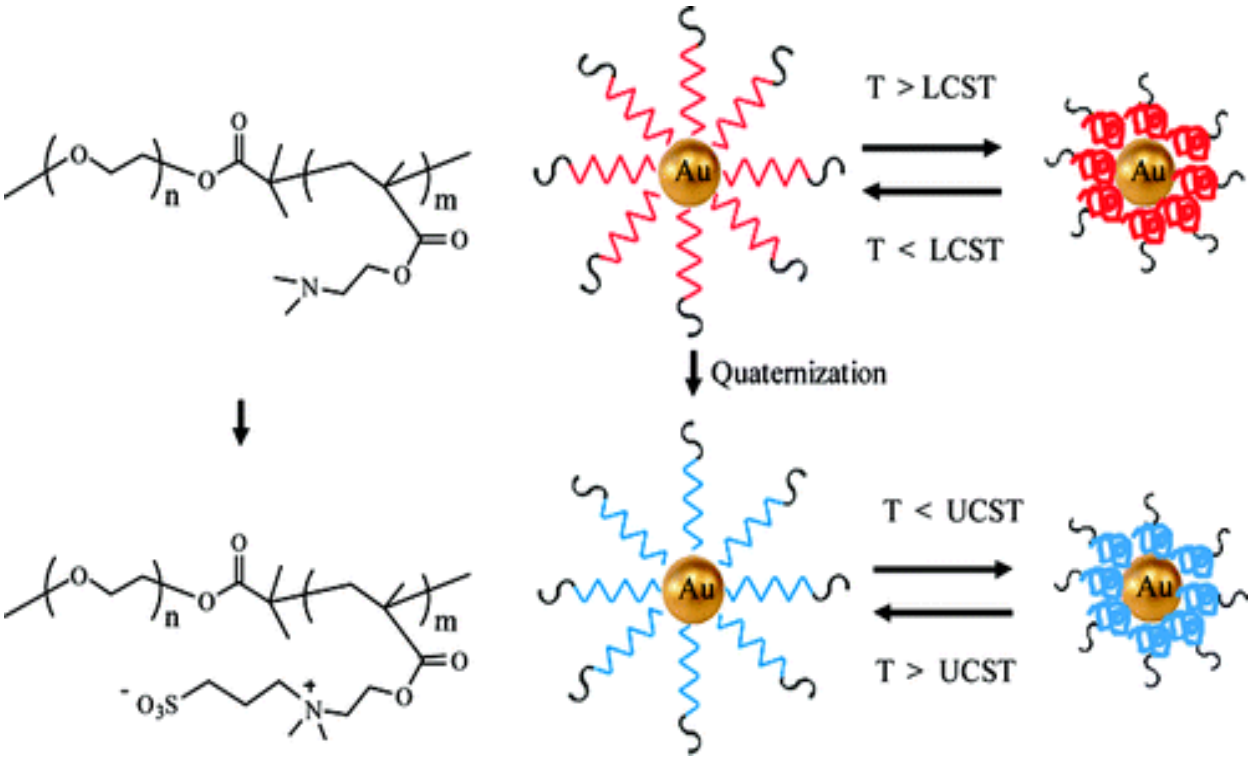

Figure 6. Chemical structures of the diblock copolymers tethered to AuNPs and schematic of both

LCST and UCST thermal phase transitions on AuNP surface. [89]

An important research topic in the area of LCST polymers is how to control and fine-tune the LCST of a given polymer that fits a particular application. In principle, such a control can be achieved by different means such as varying the polymer structure, copolymer composition or making the polymer responsive to a stimulus other than temperature change. The latter approach will be further detailed in this thesis. For instance, it has been long recognized that a photoreaction in a LCST polymer may change the phase transition temperature (93-99). One report from our group proposed a more complex control possibility by making a diblock copolymer undergo two photoreactions on the two blocks simultaneously (91). A variety of doubly photoresponsive and water-soluble diblock copolymers were synthesized, each block of which has a LCST and contains a different photoisomerizable chromophore (either azobenzene and spiropyran or two different azobenzenes). It was found that optically controlling the relative photoisomerization degrees of trans-azobenzene to cis-azobenzene and spiropyran-to-merocyanine could be used to tune the LCST of the BCP solutions.

The chain architecture or topology of a given LCST polymer may exert profound effect on the LCST. In one study, Zhao et al. found a new, simple, and efficient method to tune the LCST of thermosensitive water-soluble polymers based on a topological effect (86). The approach was schematically illustrated in Figure 7. The basic idea is to use a photocontrollable intrachain cross-linking reaction to introduce chain loops onto an initially linear polymer structure. To achieved this purpose, they designed poly P(DMAEMA-*co*-CMA). The PDMAEMA is a thermal sensitive polymer, which is soluble in cold water and becomes insoluble upon heating. The CMA bore a reversible photo dimer coumarin pendent group. By incorporating a number of CMA co-monomer units into PDMAEMA could optically control the intrachain cross-linking density that determines the number of loops formed. As shown in Figure 7, they found that the cloud point temperature was increased by increasing dimerization degree. This chain topology effect on the cloud point (or LCST) could be explored as an easy method for other water soluble polymers displaying a LCST.

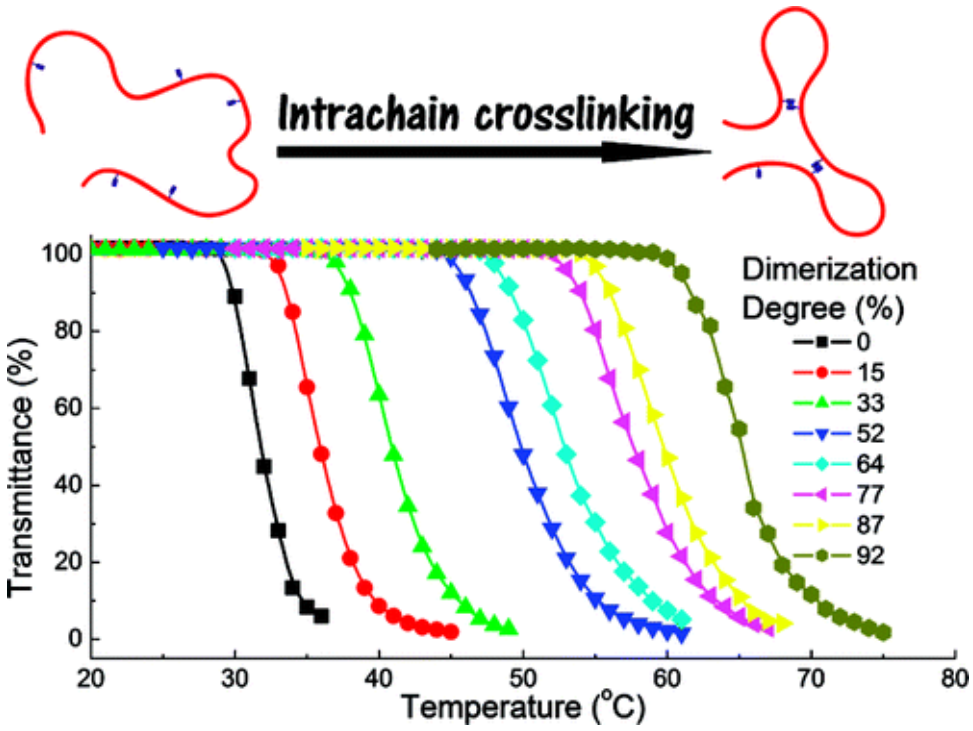

Figure 7. Schematic illustration of the formation of chain loops upon intrachain photodimerization of pendent coumarin groups and transmittance change as a function of temperature for copolymer solutions with samples photodimerized to different degrees. [86]

1.3. Light

Nature has evolved many sophisticated photoresponsive systems, such as vision and photosynthesis. These native photoresponsive systems are generally composed of a metastable photosensitive element. Without external stimuli, these groups can maintain their structures; however, upon light absorption, photosensitive element captures optical signals and converts them to physicochemical signals. If the physicochemical signals are sensed by a second functional element (such as a protein domain), it can exhibit new output functions. The optical signals also can be converted into heat through its interaction with metallic nanoparticles (such as gold nanoparticle through their surface plasmon resonance) and induce thermal changes in the systems. Photoresponsive systems, particularly, photoswitchable systems have received more and more attention in recent years since they hold great promise for many applications in broad fields

including drug release, gene delivery, biomaterials, artificial tissues, nanocontainers, microreactors, and photodynamic therapeutics (100-103).

Since our group reported the first BCP micelle that can undergo a reversibly disassemblage and assemblage upon alternating ultraviolet (UV) and visible light exposure in 2004 (104), there has been growing interest in designing and studying BCP micelles whose chain association state can be controlled or changed by light. The potential for optically controlled drug delivery applications is the main reason for this interest in the broad area of stimuli-responsive BCP self-assembled structures. If the release of drugs loaded in BCP micelles on target sites can be triggered by absorption light, the possibilities of remote activation as well as light-enabled spatial and temporal control are attractive features. Moreover, rational design of light responsive BCP micelles by exploring the photochemistry also offers interesting challenges from an academic point of view. To constitute a photoresponsive polymeric DDS, a photochromic molecule (chromophore) or metallic nanoparticles need to be incorporated or introduced into the polymer system. Upon light exposure, the absorbed light either activates a photochemical transformation in the chromophore (e.g., photoisomerization) or generates heat (photothermal effect) via the surface plasmon resonance of the nanoparticles, which gives rise to desired changes in the conformation and/or assembly of the polymers. These polymeric systems provide models by which photoswitches for reversibly controlling macromolecular recognition events can be developed. In what follows, we give a brief introduce for some photosensitive molecules often used in photo-responsive polymer or BCP-based DDSs.

In general, there are two fundamental classes of photoswitchable reactions that have been developed: single-cycle and multi-cycle photoswitches. Single-cycle photoswitches are a class of photoswitchable reactions that are irreversible. For instance, a therapeutically or biologically active molecule can be rendered temporarily inactive by attachment of such a photosensitive chemical protecting group. The molecule is activated by the removal of protective group upon light absorption. By contrast, multi-cycle photoswitches refer to reversible photoreaction processes. Upon exposure to different wavelengths of light, photoswitching chromophores can undergo a reversible photoisomerization between two isomeric forms. Due to different properties

of the two isomers, such as molecular geometry, polarity, charge or propensity for absorption/fluorescence, polymers containing such photoswitches can operate reversibly between a mute active state (switch "Off ') and an activated function (switch "On").

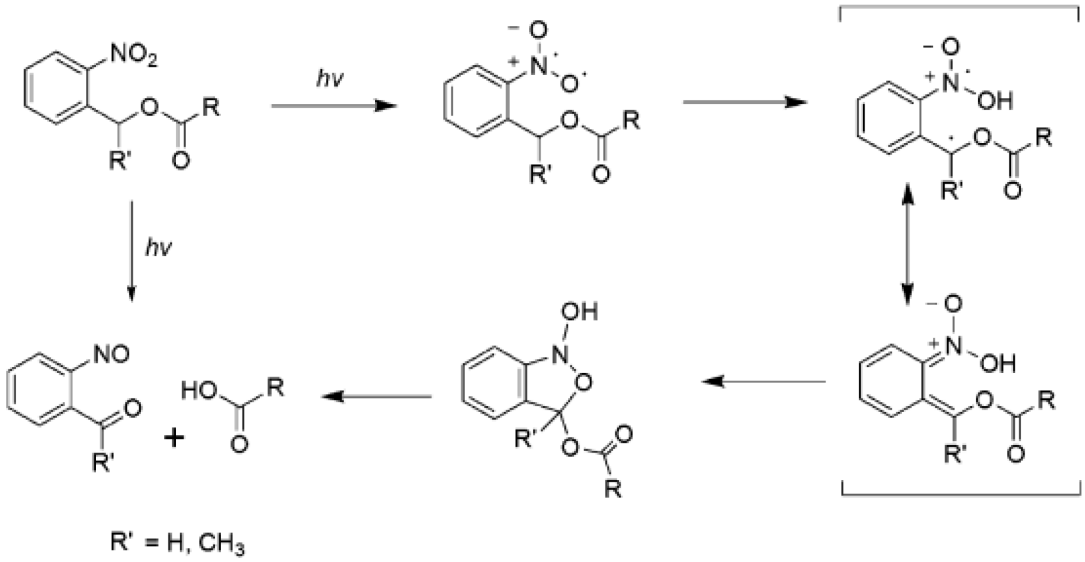

Figure 8. Photoisomerization mechanism of *o*-nitrobenzyl alcohol derivatives into an *o*-nitrosobenzaldehyde, releasing a carboxylic acid. [108]

The single-cycle photoswitchable groups have been used extensively in synthetic organic chemistry and have found numerous applications in academia and industry. Among the many photolabile groups that have been studied, *o*-nitrobenzyl (ONB) alcohol derivatives have been extensively exploited. Although they are first described in the field of synthetic organic chemistry by Schofield and co-workers in 1966, the chemistry was not widely recognized until Woodward and co-workers utilized what has become one of the most popular photolabile protecting groups (105). The application of photolabile molecules, especially ONB derivatives, is not limited to organic synthesis as can be seen by recent developments in biological applications of such photolabile compounds due to their good biocompatibility (106). The mechanism of photoreaction for an ONB alcohol derivative has been investigated in detail, most recently by Wirz and co-workers (107). Upon UV irradiation, the *o*-nitrobenzyl alcohol derivative converts into a corresponding *o*-nitrosobenzaldehyde, simultaneously releasing a free carboxylic acid (Figure 8)

(108).

Upon exposure to UV light at wavelengths near the maximum absorption wavelength of ONB derivatives, the photocleavage efficiency tends to be the highest.[107] The linkers and protecting groups based on ONB chemistry can usually be cleaved in minutes when exposed to an appropriate wavelength light, with times varying due to different light intensity (109). Thus, a remote and controlled deliver system can be achieved by introducing this photolabile group into polymer chain, since light can be delivered from outside of the system and precisely localized in a selected space at a desired time. Indeed, photo-processes usually start or stop when the light is switched on or off and no additional reagents are needed. Moreover, a number of parameters (light intensity, illumination time and wavelength) can be simply tuned during the reaction that enables good control over the photoreaction. However, photocleavage of unsubstituted ONB derivative requires UV light, which greatly restricts its utility for in-vivo applications. Fortunately, introducing substituents on the aromatic ring or at the benzyl position of the linker can shift the photocleavage wavelength. Indeed, substituting electro-donating groups onto the benzyl ring is a convenient method to increase the breadth of its absorption spectrum towards longer wavelengths (110). For example, 3, 4-dimethoxy-2-nitrobenzyl group as has the maximum absorption wavelength red-shifted to the visible region, around 400 nm. Although the excitation efficiency is quite low, some ONB derivatives can undergo two-photon absorption-based photocleavage.

As shown in Figure 9, there also are some other single-cycle photoswitchable groups, such as benzoin, 7-nitroindoline, *p*-hydroxyphenacyl and (coumarin-4-yl) methyl derivatives (111). All of them can be photocleaved upon UV or visible light irradiation. Especially for (coumarin-4-yl) methyl derivatives, they have a large two-photon absorption cross section for activation by near infrared (NIR) light (112-114). However, most of these photoswitchable groups basically suffer from the same drawback. Since they have low excitation efficiency using two-photon NIR light, high-energy UV or visible light activation is required which can be inappropriate for in-vivo applications.

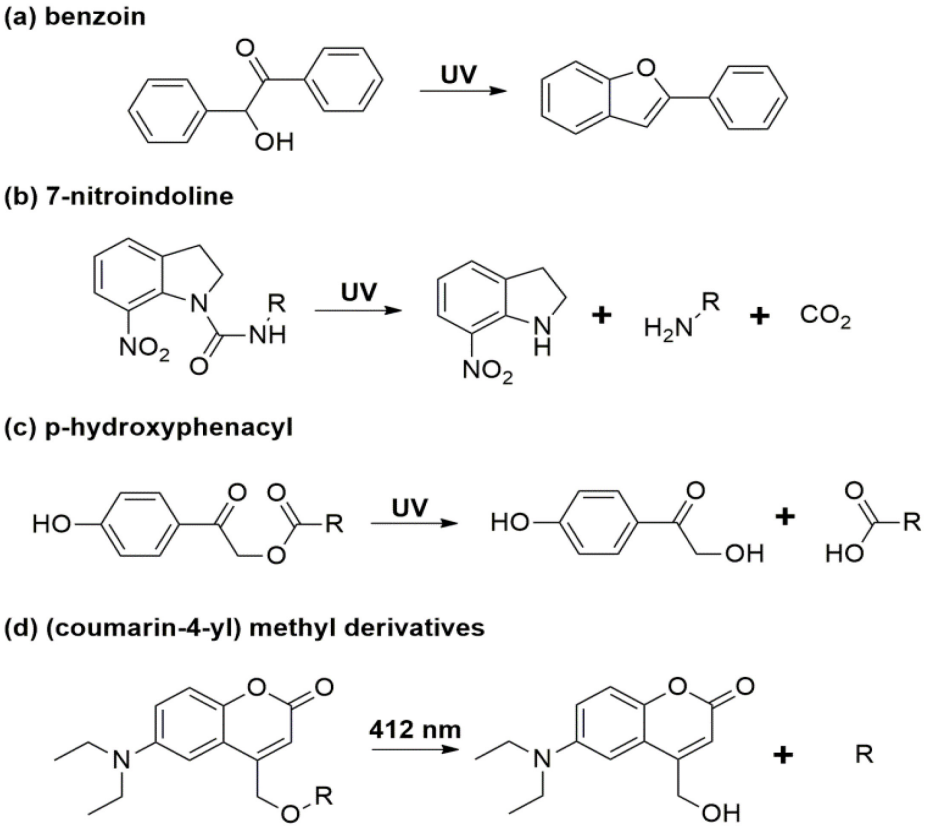

Figure 9. Chemical structures of some typical photocaging molecules and related photoreactions: (a) benzoin, (b) 7-nitroindoline, (c) *p*-hydroxyphenacyl and (d) (coumarin-4-yl) methyl derivatives.

For multi-cycle photoswitchable molecules, azobenzene and its derivatives are undoubtedly the most exploited chromophore in materials and polymer chemistry. Azobenzene is a textbook representative demonstrating the rotoresistant property of the N=N double bond, and researchers have long been aware of the two possible mechanisms of inversion and rotation for the trans-cis photoisomerization. There are many theoretical and experimental papers dealing with this subject. The azobenzene group and many of its derivatives can display a reversible photoisomerization between the generally more stable trans form to the less stable cis form via absorption of UV and visible light respectively, yielding a photostationary composition that is wavelength and temperature dependent (115,116). For unsubstituted azobenzene, upon absorption of UV light, the trans isomer is converted to the metastable cis isomer that has a higher polarity and a bent

molecular shape as compared to the trans form. This important change in polarity and molecular shape has been used in designing photoresponsive polymers and materials. For instance, trans azobenzene is a meson that can form a liquid crystal phase, while the cis form is incompatible with ordered liquid crystal phase. Consequently, the reversible trans-cis photoisomerization can be used to achieve photocontrolled isothermal phase transition between a liquid crystal phase and the isotropic state (117). The cis isomer can return back to the stable trans state either through thermal relaxation or by absorption of visible light.

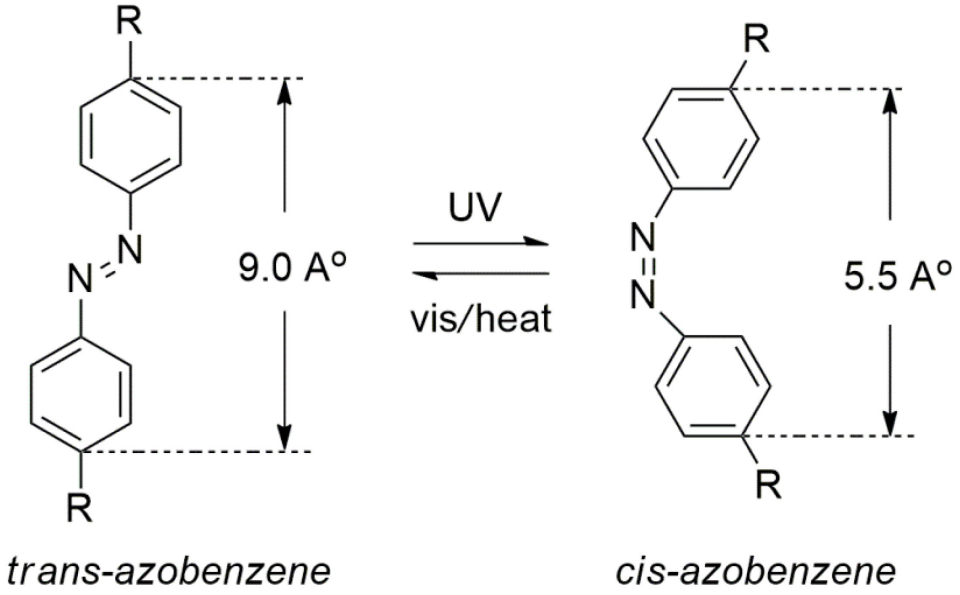

Figure 10. The reversible transformations from more stable trans form to the less stable cis form upon irradiation with UV or visible light.

One of the other popular multi-cycle photoswitchable molecules is spiropyran (SP). By absorption of UV light, it can undergo a ring-opening reaction, resulting in the formation of an open merocyanine (MC) form (118,119). The MC form possesses an extended conjugation and it is more polar and more hydrophilic than SP. It can be totally reverted back to SP by visible irradiation. Diarylethenes are another example. The molecules can undergo a reversible closed-open ring isomerization under exposure at different wavelengths of light (120). Due to the extended conjugation, the closed ring isomer is less stable and colored, while the open isomer is colorless. Coumarin is also a commonly used photoswitching group, which can undergo a

reversible photodimerization reaction (121-123). Upon absorption of longer wavelength UV light (> 310 nm), it can form a dimer through a photo-cycloaddition [2+2] reaction. When the dimer absorbs more energetic UV photons at shorter wavelengths (<250 nm), it can be reverted back to two monomeric chromophores through cleavage of the cyclobutane ring in the dimer. All the photoswitchable groups mentioned above have been much used in making photoresponsive polymers or BCPs.

As mentioned above, the design and synthesis of photoresponsive BCP micelles are now well known, and photoinduced disruption of such BCP micelles has been studied in the context of light-controlled drug delivery. Wang et al. reported that micelles or vesicles formed by an amphiphilic diblock composed of hydrophilic poly(acrylic acid) (PAA) and a hydrophobic polymethacrylate bearing azobenzene in the side group can undergo reversible dissociation and reformation under alternating UV and visible light, as a result of the reversible trans-cis photoisomerization of azobenzene (PAzoMA) (104). This is caused by a reversible change in the polarity of the PAzoMA block which shifts the hydrophilic-hydrophobic balance towards the destabilization under UV light and assembly under visible light irradiation.

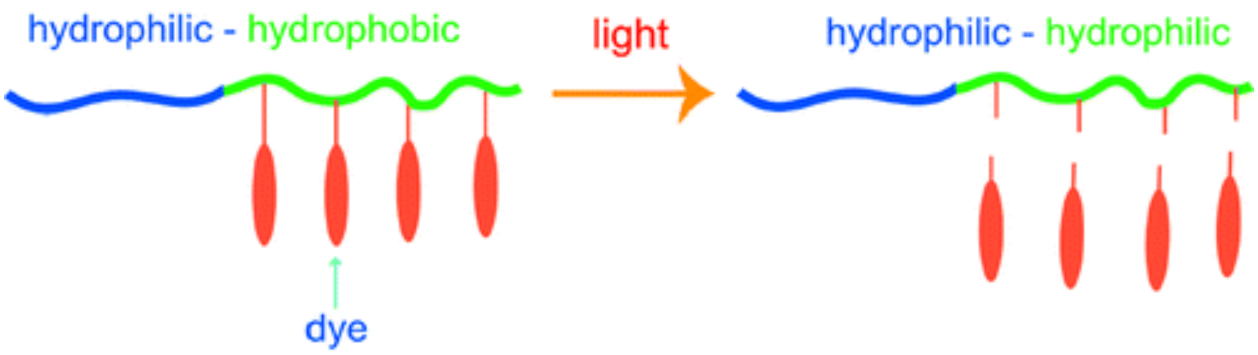

Figure 11. Schematic illustration of light-induced detachment of dye pendant groups resulting in the hydrophobic-to-hydrophilic switch. [124]

Photoinduced irreversible dissocistion or degradation of BCP micelles can also be easily prepared by using single-cycle photoswitches. Jiang et al. reported a study using the approach illustrated in Figure 11 (124). Light-breakable BCP micelles in solution can be obtained by making use of the photolysis of a photolabile chromophore on the hydrophobic block, which cleaves the

chromophore from the polymer structure and converts the hydrophobic block into a hydrophilic one. When this happens, the initially amphiphilic BCP loses the amphiphilicity required for micelle self-assembly and, consequently, the micelle is dissolved irreversibly. This design can readily be applied to many chromophores (124,125). By choosing the photolabile chromophore that interacts with light and changes the hydrophilic-hydrophobic balance, it is possible to design stable BCP micelles that can be opened or disrupted by light at a desired range of wavelengths depending upon the application (113,126). Given the many advantages of polymer micelles over small-molecule (surfactant) micelles (127-129), light-responsive BCPs represent an attractive alternative in developing materials for controlled delivery applications.

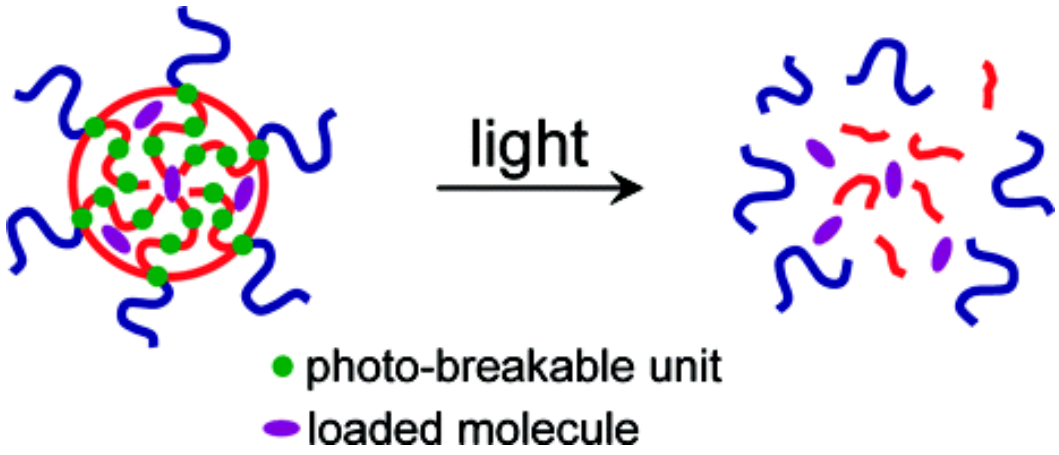

Figure 12. Schematic illustration of burst release by placing a photobreakable unit repeatedly on the hydrophobic block. [122]

With developing photocontrolled DDS in mind, there are situations where a very fast release of loaded drug (so-called “burst release”) is necessary, which demands fast degradation of BCP micelles. Figure 12 depicts the approach reported by our group (122), in which a large number of photocleavable moieties, such as ONB, are introduced into the main chain of the micelle core-forming hydrophobic block. This type of BCP micelles in aqueous solution can undergo fast photoinduced disintegration of micelle core, thus light-triggered burst release of loaded hydrophobic guest molecules could be achieved. This progress is also of fundamental interest because the approach is general and can easily be applied to design BCPs with photocleavable groups.

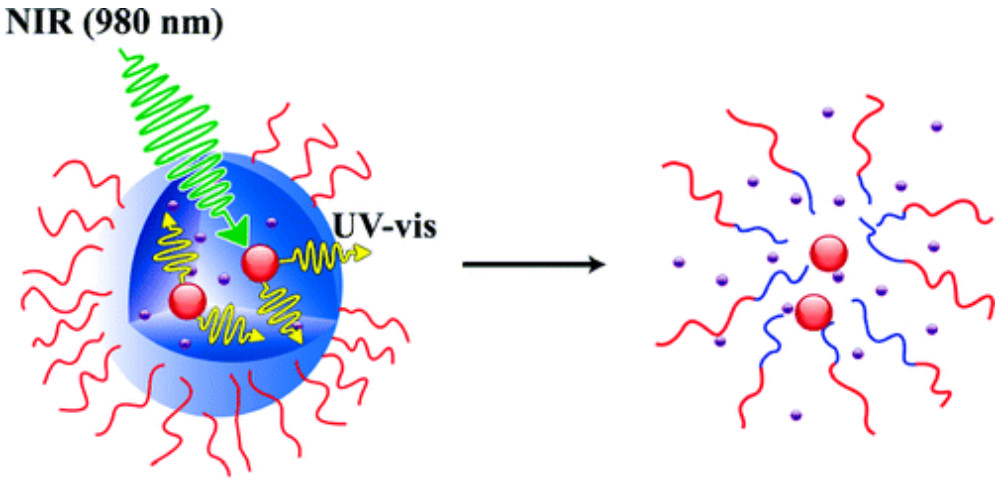

Figure 13. Schematic illustration of using NIR light excitation of UCNPs to trigger dissociation of BCP micelles. [130]

Finally, for almost all photoresponsive BCP micelles, the photochemical reaction of the photochromic groups requires the use of UV light, which, as pointed out above, is a big concern for in-vivo applications because UV light cannot penetrate deep into the tissue and is detrimental to healthy cells. The use of NIR for excitation via 2-photon absorption is a general solution, but the efficiency is low and a pulse, femtosecond laser is needed. Recently, Yan et al. demonstrated a novel strategy that makes possible the NIR excitation. The idea, shown in Figure 13, consists in co-loading upconverting nanoparticles (UCNPs) and drug in BCP micelles that can be dissociated upon UV light absorption (33,130). By exposing the BCP micellar solution to a continuous-wave diode NIR laser (such as 980 nm light), photons in the UV region are emitted by the nanoparticles inside the micelles. Those UV photons are in turn absorbed by ONB groups in the micelle core-forming hydrophobic block, which activates the photocleavage reaction and leads to the dissociation of the micelle and release of co-loaded hydrophobic species. Therefore, using UCNPs as NIR-activated internal, nanoscale UV light source, NIR light can be used for the excitation, which circumvents the need for UV light excitation. This method is general and can readily be applied to many UV-sensitive materials or systems developed for biomedical applications.

1.4. Oxidation-Reduction

A redox stimulus is defined as an electrochemical addressing of the redox-sensitive group, which causes a change in its oxidation state. Indeed, this kind of stimulus is intensively used and redox responsive polymers have recently attracted wide interest for their promising applications in controllable delivery in physiological environments, where the redox process is constantly and widely present (131-135). To design a redox responsive polymer, an easy approach is to incorporate reduction-sensitive disulfide units into the polymeric structure.

A disulfide bond (-S-S-) is a covalent linkage which is formed as a result of the oxidation of two sulfhydryl (SH) groups. Its reversibility and relative stability render the disulfide bond especially attractive in designing drug delivery systems. The oxidation, in fact primarily upon exposure to air, can induce covalently bonded disulfides formed spontaneously by autoxidation of sulfhydryls. The reversible cleavage of disulfide linkages can occur by reductive reaction. Disulfides can be cleaved into their corresponding thiols in two ways: under reducing environments in the presence of various reducing agents such as tributyl phosphine (Bu_3P) (136,137) and through a disulfide–thiol exchange in the presence of other water-soluble thiols such as dithiothreitol (DTT) (138,139) and glutathione (GSH, a tripeptide containing cysteine with a pendent thiol group) (140-143).

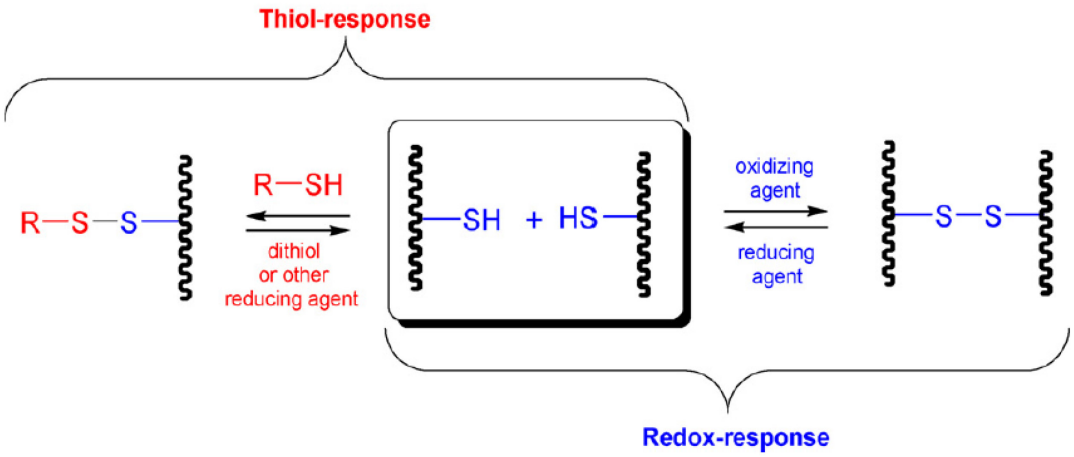

Figure 14. Redox/thiol-responsive behavior capable of being exploited in polymeric systems. [2]

GSH is an abundant reducing agent in most cells (144). It is present in a typical concentration of

about 0.002 mM in the cellular exterior, but several thousand times higher (about 10 mM) inside cells, which is enough for enabling disulfide linkages biodegradation (145-148). This dramatic difference of the GSH concentration between the extracellular and intracellular space provide an opportunity for designing intracellular specific DDSs. Thus, the incorporation of GSH-cleavable disulfide bonds into polymers or BCPs makes the disulfide bond particularly interesting in designing redox-sensitive intracellular nanocarriers. The interconversion of thiols and disulfides is a key step in many biological processes. Therefore, a reducing environment is a useful physiological stimulus that can be used as a trigger to disrupt redox-reactive BCP micelles.

Indeed, a number of studies using disulfide bonds have been published and the disulfide-based bioconjugation approach has been a popular conjugation method applied in a variety of DDS. Disulfide groups can also be directly introduced into side chains or backbone of polymers by using an appropriate monomer, initiator, or chain transfer agent (149-151). For instance, Oh's group investigated a novel thiol-responsive degradable micelle system as effective intracellular nanocarriers of anticancer drugs (152). The micelles based on a new amphiphilic block copolymer (ABP) consisting of a hydrophobic polymethacrylate bearing disulfide side groups and hydrophilic PEO. In the presence of GSH, pendant disulfide linkages in micellar cores are cleaved rendering the destabilization of the micellar nanocarriers. Such degradation leads to the enhanced release of encapsulated anticancer drugs in aqueous solutions, as well as in cellular environments. These results suggest that GSH-responsive BCP micelles are interesting candidates as intracellular nanocarriers. Based on the same principle, another controlled DDS was constructed by Chen et al. (153). Utilizing the carboxyl group as an active reaction site, paclitaxel, a chemotherapeutic drug, could be covalently linked to the backbone of a copolymer via a disulfide bond, and the loading content of paclitaxel could reach up to 32 wt%. Furthermore, they proved that the disulfide bond was stable in normal cells, but would be broken in tumor cells. This selective bond scission behavior is potentially useful for reducing the toxic and side effects of chemotherapeutic drugs.

Kataoka and co-workers demonstrated that disulfide reduction could be used to induce morphological transitions of BCP micellar aggregates in solution (154). Micelles with interpolyelectrolyte complexed cores composed of positively and negatively charged chains

contained a PEG corona linked by disulfide bonds. Upon reduction with DTT, the PEG segments were detached from the micelles, leading to a vesicular homopolymer complexes structure. Such uniform and biocompatible nanocapsules with controlled size have many potential applications in drug delivery and gene therapy. It is interesting to notice that the thiol-disulfide chemistry can be utilized not only to destabilize BCP micelles, but also to induce aggregates involving no block copolymers. For examples, Thayumanavan and co-workers demonstrated that supramolecular polymer-surfactant complexes can form micelles susceptible to thiol-induced dissociation (155). In that study, a cationic surfactant was obtained through a polymer decorated with pendant carboxylates attached via disulfides. Upon treatment with GSH, the polymer side chains were cleaved, resulting in micelle dissociation and release of a model hydrophobic compound.

Star, block, and multiblock thiol-responsive copolymers can also be obtained by placing redox-labile linkages at block junction points. For instance, Liu et al. successfully used RAFT to prepare thiol-sensitive biodegradable three-armed star polymers using both “core-first” and “arm-first” methodologies (156). This reported method could be extended to higher-armed structures by selection of appropriate functional cores. Similarly, Sun et al. reported biodegradable micelles based on disulfide-linked PEG-*b*-poly(caprolactone) (PCL) block copolymer and applied the micelles for rapid intracellular release of doxorubicin (DOX) (157). Due to the reductive cleavage of disulfide bonds, the micelles were prone to fast aggregation in the presence of DTT. These biodegradable micelles are highly promising for the efficient intracellular delivery of various lipophilic anticancer drugs to achieve improved cancer therapy. Cerritelli et al. also synthesized a BCP comprised of a hydrophilic PEG block and a hydrophobic poly(propylene sulfide) (PPS) block with an intervening disulfide (158). Under appropriate conditions, the BCP can self-assemble to form vesicles that can be disrupted in the presence of intracellular concentrations of cysteine. This system can be applied for biomolecular drugs delivery. Jeong et al. synthesized a thermo-gelling PEO-*b*-PPO-*b*-PEO (PPO: poly(propylene oxide)) disulfide multiblock copolymer as a thiol-sensitive biodegradable polymer (159). Drug release was significantly faster after treatment with GSH.

Cross-linking of micelle shells has been recognized as an effective approach to stabilizing BCP

micelles, because the chain crosslinking endows micelles with structural integrity (160,161). However, the maintenance of cross-links can act as a barrier to drug release within target cells. Therefore, shell crosslinks should be cleaved to release entrapped drugs. To this regard, the use of disulfide bonds for crosslinking can satisfy both requirements of enhanced structural stability and cell-specific drug release property. For instance, Lee and coworkers reported biocompatible, cell-permeable core-shell-corona BCP micelles bearing GSH-cleavable shell crosslinks, which allows for the release of entrapped anticancer drugs at cytoplasm in response to an intracellular GSH level (162). Zhang et al. also presented a novel reduction-responsive disulfide core-crosslinked micelle based on amphiphilic starch-*g*-PEG for efficient intracellular drug delivery (163). In the presence of reductive GSH, the hydrodynamic radii of disulfide core-crosslinked micelles would increase gradually due to the cleavage of the disulfide bonds in the micelle core. This GSH-responsive behavior is attractive for intracellular drug delivery. Upon exposure to GSH, quick release of payloads could occur.

2. Multi-Stimuli Responsive Polymers

As discussed above, during the past two decades, there have been numerous reports on stimuli-sensitive BCP micellar systems. However, a majority of them deal with response to single stimulus. This may be a limitation because in nature, the change in behavior of a macromolecule is often a result of its response not to a single stimulus, but to a combination of environmental changes. To mimic this important feature, and also to achieve a more complex level of control, design of BCPs whose micellar aggregates can sense specific changes and respond to multiple stimuli in a predictable manner would be of great interest. Therefore, fundamental research is required for engineering BCP structures combined with two or more stimuli responsive moieties, which can make BCPs to respond to stimuli in a parallel, serial or causal manner. The parallel manner means that the response of one group does not affect the response of the other and vice versa. Such BCPs are considered as an orthogonal stimuli-responsive system. The serial manner is common between two stimuli responsive groups. The stimulated response of one group can be followed by the response of the other, in such a way that the effects on the BCP are additive. By contrast, the causal manner interplays between two or more stimuli-responsive groups. One

manifestation is that when a single external stimulus is applied, a cascade of responses will be triggered. Although this interaction makes this manner exceptionally fascinating, examples are rare (164). Generally, if one can introduce different stimuli responsive groups into one polymer, it is exciting to imagine that the impact of an external stimulus can lead to a more pronounced, more specific and more controllable response of the polymer. Hence, the right combination of responsive groups will make it possible to design a multi-functional polymers or BCPs, which exhibit multifaceted behavior when applying one or more external stimuli. For BCP-based DDS, such multi-stimuli-responsive systems offer a great opportunity for fine-tuning their response to each stimulus independently, and for precisely regulating the release profile during the combined effect of multiple stimuli. This is the reason for which in recent years the development of dual- or multi-stimuli-responsive BCP micelles has become an important research topic. Since this is also the main topic of the present thesis, we present below examples of recent progresses on polymers and BCPs with two or more stimuli-responsive groups in their structures.

2.1. Thermo and Ultrasound Dual-Responsive Systems

Due to many distinctive advantages of thermal stimulus, such as easy availability, low-cost and environmental friendliness, it became the most common and used stimulus. Thus, thermo-responsive polymers and BCPs have been among the most studied stimuli-responsive materials. Naturally, to make dual-stimuli-responsive materials, thermosensitivity has often been combined with a second type of stimulus. With the other stimulus being ultrasound, there are very few examples in the literature.

The most notable thermo- and ultrasound- responsive material system, responding in a causal manner, was reported by Xia and coworkers (165). They prepared gold nanocages whose surface had been functionalized with a LCST random copolymer of poly(NIPAAm-*co*-AAm) (AAm: acrylamide). Upon HIFU treatment, the temperature in the focal volume of the sample increases rapidly. When the temperature rises above the LCST of the copolymer, the polymer chains change from a stretched conformation to a collapsed state, making the pores on the nanocages open to release pre-loaded chemicals or drugs. On the contrary, when HIFU is turned off, the temperature

cools down and the polymer chains relax back to their original extended state, blocking the pores and thus stopping the release. With this design, the released dosage can be remotely controlled by adjusting the power and/or the duration of HIFU irradiation.

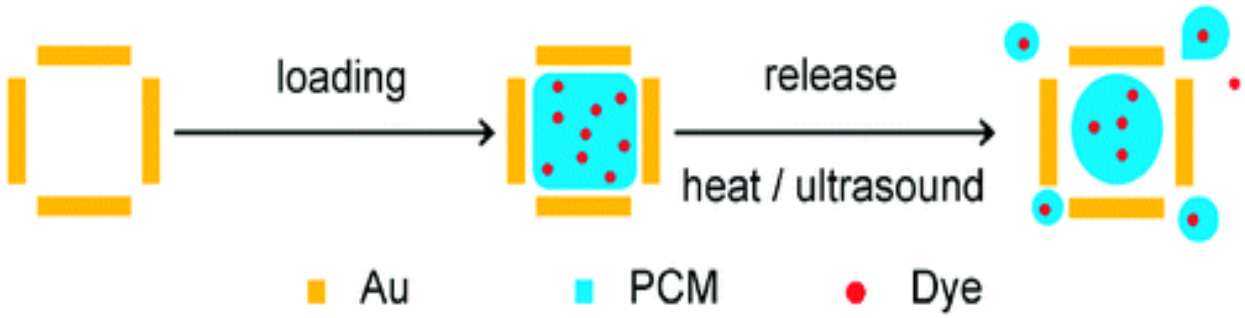

Figure 15. Schematic illustrating how to load the hollow interior of an Au nanocage with a dye-doped PCM and then have it released from the Au nanocage by direct or ultrasonic heating. [166]

Later, the same group reported another version of the thermo- and ultrasound- dual-responsive gold nanocage-based system as shown in Figure 15, by filling the hollow interiors of gold nanocages with a phase-change material (PCM) (166). The PCM can be utilized as a medium to load either hydrophobic or hydrophilic drugs, which also serve as a "gatekeeper" to control the release of drugs in response to temperature increase (167,168). Upon application of HIFU, the PCM can be melted due to ultrasound-induced heating, which allows the encapsulated drug to be released. In this case, at temperatures below the melting point, the PCM in the solid state can confine drug molecules inside gold nanocages. But when the local temperature is raised beyond the melting point of the PCM, it is melted into the liquid state, which allows the drug to be released into the surrounding medium from the melted PCM through diffusion. Thus, the new system should allow regulating the release of a drug and the release profile by controlling the temperature determined by HIFU. As long as the payload is miscible with the PCM phase, it can be conveniently loaded as its mixture with the PCM diffuses into hollow interiors of the gold nanocages.

2.2. Thermo and Light Dual-Responsive Systems

Thermo- and light dual-responsive polymers have also been investigated and applied for biomedical applications. The motivation of combining thermosensitivity with light is to provide the spatial and temporal control of the activation. An early example was reported by Kungwatchakun et al. in 1988 (169). They synthesized a random copolymer of NIPAM and N-(4-phenylazophenyl) acrylamide. By simply incorporating a number of azobenzene moieties into this LCST polymer, they showed that PNIPAM, precisely the phase transition temperature of the aqueous solution of PNIPAM could be altered by the photoisomerization of the chromophore. Upon UV light irradiation, as a result of the trans-cis isomerisation of azobenzene moieties, the phase transition temperature shifted to a higher temperature. The initial LCST could be recovered by visible light irradiation converting the cis isomer back to the trans form. Thanks to this seminal work, many studies of thermo-responsive polymers containing azobenzene moieties have been conducted, exploiting the possible photocontrol of the LCST (170-174). For instance, a recent report introduced a photo- and thermo-dual-responsive azobenzene-containing oligo-(ethylene glycol) methacrylate (OEGMA) brushes on silicon substrates (175). In this case, based on the photocontrollable water solubility of the polymer chains, the swelling degree of the brushes in water could be reversibly modulated by photoisomerization of the azobenzene moieties under alternating UV and visible light irradiation.

Many groups including ours have also studied photo- and thermo-dual-responsive BCP materials. In one of our reports (176), the LCST behavior and light-responsiveness of a diblock copolymer, PEO-*b*-P(MEO_2MA-*co*-CMA), were utilized to prepare photoresponsive nanogels via a micellar approach. At T > LCST of the,hydrophobic P(MEO_2MA-*co*-CMA) block, micelles are formed; nanogels can easily be prepared by photo-crosslinking the micelle core through dimerization of coumarin groups, followed by cooling the solution down to T<LCST. Upon exposure to UV light $\lambda < 260$ nm, the reverse photocleavage of cyclobutane rings can reduce the crosslinking density resulting in enhanced swelling of the nanogel particles. The reversibility of the photoinduced volume change of the nanogels was used to demonstrate optical control in the release of loaded guest molecules. In another study using photo-crosslinkable and thermosensitive BCPs, polymer

vesicles in aqueous solution could readily be prepared (177). The vesicular particles can undergo temperature-controlled large, reversible, and fast volume transition in aqueous solution by switching the water solubility of the vesicle membrane via the LCST.

2.3. Thermo and Redox Dual-Responsive Systems

Polymers exhibiting both thermo- and redox- sensitivity are appealing because the two stimuli of temperature variation and changing redox can exist naturally in certain pathological sites as well as in cancer cells. It is no surprise that researchers have been interested in developing materials that are responsive to both stimuli. Phillips et al. presented this type of dual-responsive polymers based on PNIPAM (178-179). By linking disulfide units to PNIPAM, the presence of GSH can cleave disulfides leading to PNIPAM fragments. Due to the molecular weight-dependent of the LCST, the thermosensitivity of PNIPAM can thus be changed by a GSH gradient. In this case, the two stimuli have a causal impact. Similarly, Oupicky and co-workers also reported a thermo and redox dual-responsive diblock copolymer made from PNIPAM and PDMAEMA blocks with disulfide bridge between them (180).

Other groups reported PNIPAM-based dual-responsive nanogels. For instance, Morimoto et al. prepared nanogels from pullulan lightly grafted with thiol-terminated PNIPAM chains whose chain ends were crosslinked through disulfide bonds at 50 °C (181). The resulting nanogels could be destructed either upon cooling to room temperature and/or upon treatment with a reducing agent. In a similar way, dual-responsive nanogels were also obtained by using dextran grafted with thiol-terminated PNIPAM (182), and thiolated hydroxypropyl cellulose (183). You et al. obtained core-shell nanoparticles based on a redox-sensitive hyperbranched poly(amido amine) core and thermo-sensitive PNIPAM shell (184). In that case, the polymer particles can have their sizes changed reversibly by varying the solution temperature and their payloads released by addition of DTT. The system responds to the two stimuli in a parallel manner.

By increasing aqueous solution temperature of PEG-*b*-PAA-*b*-PNIPAM triblock copolymers to above the LCST of PNIPAM and subsequent crosslinking with cystamine via carbodiimide chemistry, Zhong et al. obtained thermo- and redox dual-responsive crosslinked polymersomes

(185,186). Owning to the crosslinking, polymersomes were found to be stable against dilution, organic solvent, high salt conditions or change of temperature in water. However, they were rapidly dissociated under reductive conditions mimicking the intracellular environment. One more special example of the systems that respond to the two stimuli in a serial manner is an alkylacrylamide-based BCP bearing vinylferrocene moieties; the LCST of the polymer can be reversibly increased by transferring into the hydrophilic cationic state (187).

3. Objectives of the Thesis

The main objective of this thesis is to make contributions to our fundamental knowledge and understanding about dual-stimuli-responsive BCP micelles. Our approach is to synthesize BCPs based on rational structural design toward a specific new approach or mechanism, to make them self-assemble into micellar structures, to study the effect of the stimuli on the micelles and, at the same time, explore their potential use as nanocarriers for stimuli-controlled drug delivery. The research works presented in this thesis can be divided into two parts. In the first part, Chapters 1 and 2, our studies aim at developing a new approach for rendering BCP micelles sensitive to ultrasounds, more specifically to HIFU. The basic idea is to prepare an amphiphilic diblock copolymer of which the hydrophobic block is a LCST polymer bearing ultrasound-labile co-monomer units. Upon HIFU irradiation, the co-monomer units are expected to undergo a reaction and increase its polarity. If this happens, the LCST may be shifted above the solution temperature resulting in BCP micelle dissolution.

To achieve this purpose, in the first project, discussed in Chapter 1, we tried to find such a HIFU-labile co-monomer. A series of amphiphilic BCPs with different hydrophobic blocks of polymethacrylayes were synthesized and the reaction of their micelles to HIFU irradiation was investigated. The comparative study allowed us to identify the one relatively most reactive to the ultrasound, namely, poly(2-tetrahydropyranyl methacrylate) (PTHPMA). In the second project that followed, detailed in Chapter 2, we synthesized a model diblock copolymer having one block displaying LCST and containing THPMA co-monomer units. We found that the BCP forms micelles at solution temperature above LCST, and that the micelles can be dissociated under HIFU

irradiation inducing hydrolysis of THPMA. This work demonstrates the validity of the new approach for developing ultrasound-responsive BCP micelles.

The second part of this thesis, presented in Chapter 3, deals with a new light and redox dual-stimuli-responsible copolymer. The project has a specific purpose: developing a BCP structural design that allows the micelles to respond to exposure of both light and a reducing medium, while having the minimum number of photo- and redox- reactive groups per chain of the BCP. We proposed and investigated a strategy that consists in making an amphiphilic ABC-type triblock copolymer that contains a redox-cleavable linkage at the junction of the A and B blocks as well as a photo-cleavable junction unit between the B and C blocks. Our study demonstrates the efficiency of this BCP design for endowing the BCP micelles with dual-stimuli-responsiveness by using few stimuli-reactive moieties, which is of both fundamental and applied interest.

In Chapter 4, we concluded our studies and discussed a number of future works that are worth being pursued.

CHAPTER 1. ULTRASOUND-INDUCED DISRUPTION OF AMPHIPHILIC BLOCK COPOLYMER MICELLES

1.1. About the Project

As an external stimulus, ultrasound has not been much exploited as a trigger for stimuli-responsive BCP micelles as compared to, for example, the use of pH or temperature change or even light. And yet ultrasound may have some unique advantages over other types of stimuli, in particular with high-frequency diagnostic high-intensity focused ultrasound (HIFU). In addition to the temporal and spatial control by selecting the time of ultrasound application and the place where the focus of the ultrasound beams is located, ultrasound can easily penetrate deep through the tissue in the body, in contrast with light that does have the time and location selectivity, but a limited penetration depth. An important challenge is to develop polymer micelles that can be disrupted effectively by HIFU that is harmless to healthy cells and tissues (thus more suitable for drug delivery), but has a weaker cavitation effect than low-frequency power ultrasound. To achieve this goal, systematic investigations are required to unveil and understand the effect of BCP chemical structures on the disruption of micelles to ultrasound irradiation. This would be a first step toward rationally designed BCP micelles for HIFU-controllable micellar disruption and release of loaded drugs. Therefore, in the present study, we synthesized a series of four BCPs that have the same hydrophilic block but differ in the micelle-core-forming hydrophobic polymethacrylate block. We conducted a comparative study on the disruption of their micelles by high-frequency HIFU under the same conditions, with the purpose of identifying a monomer structure that is more susceptible to HIFU-induced reactions.

This work was published in *Macromolecular Chemistry and Physics* **2011**, *212*, 498-506 by Juan Xuan, Maxime Pelletier, Hesheng Xia and Yue Zhao. This research work was conducted in the Université de Sherbrooke and Sichuan University under the supervision of Prof. Zhao and co-supervision of Prof. Xia. The block copolymer samples were synthesized by Maxime Pelletier. I performed all the other experiments reported in this publication. I wrote the first draft of the manuscript. Prof. Zhao finalized the manuscript with revision contributions from Prof. Xia.

1.2. Paper Published in Macromolecular Chemistry and Physics 2011, 212, 498

Ultrasound-Induced Disruption of Amphiphilic Block Copolymer Micelles

Juan Xuan,[1] Maxime Pelletier,[2] Hesheng Xia,[1,*] Yue Zhao[2,*]

[1] State Key Laboratory of Polymer Materials Engineering, Polymer Research Institute, Sichuan University, Chengdu 610065

[2] Département de chimie, Université de Sherbrooke, Sherbrooke, Québec, J1K 2R1, Canada,

* Corresponding authors: xiahs@scu.edu.cn; yue.zhao@usherbrooke.ca

1.2.1. Abstract

Ultrasound-induced disruption of block copolymer micelles in aqueous solution was investigated. Four amphiphilic block copolymers (BCPs) composed of a hydrophilic block of poly(ethylene oxide) (PEO) and different hydrophobic blocks of polymethacrylayes were used in this study, which are 1) PEO-*b*-PTHPMA, PTHPMA being poly(2-tetrahydropyranyl methacrylate), 2) PEO-*b*-PIBMA, PIBMA being poly(1-(isobutoxy)ethyl methacrylate), 3) PEO-*b*-PTHFEMA, PTHFEMA being poly((2-tetrahydrofuranyloxy)ethyl methacrylate) and 4) PEO-*b*-PMMA, PMMA being poly(methyl methacrylate). Under the same conditions (pH 7, same ultrasound power, micellar solution volume and irradiation time), combined characterization results of fluorescence change of loaded Nile Red (NR), dynamic light scattering, infrared spectroscopy, atomic force and scanning electron microscopy show that those micelles, differing in the chemical structure of the micelle-core-forming polymethacrylate, could be disrupted differently by high-frequency (1.1 MHz) high-intensity focused ultrasound (HIFU) beams. Of the used BCPs, micelles of PEO-*b*-PIBMA and PEO-*b*-PTHPMA, whose polymethacrylates bear a labile acetal unit and are much less stable than the two other BCPs, appear to be more sensitive to ultrasound irradiation resulting in a more severe micellar disruption and; infrared spectra recorded after HIFU irradiation of their micellar solutions show evidence of ultrasound-induced chemical reactions, most likely hydrolysis. By contrast, micelles of PEO-*b*-PMMA, with the more stable polymethacrylate block, appear to resist better HIFU irradiation, while infrared analysis found no evidence of chemical reactions. Moreover, the effects of adjusting the focal area of HIFU beams and ultrasound power on BCP micellar disruption were also investigated and discussed. This study provides new evidence for the interest of developing ultrasound-responsive BCP micelles for controlled delivery applications.

1.2.2. Introduction

In the research and development of stimuli-responsive block copolymer (BCP) micelles for controlled delivery applications, to date the use of ultrasound[1] as an external stimulus has been less explored as compared to the use of pH[2] or temperature[3] or even light.[4] And yet ultrasound

may have some unique advantages over other types of stimuli, in particular with focused, high-frequency diagnostic ultrasound. In addition to possible temporal and spatial control by selecting the time of ultrasound application and the place of its action (around the focal region of the sound beams), ultrasound can easily penetrate deep in the body, in contrast with light that does have the time and location selectivity, but a limited penetration depth.[5] Generally, the disruption of BCP micelles by ultrasound is believed to originate from some thermal and hydrodynamic shear effects associated with the acoustic cavitation phenomenon in solution (formation, growth and collapse of micrometer-sized bubbles).[6] An important challenge is to develop polymer micelles that can be disrupted effectively by high-frequency, high-intensity focused ultrasound (HIFU) that is harmless to healthy cells and tissues (thus more suitable for drug delivery), but has a weaker cavitation effect than low-frequency power ultrasound. To achieve this goal, systematic investigations are required to unveil and understand the effect of BCP chemical structures on the reaction of micelles to ultrasound irradiation. This would be a first step toward rationally designed BCP micelles for HIFU-controllable micellar disruption and release of loaded guest molecules.

In a previous study,[7] we found that micelles of an amphiphilic diblock copolymer comprised of poly(ethylene oxide) and poly(2-tetrahydropyranyl methacrylate) (PEO-*b*-PTHPMA) could be disrupted by high-frequency HIFU (1.1 MHz). The micellar disruption in aqueous solution was evidenced by the characterization results obtained with dynamic light scattering, atomic force microscopy, fluorescence and infrared spectroscopy. Although the hypothesis of hydrolysis was supported by an infrared analysis,[7] the observed decrease in pH upon ultrasound expose could be a reaction of water under certain conditions.[8] As a continuing effort on ultrasound-sensitive BCP micelles, in the present work, we have synthesized three new diblock copolymers in addition to PEO-*b*-PTHPMA, which are poly(ethylene oxide)-*block*-poly(1-(isobutoxy)ethyl methacrylate) (PEO-*b*-PIBMA), poly(ethylene oxide)-*block*-poly((2-tetrahydrofuranyloxy)ethyl methacrylate) (PEO-*b*-PTHFEMA) and poly(ethylene oxide-*block*-poly(methyl methacrylate) (PEO-*b*-PMMA). Using the four BCPs that differ in the micelle-core-forming hydrophobic polymethacrylate block, we conducted a comparative study on disruption of their micelles by high-frequency HIFU under well controlled conditions with no change in pH (buffer solutions at pH=7). The chemical structures of the BCPs are shown in Figure 1-1, together with the acronyms and the BCP

compositions as determined by ^{1}H NMR. While PTHPMA has a tetrahydropyrane ring linked to the ester group, PTHFEMA has a tetrahydrofurane ring with an ethoxy spacer, PIBMA isobuthyl ether and PMMA a methyl group. The results reported herein show that all BCP micelles could be disrupted by high-frequency HIFU, but the extent of disruption appears to be influenced by the chemical structure of the hydrophobic block, as revealed by the characterization results.

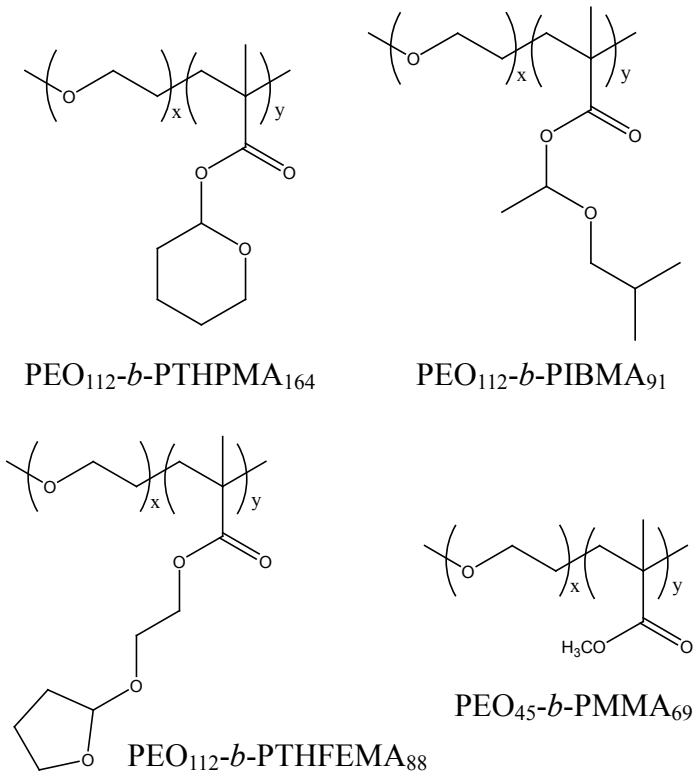

Figure 1-1. Chemical structures, acronyms and compositions of the used amphiphilic block copolymers.

1.2.3. Experimental

Synthesis of Diblock Copolymers

Materials. Dichloromethane (99%) was purified by distillation from calcium hydride. All the monomers were purified by passing through a column of basic aluminum oxide before use. 2-Hydroxyethyl methacrylate (98%), 2,3-dihydrofuran (99%), isobutyl vinyl ether (99%),

poly(4-vinylpyridine hydrochloride), phenothiazine, sodium carbonate anhydrous, calcium hydride, N,N,N`,N``,N``-pentamethyldiethylenetriamine (PMDETA, 99%), copper(I) chloride (Cu(I)Cl, 98%) were purchased from Aldrich and used without further purification. The synthesis of PEO-*b*-PTHPMA was reported previously.[9] Detailed below are the syntheses of PEO-*b*-PIBMA and PEO-*b*-PTHFEMA using atom transfer radical polymerization (ATRP) and their respective methacrylate monomer. PEO-*b*-PMMA is a well-known block copolymer; its synthesis using ATRP will not be described here.

Synthesis of 1-(isobutoxy)ethyl methacrylate (IBMA). Methacrylic acid (4.0 g, 46.5 mmol), isobuthyl vinyl ether (9.3 g, 93.0 mmol), P4VP.HCl (168 mg, 1.1 mmol) and phenothiazine (15 mg, inhibitor) were mixed in a round-bottom flask. The mixture was then heated to 70 ^{o}C overnight. The mixture was filtered to remove P4VP.HCl and phenothiazine (15 mg, inhibitor); then Na_2CO_3 (500 mg, 4.7 mmol) and CaH (500 mg, 11.9 mmol) were added carefully. After concentration in a rotary evaporator, the solution was distilled under reduced pressure at 25 ^{o}C (water bath) to give a transparent liquid (4.1g, yield 48%).^{1}H NMR ($CDCl_3$) (ppm): 6.13 (s, 1H, -CH_2CC-), 5.95 (q, 1H, -OCHO-), 5.56 (s, 1H, -CH_2CC-), 3.32 (m, 2H, -$CH_2CH(CH_3)_2$-), 1.95 (s, 3H, -CH3CCO-), 1.85 (s, 1H, -$CH(CH_3)_2$-), 1.46 (d, 3H, -CH_3CHO-), 0.91 (d, 6H, -$(CH_3)_2$CH-).

Synthesis of (2-tetrahydrofuranyloxy)ethyl methacrylate (THFEMA). 2-Hydroxyethyl methacrylate (3.0 g, 23.0 mmol), 2,3-dihydrofuran (3.2 g, 45.7 mmol), poly(4-vinylpyridine hydrochloride) (P4VP.HCl) (77 mg, 0.5 mmol) and phenothiazine (10 mg, inhibiter) were charged in a round-bottom flask. The solution was heated to 70 ^{o}C and stirred overnight. Afterward, the mixture was filtered to remove P4VP.HCl. Before distillation, phenothiazine (10 mg, inhibiter), Na_2CO_3 (500 mg, 4.7 mmol) and CaH (500 mg, 11.9 mmol) were added. The excess of 2,3-dihydrofuran was removed by evaporation under reduced pressure. Finally, the solution was distilled under reduced pressure at 30 ^{o}C to give a transparent liquid (4.1 g, yield 90%) ^{1}H NMR ($CDCl_3$)(ppm): 6.13 (s, 1H, -CH_2CC-), 5.56 (s, 1H, -CH_2CC-), 5.10 (t, 1H, -OCHO-), 4.22 (m, 2H, -CH_2CH_2O-), 3.85 (m, 2H, -CH_2OCH-), 3.60 (m, 2H, -$CH_2CH_2CH_2$CH-), 1.85 (7H, CH_3C, CH_2CH_2CH).

Synthesis of diblock copolymer PEO-*b*-PIBMA. Bromine end–capped PEO macroinitiator with a molecular weight of 5000 g mol^{-1}, designated as PEO_{112}-Br, was prepared following a literature method.[10] IBMA (744 mg, 4.00 mmol), PMDETA (41.6 mg, 0.24 mmol) and Cu(I)Cl (11.9 mg, 0.12 mmol) were added to a solution of PEO_{112}-Br (400 mg, 0.079 mmol) dissolved in anisole (700 mg). The reaction mixture placed in a flask was degassed three times using the freeze-pump-thaw procedure. After 30 min of stirring at room temperature, it was immersed in a preheated oil bath at 50 ^{o}C for 2 h. Afterward, the mixture was passed through a neutral Al_2O_3 column with dichloromethane as eluent to remove the catalyst. The solution was concentrated upon solvent evaporation under reduced pressure and then precipitated twice in cold ether (ice bath). A white powder of the diblock copolymer (469 mg, yield 41%) was collected by filtration and dried in a vacuum oven. The reaction gave the sample PEO_{112}-*b*-$PIBMA_{91}$ whose composition was determined from the ^{1}H NMR spectrum by comparing the integrals of the resonance peaks of PEO (3.73 ppm) and PIBMA (5.65 ppm). ^{1}H NMR ($CDCl_3$) (ppm): 5.65 (broad, 1H, -OCHO-), 3.73 (broad, 4H, CH_2CH_2O), 3.35 (m, 2H, -$CH_2CH(CH_3)_2$-), 1.95 (m, 1H, -$CH(CH_3)_2$-), 1.35 (broad, 3H, -CH_3CHO-), 0.91 (broad, 6H, -$(CH_3)_2CH$-). M_n (^{1}H NMR)= 22000 g mol^{-1}, M_n (GPC)= 31000 g mol^{-1}, M_w/M_n=1.23

Synthesis of diblock copolymer PEO-*b*-PTHFEMA. THFEMA (856 mg, 4.00 mmol), PMDETA (41.6 mg, 0.24 mmol) and Cu(I)Cl (11.9 mg, 0.12 mmol) were added to a solution of PEO_{112}-Br (400 mg, 0.079 mmol) dissolved in anisole (800 mg). The reactive mixture placed in a flask was degassed three times using the freeze-pump-thaw procedure. After 30 min of stirring at room temperature, it was immersed in a preheated oil bath at 50 ^{o}C for 2 h. Then, the mixture was passed through a neutral Al_2O_3 column with dichloromethane as eluent to remove the catalyst. After concentration of the solution by solvent evaporation under reduced pressure, the polymer was precipitated from the dichloromethane solution in cold ether (dry ice bath), and the purification was repeated once. A white powder of diblock copolymer (376 mg, yield 30%) was collected by filtration and dried in a vacuum oven. The reaction gave the sample PEO_{112}-*b*-$PTHFEMA_{88}$, whose composition was determined from the ^{1}H NMR spectrum by comparing the integrals of the resonance peaks of PEO (3.73ppm) and PTHFEMA (5.10 ppm). ^{1}H NMR ($CDCl_3$)(ppm): 5.10 (broad, 1H, -OCHO-), 4.22 (m, 2H, -CH_2CH_2O-), 3.85 (m, 2H,

-CH_2OCH-), 3.73 (broad, 4H, CH_2CH_2O), 3.60 (m, 2H, -$CH_2CH_2CH_2CH$-), 1.85 (7H, CH_3C, CH_2CH_2CH) M_n (^{1}H NMR)= 23000 g mol^{-1}, M_n (GPC)= 33000 g mol^{-1}, M_w/M_n=1.19

Micelle Preparation and Ultrasound Irradiation

Basically the same micelle preparation and ultrasound irradiation procedures as in the previous report [7] were utilized in the present work. Precaution was taken to ensure that micelles of the four BCPs (with or without loaded Nile Red) were prepared and subjected to ultrasound irradiation under exactly the same conditions. To separate the possible effect of a pH change on the micellar disruption (hydrolysis at acidic pH, for instance) from the ultrasound action, comparisons of all the BCPs were made using their micelles in buffer solutions at pH 7. For micelle preparation, briefly, a BCP sample (3.0 mg) was dissolved in THF (4.6 mL) before water was added first slowly (1.2 mL) and then quickly (1.0 mL) to induce micelle formation. The micellar solution was then diluted by water and after removal of THF by evaporation at 45 ^{o}C for 24 h, an initial polymer concentration of 0.15 mg/mL was obtained. To load Nile Red (NR) in the micelles, which is a model hydrophobic compound, the same procedure was used except that the THF solution contained both dissolved BCP and the hydrophobic dye (0.1 mg/mL); upon addition of water, the aggregation of the hydrophobic block allowed some NR molecules to be solubilized by polymer chains forming the core of micelle. During the removal of THF, unloaded NR was precipitated in aqueous solution and removed by filtration using a 0.22 μm membrane.

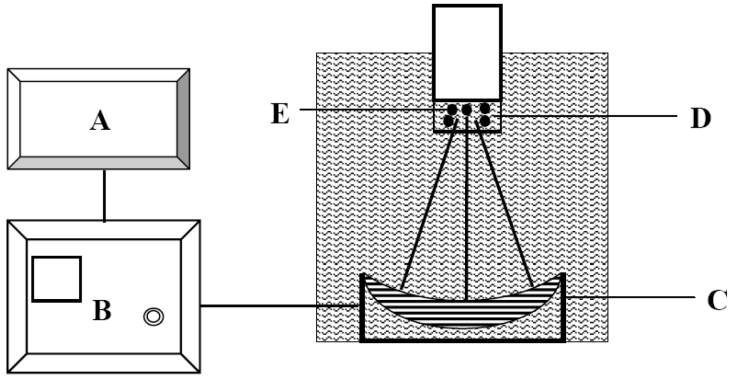

Figure 1-2. Experimental setup with a schematic diagram of the high-frequency high-intensity focused ultrasound apparatus: arbitrary waveform generator (A), radio-frequency power amplifier

(B), acoustic lens transducer (C), water bath (D) and polymer micelles (E).

In the present study, high-frequency HIFU irradiation was generated by a commercially available ultrasound apparatus that comprises three main components: an arbitrary waveform generator (Agilent 33220A Function Generator), a RF power amplifier (A150, Electronics & Innovation) and an acoustic lens transducer (H-101, Sonic Concept, USA). As schematized in Figure 1-2, the acoustic lens transducer could generate focused ultrasound beams of adjustable power (up to 100W) at a high frequency (1.1 MHz). The focal spot has a circular diameter of ~ 1.26 mm and a height of ~ 11 mm, and the focal length is about 63 mm. In all ultrasound irradiation experiments, the focal spot of the beams were set at the center of the micellar solution (5 mL) placed in a tube reactor immersed in a water tank, unless otherwise stated. After a certain time of ultrasound irradiation, the tube reactor was removed from the water tank and the micellar solution was used for characterizations at room temperature, the irradiation time being cumulative. We mention here that based on change in fluorescence of loaded Nile Red, this ultrasound system is more efficient than a home-built apparatus utilized in our previous work,,[7] allowing the use of smaller ultrasound powers in the present study.

Characterizations

The fluorescence of Nile Red (NR) entrapped in BCP micelles was used to probe the ultrasound-induced micellar disruption as it is sensitive to the polarity of the environment in which the dye is located.[11] For these measurements, a fluorescence spectrophotometer (970CRT, Shanghai Precision & Scientific Instrument) was used, with the excitation wavelength set at 540 nm. Unless otherwise stated, excitation and emission slit were set to 5 and 10 nm respectively. Direct evidence for perturbation of BCP micelles in solution could be obtained by using dynamic light scattering (DLS) that measures the average hydrodynamic diameter (D_H) and the size distribution of micellar aggregates, as well as the scattering intensity. DLS measurements were performed on a Brookhaven BI-200 goniometer with vertically polarized incident light of wavelength λ=532 nm supplied by an argon laser operating at 400 mW, and a Brookhaven

BI-9000 digital autocorrelator. All measurements were carried out at 25°C at a scattering angle of 90°, with the autocorrelation functions analyzed by using the non-negatively constrained least square algorithm. Unless otherwise stated, only the initial micellar solution prior to ultrasound irradiation was microfiltered through a 0.22 μm membrane. Using a Nicolet 560 Fourier transform infrared (FTIR) spectrometer, infrared spectra of the samples prepared from ultrasound-irradiated micellar solutions were recorded at room temperature. To prepare the samples used for the infrared analysis, micellar solutions after ultrasound irradiation were first dried under vacuum at 40 °C to remove water, then redissolved in THF and finally cast on a KBr window and dried. Moreover, atomic force microscopy (AFM, NanoScope MultiMode IIIa) and scanning electron microscopy (SEM, Inspect F, Philips) were used to observe the micellar aggregates in dried state. The samples were obtained by casting a drop of the micellar solution on clean mica, followed by drying.

1.2.4. Results and Discussion

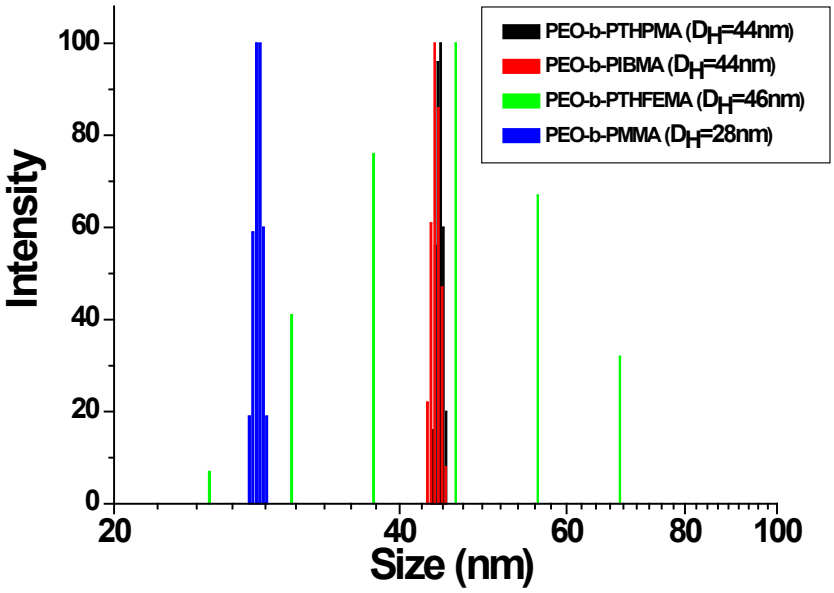

Figure 1-3. Size distributions of different BCP micelles in aqueous solution as revealed by DLS (the average hydrodynamic diameters are indicated in the figure).

The formation of micelles by the four amphiphilic BCPs under the same preparation conditions

(Experimental section) was first examined. Figure 1-3 shows the intensity-averaged size distributions for all samples in aqueous solution as measured by DLS. Though they all self-assemble into micellar aggregates, their average sizes and size distributions are different. Of them, PEO-*b*-PMMA form small micelles with average D_H ~ 28 nm, while the three others give rise to micellar aggregates of larger sizes in the range of 40-50 nm, with PEO-*b*-PTHFEMA exhibiting a much wider distribution of D_H than the other BCPs. This observation is not surprising, since these BCPs have different hydrophobic blocks, and thus different amphiphilicity with respect to the PEO block. The shorter PEO block for the PEO-*b*-PMMA sample may also account for the smaller micelles.

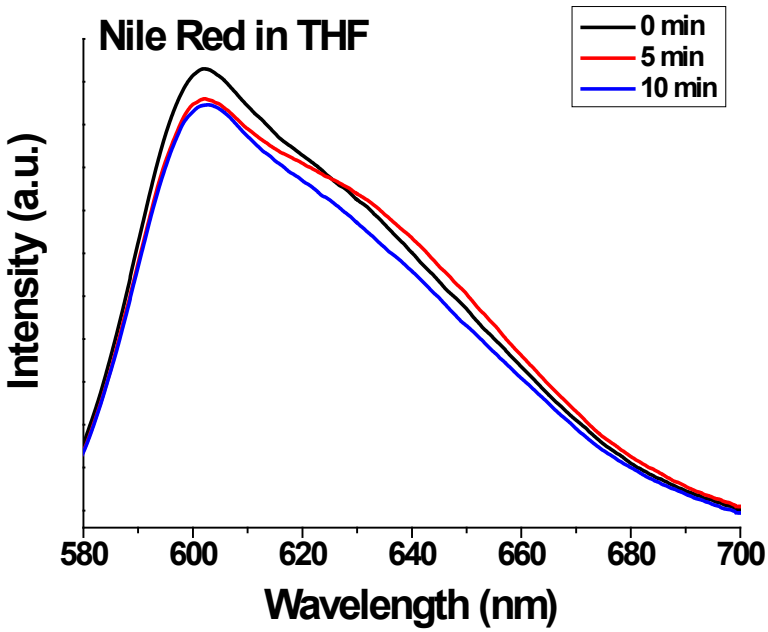

Figure 1-4. Fluorescence emission spectra of Nile Red dissolved in THF (excitation: 540 nm) recorded before (0 min) and after exposure to ultrasound irradiation (5 and 10 min) (ultrasound power: 40 W, solution volume: 5 mL).

NR solubilized by BCP micelles emits fluorescence whose change can be used as a probe to detect micellar disruption.[11] For micelles in aqueous solution, a quenching of fluorescence can be observed if NR is released or exposed to water, in which it is insoluble and can aggregate, as a result of stimuli-induced dissociation or swelling of micelles.[9,11] Before using the fluorescence of

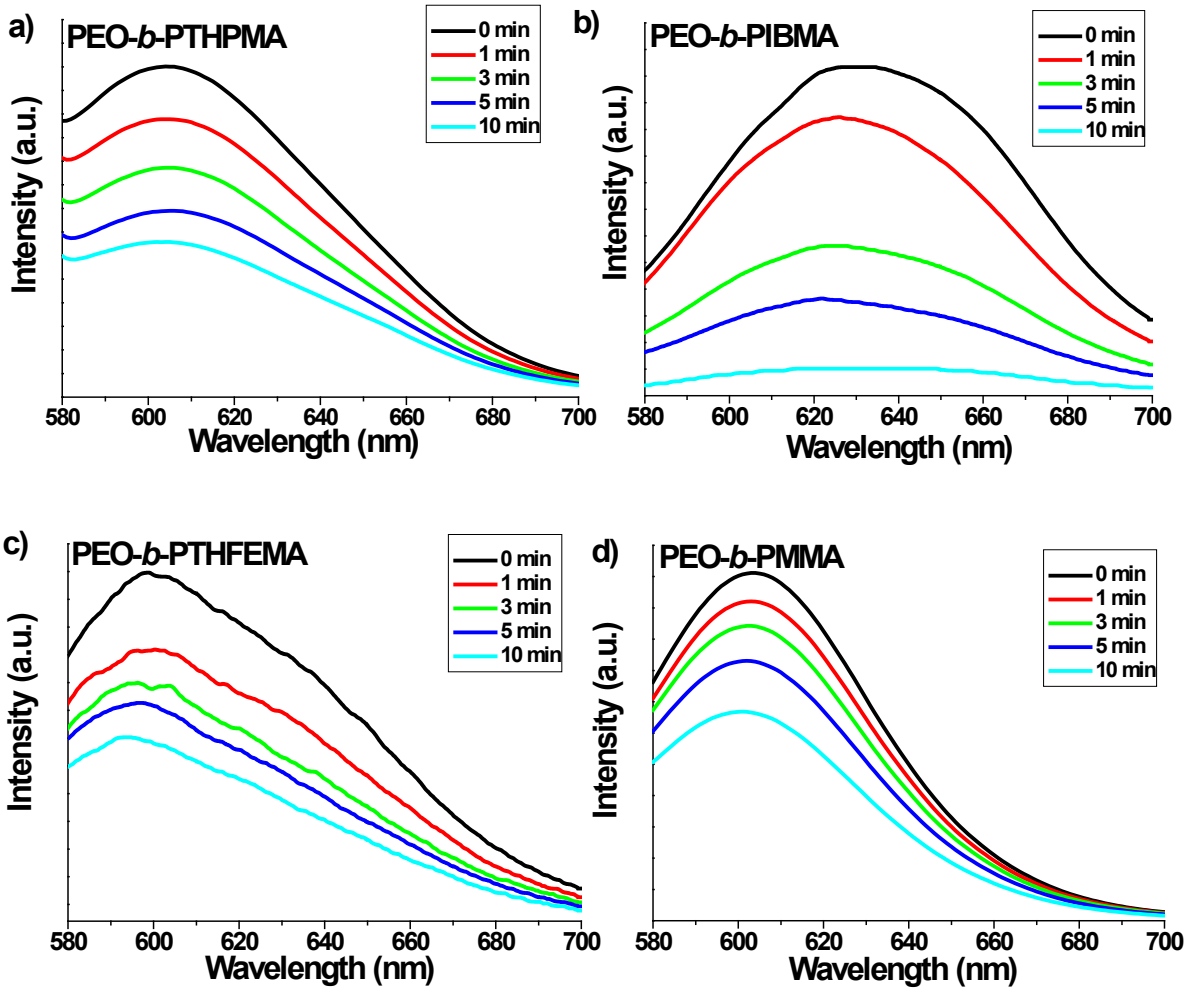

Figure 1-5. Fluorescence emission spectra of Nile Red-loaded BCP micelles (excitation: 540 nm) recorded at different ultrasound irradiation times for (a) PEO-*b*-PTHPMA, (b) PEO-*b*-PIBMA, (c) PEO-*b*-PTHFEMA and (d) PEO-*b*-PMMA, all experiments being carried out under the same conditions (ultrasound power: 40 W, micellar solution volume: 5 mL).

NR to monitor ultrasound-induced disruption of BCP micelles, we performed control tests to make sure that under the used experimental conditions, the high-frequency HIFU causes no degradation of NR resulting in decrease of its fluorescence intensity. Figure 1-4 shows the result obtained by dissolving NR in THF. Only a slight fluorescence decrease can be noticed after 5 or 10 min irradiation at an ultrasound power of 40 W, suggesting that the used ultrasound beams could not degrade seriously NR in solution. By contrast, significant changes were observed for NR-loaded micellar solutions of the four BCPs subjected to high-frequency HIFU at a power of 40W. Figure

1-5 shows their fluorescence emission spectra recorded at different ultrasound irradiation times. In all cases, the intensity decreases with increasing the cumulative irradiation time. Considering the result of the control test in Figure 1-4, the large decrease in the fluorescence intensity of NR should be the consequence of BCP micellar disruption by the ultrasound, bringing an increased amount of NR into contact with water that quenches the fluorescence of the dye. On the other hand, the emission spectra of NR loaded in the four BCP micelles display different shapes and emission maximums, which reflect different polarities of the micelle cores sensed by NR molecules.

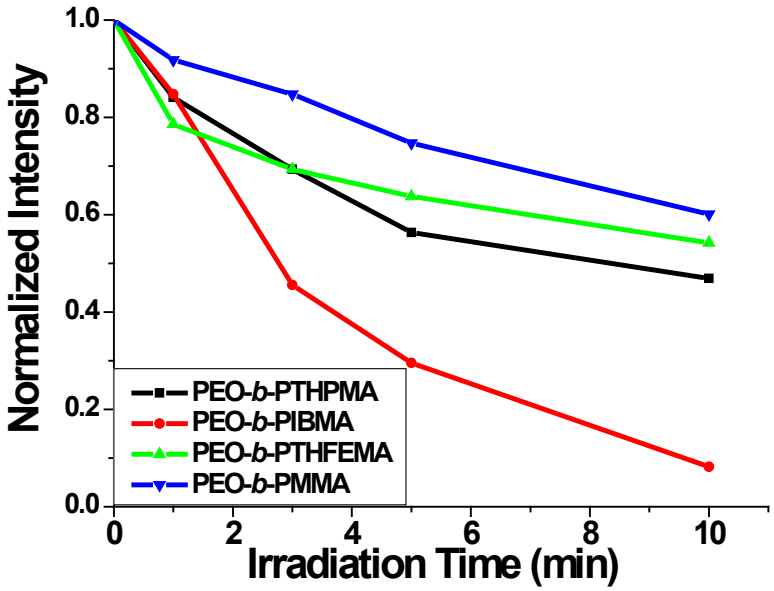

Figure 1-6. Normalized fluorescence emission intensity of Nile Red vs. ultrasound irradiation time for various BCP micellar solutions, using data in Figure 1-4 with the intensity measured at the respective emission maximum of each BCP.

To better compare the kinetics of apparent release of NR with different BCPs, shown in Figure 1-6 are the normalized emission intensity (measured at their respective emission maximum) vs. ultrasound irradiation time. It is seen that PEO-*b*-PIBMA displays the fastest NR fluorescence decrease than the others, presumably due to a greater disruption of micelles in response to ultrasound waves; whereas the change rate with micelles of PEO-*b*-PMMA is the slowest. These results show that all the BCP micelles, having a polymethacrylate core, could be more or less

disrupted by ultrasound irradiation. The chemical structure of the hydrophobic micelle-core-forming polymer appears to affect the extent of disruption and the rate of the apparent release of NR. A qualitative assessment of the NR loading capacity by the four BCP micelles is worth being mentioned. Under the same preparation conditions, and based on the fluorescence intensity, PEO-*b*-PMMA appears to solubilize the most of NR, which is followed by, in the decreasing order, PEO-*b*-PTHFEMA, PEO-*b*-PIBMA and PEO-*b*-PTHPMA.

The disruption of the BCP micelles by ultrasound was confirmed by DLS, AFM and SEM. Figure 1-7 shows the DLS results of all BCP micellar solutions subjected to ultrasound irradiation (40 W). Although no clear common trend for the evolution of size distribution over irradiation time can be observed, it is clear that ultrasound could disrupt the initial BCP micelles quickly in all the solutions, and that disrupted micelles become less stable in aqueous solution and coalesce into larger aggregates. In all cases except PEO-*b*-PMMA, 1 min HIFU irradiation is enough to change quite drastically the sizes of the aggregates, with apparently the formation of larger aggregates than the initial ones and an increased polydispersity (Fig.1-7a-1-7c). As the irradiation went on, their sizes undergo a continuous change, with, in some cases, the appearance of some smaller aggregates. The micelles of PEO-*b*-PMMA seem to be more resistant to ultrasound; larger aggregates were formed only after irradiation longer than 3 min (Fig.1-7d). By plotting the average D_H vs. irradiation time, the differences between the four BCPs become clear. Much larger aggregates are formed upon ultrasound exposure for BCP solutions of PEO-*b*-PTHFEMA and PEO-*b*-PIBMA than with PEO-*b*-PTHPMA and PEO-*b*-PMMA (Fig.1-7e). For the former two BCPs, the average size of their aggregates increases first over the first 3-5 min of irradiation, before decreasing at longer times. The changes in light scattering intensity (measured at 90^o) essentially echo the changes in the average size of the aggregates (Fig.1-7f). It is interesting to notice that the less ultrasound-sensitive micelles of PEO-*b*-PMMA show no significant size change within the first 3 min of irradiation, which corroborates with the slower ultrasound-induced fluorescence change of NR (Fig.1-6).

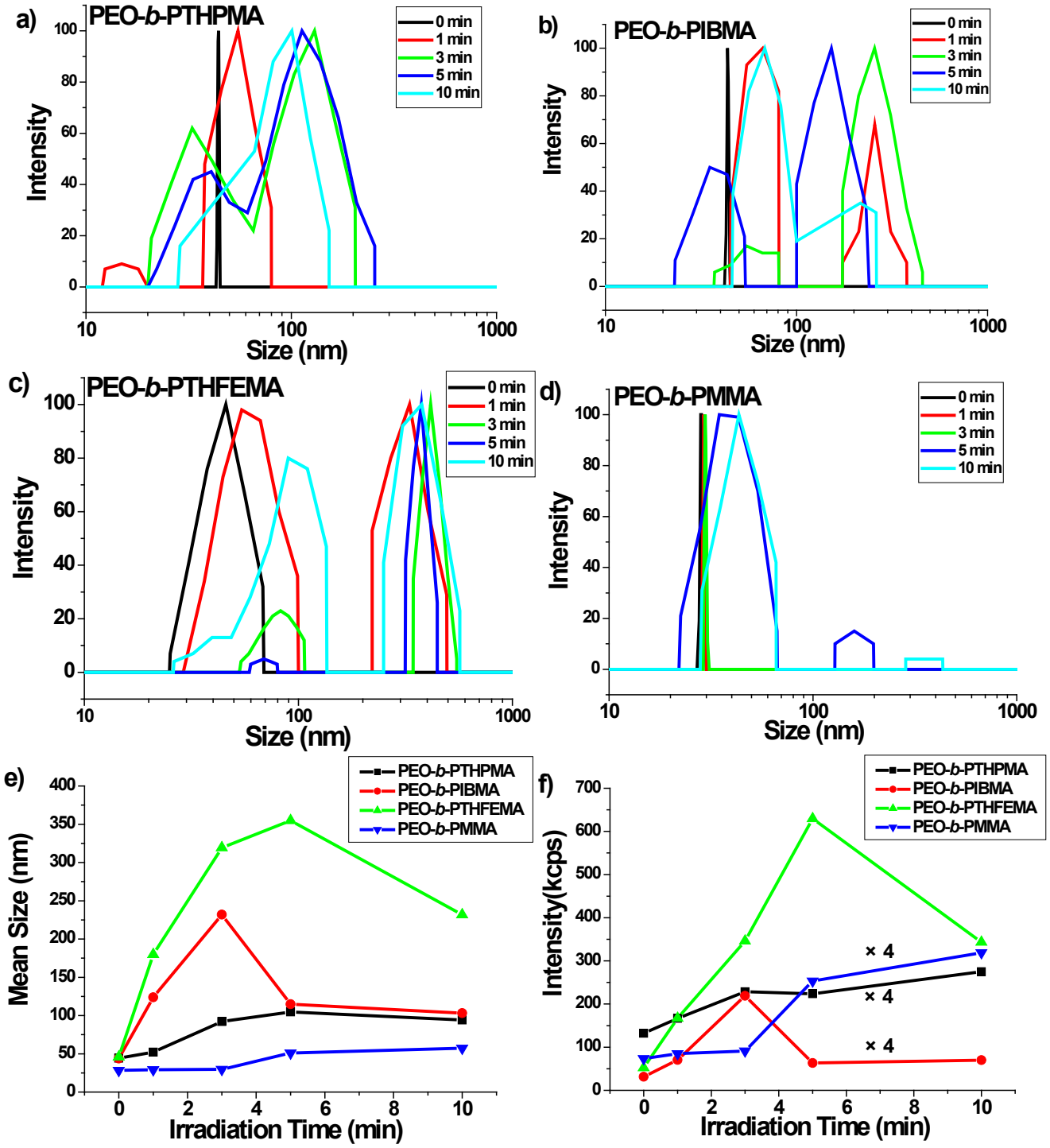

Figure 1-7. (a-d) Evolution of size distribution over ultrasound irradiation time for micellar aggregates of PEO-*b*-PTHPMA (a), PEO-*b*-PIBMA (b), PEO-*b*-PTHFEMA (c) and PEO-*b*-PMMA (d). (e) Mean hydrodynamic diameter (D_H) vs. ultrasound irradiation time, and (f) light scattering intensity (measured at 90°) vs. ultrasound irradiation time for various BCP micellar

solutions. All experiments were carried out under the same conditions (ultrasound power: 40 W, micellar solution volume: 5 mL).

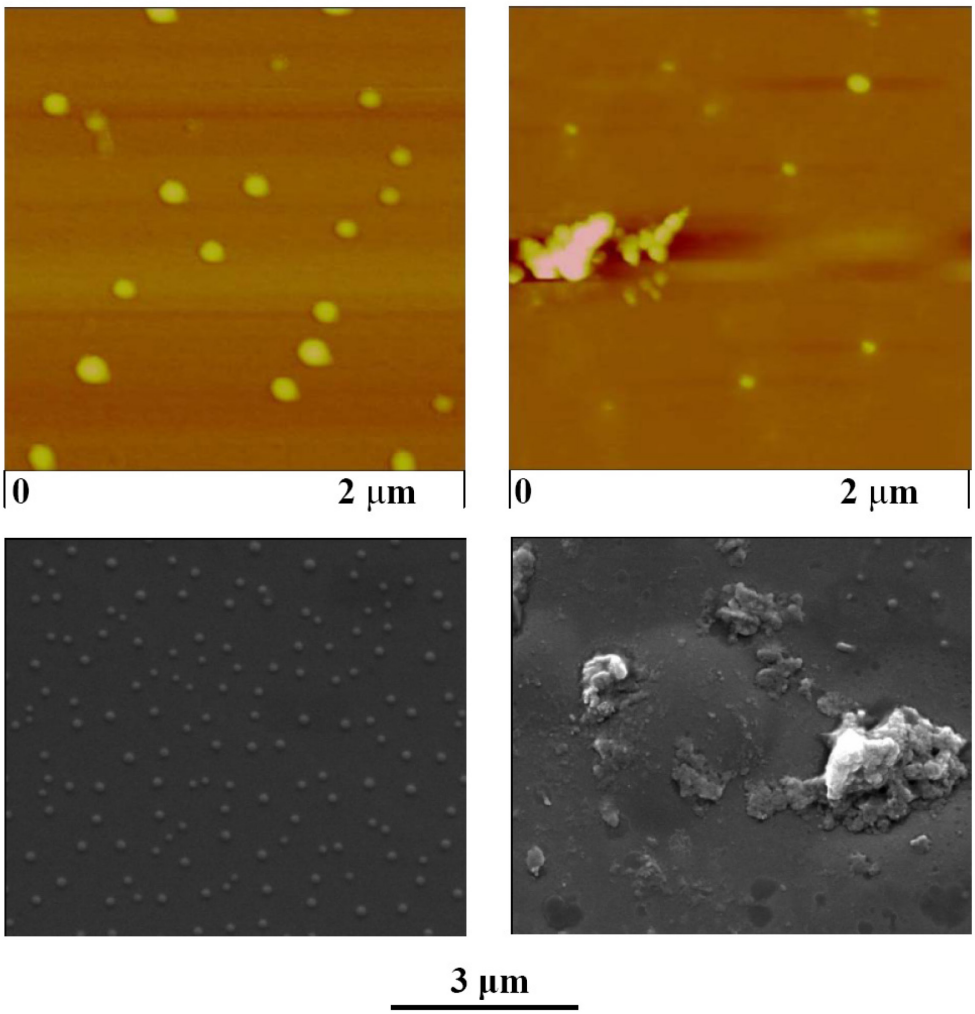

Figure 1-8. Images of AFM (upper) and SEM (lower) showing micelles of PEO-*b*-PIBMA before ultrasound (left) and large aggregates formed from disrupted micelles after ultrasound irradiation (right).

Figure 1-8 shows an example of AFM and SEM images obtained with the micellar solution of PEO-*b*-PIBMA before and after ultrasound irradiation (10 min, 40 W). Being consistent with the DLS results, larger aggregates were formed upon irradiation, which coexist with a certain amount of smaller micelles. The SEM images are particularly clear; small micelles quite uniform in size

prior to ultrasound exposure are replaced by irregular large aggregates after the irradiation.

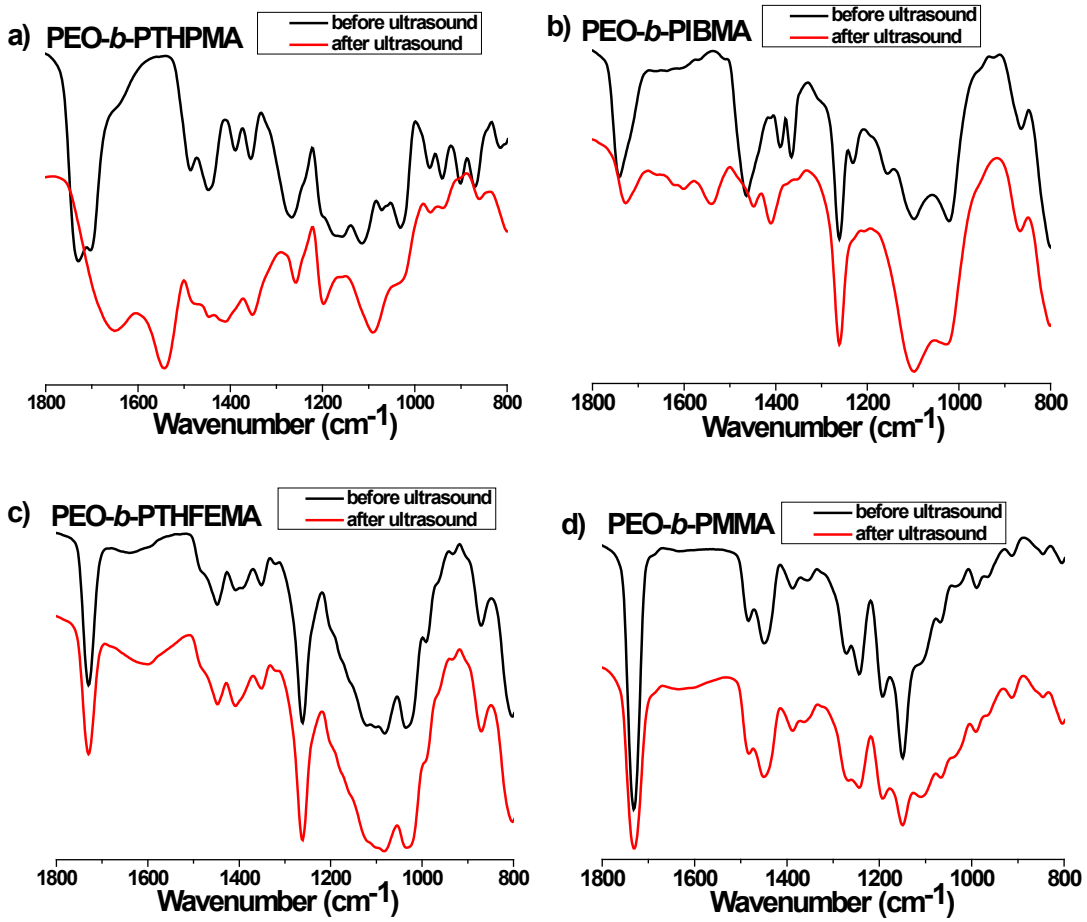

Figure 1-9. Infrared spectra of solid samples obtained from various BCP micelles before and after ultrasound irradiation (10 min, ultrasound power 40 W).

In order to get some insight into the origin of the micellar disruption and related structural changes, infrared spectra of all BCP micelles were recorded before and after their ultrasound treatment in solution (10 min, 40 W). In this experiment, BCP micelles were prepared under the same conditions as described above, but the solutions contained no NR and were not treated with buffer in order to avoid spectral complications. The obtained spectra in the 800-1800 cm^{-1} region are shown in Figure 1-9. Although a specific analysis is difficult, some observations can be made. Firstly, the spectral changes indicate the occurrence of ultrasound-induced chemical reactions, particularly with micelles of PEO-*b*-PIBMA and PEO-*b*-PTHPMA. These two BCPs display much more prominent spectral changes induced by ultrasound exposure than PEO-*b*-PTHFEMA

and PEO-*b*-PMMA, which, again, is consistent with the observed differences in the fluorescence change rate of NR upon ultrasound irradiation (Fig.1-6).

Secondly, prominent spectral changes occur in the 1400-1800 cm^{-1} region; for PEO-*b*-PTHPMA, the characteristic carbonyl stretch band at ~1735 cm^{-1} is replaced by a broad band peaked at ~ 1650 cm^{-1} after ultrasound irradiation, while PEO-*b*-PIBMA displays a shift of about 15 cm^{-1} to lower wavenumbers. This spectral change is likely due to the formation of some carboxylic acid groups whose hydrogen-bonded dimers are known to absorb at lower wavenumbers.[12] Should ultrasound induce cleavage of side groups, some of generated small molecules may be removed during the thermal treatment of the sample at 40 ^{o}C in vacuum, which can also contribute to the spectra changes. Thirdly, while PEO-*b*-PMMA exhibits the smallest spectral changes among the four BCPs, PEO-*b*-PTHFEMA shows a more intense absorption band around 1600 cm^{-1} after ultrasound irradiation.

Of the four BCPs, the micelle-core-forming hydrophobic PTHPMA, PIBMA and PTHFEMA have a labile acetal unit in their side group, and among them, PTHPMA and PIBMA indeed are much less stable and more likely to undergo a hydrolysis reaction. The above characterization results points out that micelles based on PTHPMA- and PIBMA-containing BCPs respond more importantly to high-frequency UIFU irradiation. By contrast, PMMA is the hydrophobic block used that is less likely to have a hydrolysis reaction and, indeed, micelles of PEO-*b*-PMMA appear to be less sensitive to ultrasound. Therefore, the whole of the results of this comparative study show that the chemical structure of the hydrophobic, micelle-core-forming polymethacrylate could influence greatly the extent of ultrasound-induced disruption of BCP micelles. It appears that with ester groups more likely to undergo hydrolysis reaction, high-frequency HIFU irradiation could induce more significant chemical reactions, most likely hydrolysis, which leads to a more severe micellar disruption. We mention that under the used ultrasound irradiation conditions (power and time), the temperature of the aqueous solution in the tube reactor is around 30 ^{o}C. No thermally induced hydrolysis of the BCP could occur in this range of temperatures. Of course, there may also be differences in terms of ultrasound-induced physical disruption for micelles of BCPs of different chemical structures. It is easy to imagine that for a micelle core that is softer, i.

e., less compact or rigid, it should be more probable to be perturbed by any mechanical shearing effect associated with the ultrasound. The observed micellar disruption should be the overall result of the chemical and physical disruption effects exerted on the micelles by ultrasound waves. At this time, we are unable to assess separately their respective role in the process. One difficulty is the very small amount of polymers involved in this type of experiments, which prevents the use of such methods as size exclusion chromatograph and HPLC to detect possible chain scission or to further identify new chemical species after ultrasound irradiation. We note that more thorough and quantative characterizations will be targeted in a future work, which is out of the scope of the present study.

An important potential advantage of ultrasound-based release is that it may have a temporal and spatial selectivity similar to the use of light-controllable nanovectors, while affording a much greater tissue penetration depth than light. The spatial selectivity can be enhanced if the ultrasound-induced disruption of micelles takes place predominantly around the focal area of the beams. We conducted the experiment described in Figure 1-10 to evaluate this aspect. Using NR-loaded micellar solutions of PEO-*b*-PIBMA and PEO-*b*-PTHPMA, the apparent release of NR, monitored by the change in fluorescence emission, was allowed to occur under exactly the same conditions except the position of the focal spot of the ultrasound beams with respect to the solution. As depicted in Figure 1-10a, the focal point was placed right in the middle of the solution (position 1), above and beneath the center of solution by 2 cm (positions 2 and 3) and at the level of the solution center but just outside a wall of the tube reactor (position 4). With both PEO-*b*-PIBMA (Fig.1-10b) and PEO-*b*-PTHPMA (Fig.1-10c), it is seen that the release of NR was much more important with position 1 than with positions 2-4, for which the solution was subjected to non-focused (or less focused) ultrasound beams. These results indicate that ultrasound-induced micellar disruption is more severe under focused beams, which makes it possible to choose the place of action by controlling the location of the focal spot of ultrasound beams.

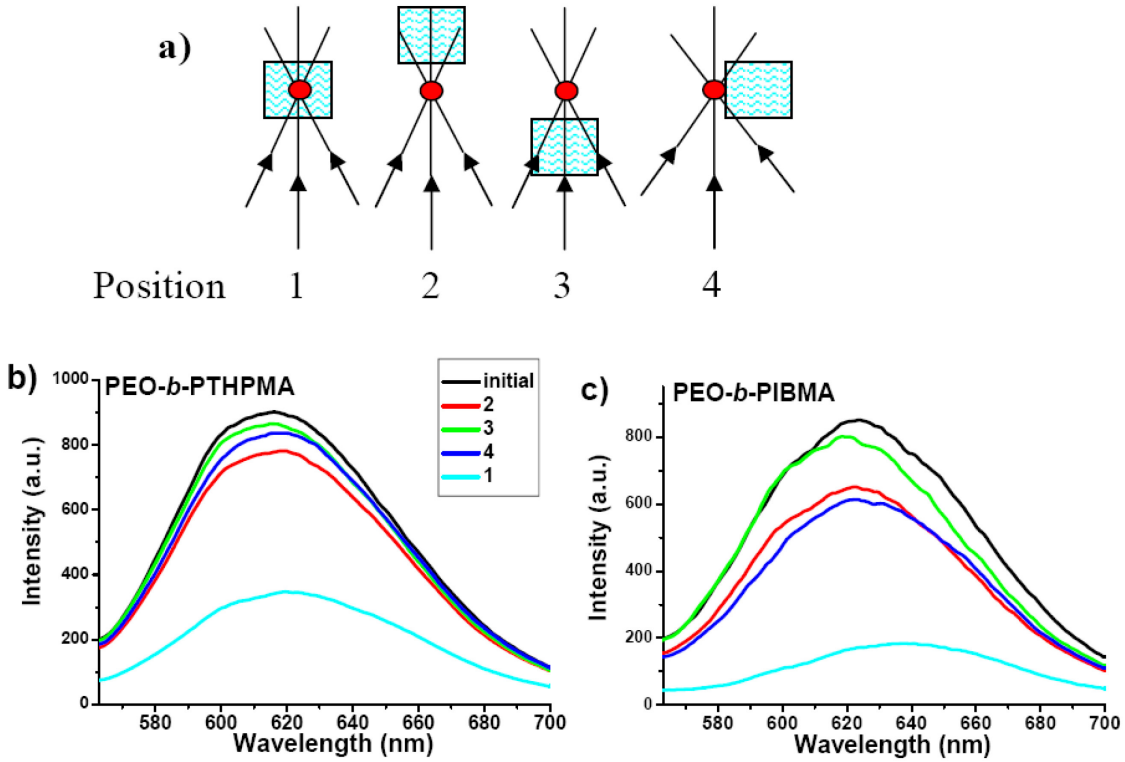

Figure 1-10. (a) Schematic of different positions of the focal spot of ultrasound beams with respect to micellar solution. (b) and (c) Fluorescence emission spectra of Nile Red (excitation 540 nm) recorded after 5 min ultrasound irradiation (40 W) with different focal spot positions for micelles of PEO-*b*-PTHPMA (b) and PEO-*b*-PIBMA (c).

Finally, given in Figure 1-11 are two examples of results that show the effect of ultrasound power (beam intensity) on the fluorescence change rate of NR. With both micelles of PEO-*b*-PTHPMA (Fig.1-11a) and PEO-*b*-PIBMA (Fig.1-11b), it is no surprise to find out that the release becomes faster with increasing the power. This clearly is the result of a faster and more severe disruption of BCP micelles by a more powerful ultrasound irradiation. At a power output of 100 W, 5 min exposure to high-frequency HIFU is enough to quench almost completely the fluorescence of NR. Actually, with this high power, the shift of fluorescence emission maximum to ~ 640 nm indicates that most dye molecules are in an aqueous medium. In addition to irradiation time, adjusting the ultrasound power is another way to control the extent of micellar disruption and the concomitant release of encapsulated molecules. As more NR molecules are brought into water by ultrasound, the color of the micellar solution due to absorption of encapsulated dye molecules becomes

increasingly faded (pictures not shown).

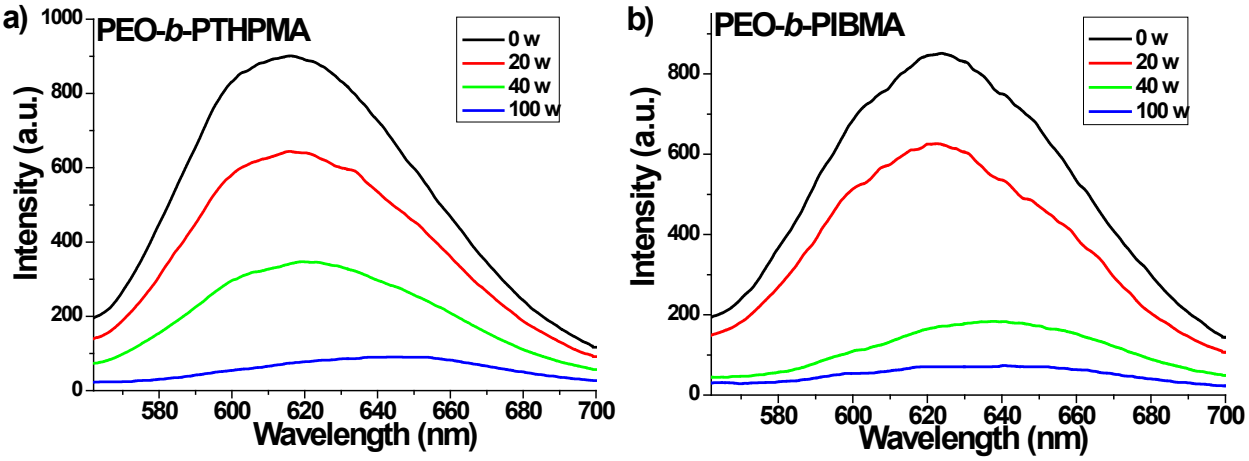

Figure 1-11. Fluorescence emission spectra of Nile Red-loaded BCP micelles (excitation 540 nm) recorded after 5 min ultrasound irradiation with different powers for PEO-*b*-PTHPMA (a) and PEO-*b*-PIBMA (b).

1.2.5. Conclusion

We conducted a comparative study on the disruption of BCP micelles and the concomitant release of encapsulated NR molecules by high-frequency HIFU irradiation. We found that all micelles formed by the four BCPs composed of a PEO hydrophilic block and a different polymethacrylate hydrophobic block could be disrupted by ultrasound resulting in release of NR. However, the extent of micellar disruption and release was found to be influenced by the chemical structure of the micelle-core-forming hydrophobic polymethacrylate. On the one hand, micelles of PEO-*b*-PIBMA and PEO-*b*-PTHPMA, whose hydrophobic blocks have a labile acetal unit in the side group and are more likely to undergo ester hydrolysis, could be disrupted more severely by ultrasound, giving rise to a faster release of NR. On the other hand, micelles of PEO-*b*-PMMA, whose polymethacrylate block is more stable, appear to be more resistant to ultrasound and exhibit a slower rate of release of NR than other BCPs. Moreover, infrared spectra recorded with micelles before and after ultrasound irradiation of their aqueous solution show evidence for the occurrence of chemical reactions, most likely hydrolysis, for PEO-*b*-PIBMA and PEO-*b*-PTHPMA, but absence of chemical reactions for PEO-*b*-PMMA. The effect of BCP chemical structure on the

reaction of micelles to high-frequency UIFU irradiation, as evidenced by the present study, shows the perspective of designing and developing ultrasound-sensitive BCP micelles for ultrasound-based delivery applications.

Acknowledgment

This study is funded by National Natural Science Foundation (NSFC) of China (Grant No: 51073100). H. X. also thanks the support by the Program for New Century Excellent Talents in Universities, China. Y.Z. acknowledges financial support from the Natural Sciences and Engineering Research Council of Canada (NSERC) and le Fonds québecois de la recherche sur la nature et les technologies of Quebec (FQRNT). We are grateful to St-Jean Photochemicals Inc. (St-Jean-sur-Richelieu, Quebec, Canada) for providing us with the monomer of tetrahydropyranyl methacrylate. We also thank Prof. Yves Dory (University of Sherbrooke) for helpful discussion.

Keywords: block copolymers, micelles, stimuli-sensitive polymers, ultrasound

References

[1] [1a] Rapoport, N. Y. *Colloids Surf. B: Biointerfaces* **1999**, *16*, 93; [1b] Husseini, G. A.; Myrup, G.; Pitt, W. G.; Christensen, D. A.; Rapoport, N. Y. *J. Control. Release* **2000**, *69*, 43; [1c] Marin, A.; Sun, H.; Husseini, G. A.; Pitt, W. G.; Christensen, D. A.; Rapoport, N. Y. *J. Control. Release* **2002**, *84*, 39.

[2] See, for example, [2a] Gillies, E. R.; Frechet, J. M. J. *Chem. Commun.* **2003**, 1640-1641; [2b] Bellomo, E. G.; Wyrsta, M. D.; Pakstis, L.; Pochan, D. J.; Deming, T. J. *Nat. Mater.* **2004**, *3*, 244-248; [2c] Bae, Y.; Fukushima, S.; Harada, A.; Kataoka, K. *Angew. Chem. Int. Ed*. **2003**, *42*, 4640-4643; [2d] Xu, X.; Smith, A. E.; Kirkland, S. E.; McCormick, C. L. *Macromolecules* **2008**, *41*, 8429–8435; [2e] Jiang, X.; Zhao, B. *Macromolecules* **2008**, *41*, 9366–9375.

[3] See, for example, [3a] Chung, J. E.; Yokoyama, M.; Okano, T. *J. Controlled Release* **2000**, *65*, 93-103; [3b] Schilli, C. M.; Zhang, M.; Rizzardo, E.; Thang, S. H.; Chong, Y. K.; Edwards, K.; Karlsson, G.; Muller, H. E. *Macromolecules* **2004**, *37*, 7861-7866; [3c] Qin, S.; Geng, Y.;

Discher, D. E.; Yang, S. *Adv. Mater.* **2006**, *18*, 2905-2909; [3d] Rodriguez-Hernandez, J.; Checot, F.; Gnanou, Y.; Lecommandoux, S. *Prog. Polym. Sci.* **2005**, *30*, 712-724.

[4] [4a] Zhao, Y. *J. Mater. Chem.* **2009**, *19*, 4887–4895; [4b] Wang, Y.; Xu, H.; Zhang, X. *Adv. Mater.* **2009**, *21*, 2849-2864; [4c] Wang, G.; Tong, X.; Zhao, Y. *Macromolecules* **2004**, *37*, 8911-8917; [4d] Jiang, J.; Tong, X.; Zhao, Y. *J. Am. Chem. Soc.* **2005**, *127,* 8290-8291; [4e] Babin, J.; Pelletier, M.; Lepage, M.; Allard, J.F.; Morris, D.; Zhao, Y. *Angew. Chem. Int. Ed.* **2009**, *48*, 3329-3332.

[5] [5a] Pitt, W. G.; Husseini, G. A.; Staples, B. *J. Expert Opin. Drug Delivery* **2004**, *1*, 37; [5b] Kost, J.; Leong, K.; Langer, R. *Proc. Natl. Acad. Sci. U.S.A* **1989**, *86*, 7663; [5c] Kennedy, J. E. *Nat. Rev. Cancer.* **2005**, *5*, 321-327.

[6] [6a] Suslick, K. S. *Science **1990***, *3*, 1439; [6b] Zhu, C. P.; He, S. C.; Shan, M. L.; Chen, J. C. *Ultrasonics* **2006**, *44*, e349; [6c] Thomas, C. R.; Farny, C. H.; Coussios, C. C.; Roy, R. A. *Acoust. Res. Lett.* **2005**, *6*, 182.

[7] Wang, J.; Pelletier, M.; Zhang, H.; Xia, H.; Zhao, Y. *Langmuir* **2009**, *25*, 13201-13205.

[8] Shinobu, K.; Kenji, E.; Yoshihiro, K.; Hiroyasu, N.; Kogaku, K. *Ronbunshu* **1999**, *25*, 290-293

[9] Pelletier, M.; Jerome, B.; Tremblay, L.; Zhao Y. *Langmuir* **2008**, *24*, 12664.

[10] Tian, Y.; Watanabe, K.; Kong, X.; Abe, J.; Iyoda, T. *Macromolecules* **2002**, *35*, 3739.

[11] Goodwin, A. P.; Mynar, J. L.; Ma, Y.; Fleming, G. R.; Frechet, J. M. J. *J. Am. Chem. Soc*. **2005**, *127*, 9952.

[12] Dong, J.; Ozaki, Y.; Nakashima, K. *Macromolecules* **1997**, *30*, 1111-1117.

1.3. Conclusion of the Project

In this project, we have performed a comparative study on the disruption of BCP micelles and the concomitant release of encapsulated dye (Nile Red) molecules by high-frequency HIFU irradiation. By synthesizing four BCPs whose structures differ only on the ester side group of the hydrophobic polymethacrylate, we have been able to investigate the effect of the BCP structure on the reaction of the BCP micelles in response to HIFU. The results show that all BCP micelles could be disrupted by focused ultrasound beams resulting in release of the dye. However, the extent of micellar disruption and release was found to be influenced by the chemical structure of the micelle-core-forming hydrophobic polymethacrylate. The main findings can be summarized as follows. First, the micelles of PEO-*b*-PIBMA and PEO-*b*-PTHPMA, whose hydrophobic blocks have a labile acetal unit in the side group and are more likely to undergo ester hydrolysis, could be disrupted more severely by ultrasound, giving rise to a faster dye release. Secondly, the micelles of PEO-*b*-PMMA, whose polymethacrylate block is more stable, appear to be more resistant to ultrasound and exhibit a slower rate of dye release than the other BCPs. Moreover, infrared spectra recorded with micelles before and after ultrasound irradiation of their aqueous solution show evidence for the occurrence of chemical reactions, most likely the hydrolysis of ester groups, for PEO-*b*-PIBMA and PEO-*b*-PTHPMA. By contrast, no evidence of chemical reactions was found for the micelles of PEO-*b*-PMMA. The effect of BCP chemical structure on the reaction of micelles to high-frequency HIFU irradiation, as evidenced by the present study, could help designing and developing ultrasound-sensitive BCP micelles for ultrasound-based delivery applications.

CHAPTER 2. ULTRASOUND-RESPONSIVE BLOCK COPOLYMER MICELLES BASED ON A NEW AMPLIFICATION MECHANISM

2.1. About the Project

Although high intensity focused ultrasound (HIFU) is emerging as an interesting trigger for the release of substances BCP micelles and other types of nanocarriers, a major challenge remains in developing ultrasound-responsive BCP micelles. BCP micelles must have a high sensitivity to ultrasound in order to reduce the ultrasound intensity required for an effective micellar disruption. To achieve this goal eventually, a useful strategy consists in introducing into BCP structures weak chemical bonds which are more susceptible to be broken by ultrasound. In our previous studies presented in Chapter 1, we found evidence that the micelle core-forming PTHPMA chains, whose side groups bear labile acetal units, could undergo hydrolysis reaction under HIFU irradiation at room temperature, resulting in cleavage of the THP groups and formation of the hydrophilic methacrylic acid (MAA). This finding allowed us to conduct the present study, in which a new approach, based on combining the ultrasound reactivity with the thermosensitivity of LCST polymers, was proposed and demonstrated that could amplify the ultrasound-induced effect and thus help designing ultrasound-sensitive BCP micelles.

This work was published in *Langmuir* **2012**, *28*, 16463−16468, by Juan Xuan, Olivier Boissière, Yi Zhao, Bin Yan, Luc Tremblay, Serge Lacelle, Hesheng Xia and Yue Zhao. This research work was conducted in the Université de Sherbrooke and Sichuan University under the supervision of Prof. Zhao and co-supervision of Prof. Xia. The block copolymer used was synthesized by Yi Zhao and Bin Yan. The NMR experiments were carried out by Olivier Boissière, Luc Tremblay and Serge Lacelle. I performed the rest of the experiments described in this publication. I wrote the first draft of the manuscript. Prof. Zhao finalized the manuscript with revision contributions from Prof. Xia.

2.2 Paper Published in Langmuir 2012, 28, 16463

Ultrasound-Responsive Block Copolymer Micelles Based on a New Amplification Mechanism

Juan Xuan,[a,b] Olivier Boissière,[b] Yi Zhao[b], Bin Yan,[b] Luc Tremblay,[c] Serge Lacelle,[b] Hesheng Xia[a*] and Yue Zhao[b*]

[a] State Key Laboratory of Polymer Materials Engineering, Polymer Research Institute, Sichuan University, Chengdu 610065, China

xiahs@scu.edu.cn

[b] Département de chimie, Université de Sherbrooke, Sherbrooke, Québec, J1K 2R1, Canada.

yue.zhao@usherbrooke.ca

[c] Département de médecine nucléaire et de radiobiologie and Centre d'imagerie moléculaire de Sherbrooke, Université de Sherbrooke, Sherbrooke, QC, Canada J1K 2R1

2.2.1 Abstract

A new approach for amplifying the effect of high intensity focused ultrasound (HIFU) in disassembling amphiphilic block copolymer (BCP) micelles in aqueous solution was investigated. The diblock copolymer is comprised of a water-soluble poly(ethylene oxide) (PEO) block and a block of poly(2-(2-methoxyethoxy)ethyl methacrylate) ($PMEO_2MA$) that is hydrophobic at temperatures above its lower critical solution temperature (LCST). We show that by introducing a small amount of HIFU-labile 2-tetrahydropyranyl methacrylate (THPMA) co-monomer units into the $PMEO_2MA$ that forms the micelle core at T>LCST, an ultrasound irradiation of a micellar solution could induce the hydrolysis of THPMA groups. As a result, the LCST of the thermosensitive polymer increases due to the conversion of hydrophobic THPMA co-monomer units onto hydrophilic methacrylic acid (MAA). Consequently, the BCP micelles disassemble without actually changing the solution temperature. In addition to the characterization results of transmittance measurements, variable-temperature ^{1}H NMR, SEM and DLS, a ^{13}C NMR spectral analysis provided critical evidence for the hydrolysis reaction of THPMA groups under HIFU irradiation.

2.2.2 Introduction

Block copolymer (BCP) micelles have been extensively studied as delivery systems for biomedical applications. Generally, hydrophobic drugs can be loaded into their interior and released upon their disruption in response to a variety of stimuli such as pH change,[1-2]temperature change,[3-4] exposure to light[5-6] or enzyme,[7-8] to name a few. In recent years, there has been growing interest in using ultrasound as a stimulus to induce the disruption of BCP micelles and trigger the release of their payloads.[9-11] As compared to other external stimuli allowing for remote control of the disruption process of BCP micelles, ultrasound has an important advantage. It can penetrate deep into the body in a noninvasive way and be applied locally with focused beams. In general, two types of ultrasound technology can be utilized: low frequency (e.g. 20 kHz) and high frequency diagnostic ultrasounds (e.g. 1 MHz). The former have longer wavelengths and are difficult to focus; when they pass through the body, the resulting ultrasonic cavitation is severe

and can be damaging. By contrast, the latter can be focused, and the intensity is quite high only on the focal spot, while in other areas it is low enough to be acceptable by the human body. Therefore, high intensity focused ultrasound (HIFU) is emerging as an interesting trigger for the release of substances from BCP micelles[12-13]and other types of nanocarriers.[14-16]

However, a major challenge remains in developing ultrasound-responsive BCP micelles. The sensitivity of the responsiveness of BCP micelles to ultrasound needs to be improved in order to further reduce the ultrasound intensity required for effective activation. To achieve this goal eventually, a useful strategy consists in introducing into BCP structures weak chemical bonds which are more susceptible to be broken by ultrasound. This level of control also allows BCP micelles to be disrupted in a predictable and understandable fashion. Recent progress on mechanophores[17-19] may suggest the use of certain ultrasound-labile moieties in BCPs. However at this point, most mechanophores need to be positioned at the chain center in order to be subjected to ultrasound-generated mechanical force, inducing chemical reactions in dilute solutions of dissolved polymer chains with low frequency ultrasound. In other words, their responsiveness to ultrasound in an aggregated polymer chain, solid-like state, such as a micelle core, may not be effective.[20] In our previous studies of micelles formed by a diblock copolymer comprised of hydrophilic poly(ethylene oxide) (PEO) and hydrophobic poly(2-tetrahydropyranylmethacrylate) (PTHPMA),[21,22] we found evidence that the micelle core-forming PTHPMA chains, whose side groups bear labile acetal units, could undergo hydrolysis reaction under HIFU irradiation at room temperature, resulting in cleavage of THP groups and formation of methacrylic acid (MAA). Based on this finding, in the present study, we propose and demonstrate a new approach that could amplify the ultrasound-induced effect and help designing ultrasound-sensitive BCP micelles.

This amplification mechanism is schematically illustrated in Figure 2-1. The basic idea is to incorporate a number of ultrasound-reactive co-monomer units, such as THPMA, into the hydrophobic block that is chosen to be a thermosensitive polymer exhibiting a lower critical solution temperature (LCST) in aqueous solution. With this design, micelles can be formed at $T_{solution}$>LCST since the thermosensitive polymer is hydrophobic. Under HIFU irradiation, if the ultrasound-induced reaction of the co-monomer units increases their polarity, like in the case of

MAA formation due to removal of THP groups, the LCST could shift to a higher temperature $LCST_{new}$. This shift in LCST due to the enhanced polarity of co-monomer units is well known.[23-26] If the ultrasound irradiation displaces the new LCST above $T_{solution}$, the micelles would be dissolved because the thermosensitive polymer becomes soluble in water and the BCP is no longer amphiphilic. Through this mechanism, the reaction of a limited number of co-monomer units to HIFU could result in BCP micelles disassembly on account of a change in the phase transition temperature of the hydrophobic block. The present study confirmed the validity of this approach for the amplification of the ultrasound effect.

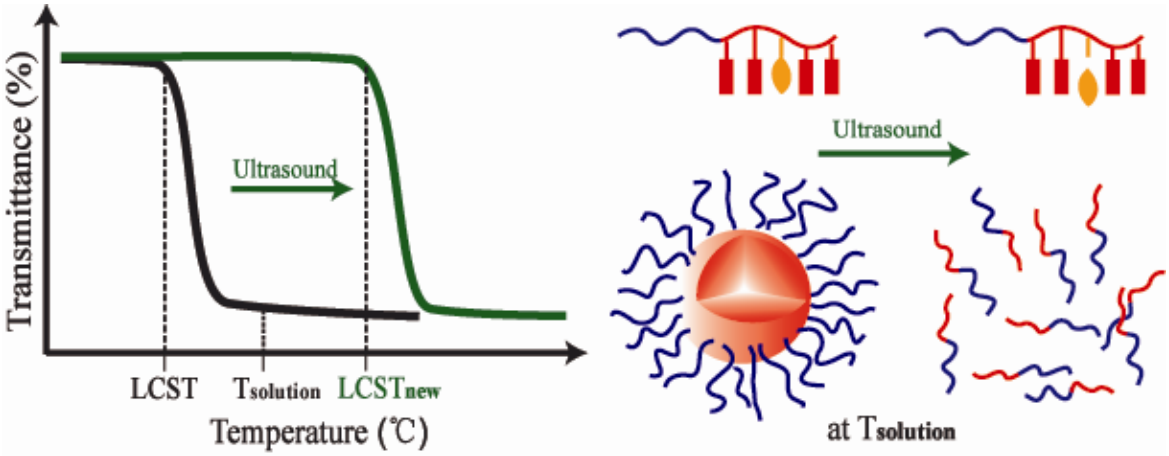

Figure 2-1. Schematic illustration of the amplification mechanism for ultrasound-disrupted block copolymer micelles based on ultrasound-induced increase in the lower critical solution temperature (LCST) of the hydrophobic block.

2.2.3. Results and Discussion

To test the approach depicted in Figure 2-1, we synthesized a diblock copolymer of which PEO is the permanent hydrophilic block, while the LCST-thermosensitive block is poly(2-(2-methoxyethoxy)ethyl methacrylate) ($PMEO_2MA$) containing a small amount of THPMA co-monomer units as the ultrasound-reactive trigger. The BCP sample used in this study, denoted as PEO_{112}-*b*-P(MEO_2MA_{189}-*co*-$THPMA_{21}$), was synthesized using ATRP and characterized by means of various techniques (details in the Experimental Section). The content of THPMA in the hydrophobic block is 10 mol%. The effect of 1.1 MHz HIFU on the LCST of the

P(MEO_2MA-*co*-THPMA) block was first investigated by solution transmittance measurements. Figure 2-2a shows the result obtained with a BCP solution (2 mg/mL). Prior to HIFU exposure, there is a decrease in transmittance at about 22 °C on heating. This apparent cloud point should arise from the LCST of the P(MEO_2MA-*co*-THPMA) block, indicating dehydration of this thermosensitive block and formation of BCP micelles. Indeed, micelles were observed at temperatures higher than 25 °C (see below). The relatively small decrease in transmittance indicates the presence of well-dispersed BCP micelles. By contrast, after HIFU treatment of the aqueous solution at room temperature, the transmittance measurements reveal a cloud point at a much higher temperature of about 42 °C. Moreover, the drop in transmittance of the BCP solution after HIFU is much more prominent than that observed for the solution before the ultrasound treatment, implying the formation of larger aggregates of BCP chains resulting from the HIFU exposure.

The transmittance measurements shown in Figure 2-2a provide the first direct support to our working hypothesis. That is, HIFU cleaves THP side groups and the arising polarity increase of the co-monomer shifts the LCST of the thermosensitive block to higher temperatures. In order to further confirm this effect and to demonstrate that the transmittance decrease on heating originates from chain aggregation of the dehydrated P(MEO_2MA-*co*-THPMA) block, we recorded variable-temperature ^1H NMR spectra of the BCP solution (in D_2O) before and after the ultrasound treatment.

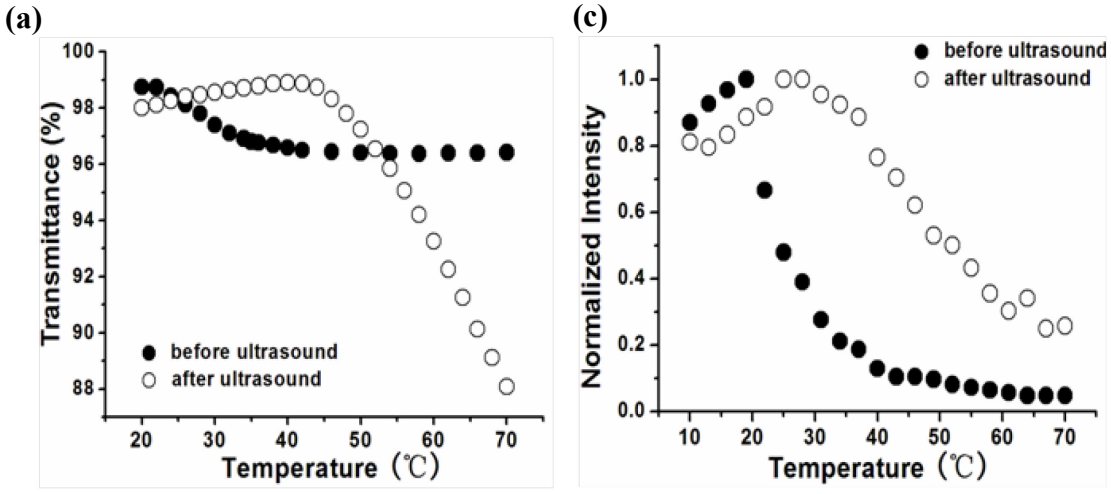

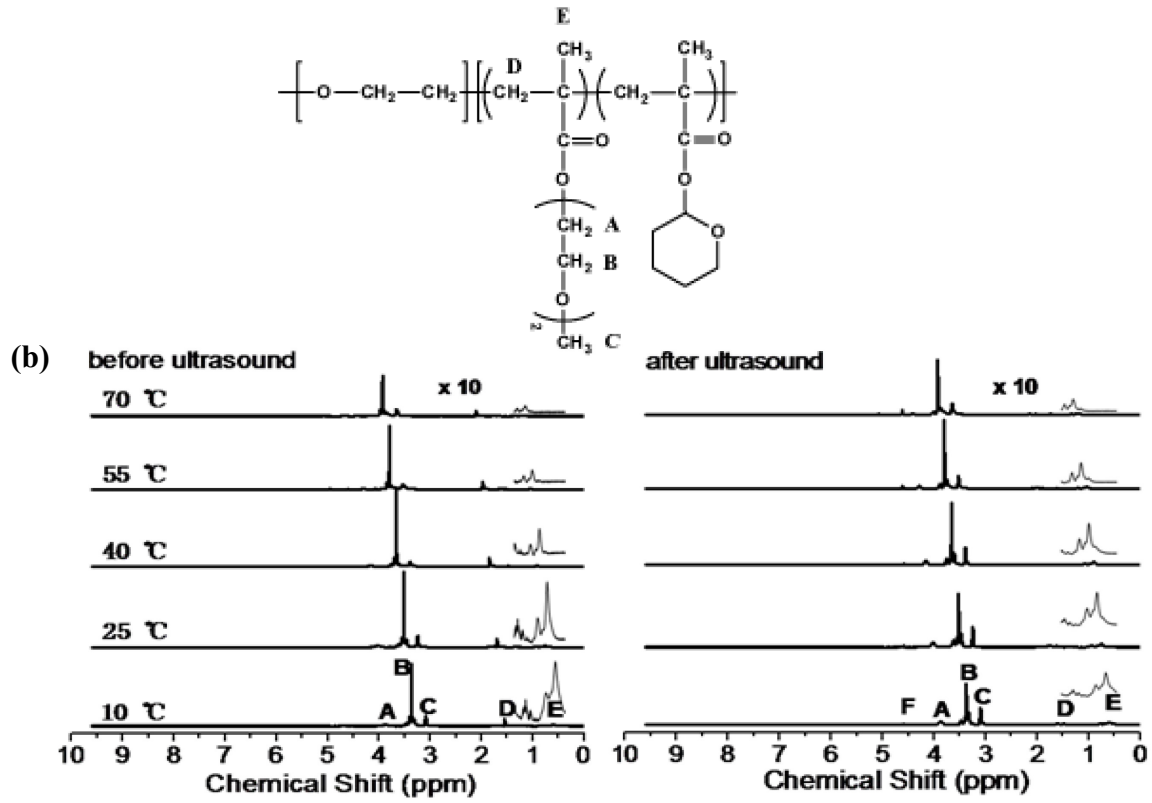

Figure 2-2. (a) Transmittance (at 600 nm) vs. temperature for an aqueous solution of PEO-*b*-P(MEO_2MA-*co*-THPMA) (2 mg/mL) before and after ultrasound irradiation (1.1 MHz, 100 W, 20 min). (b) Variable-temperature ^1H NMR spectra of the block copolymer solution (in D_2O) before and after ultrasound irradiation; the 0.4–1.4 ppm spectral region being magnified for clarity and the block copolymer chemical structure shown for assignment of the resonance peaks. (c) Normalized integrals of the resonance peak at 0.6 ppm vs. solution temperature.

Figure 2-2b shows the spectra only at some chosen temperatures for the sake of clarity. For both aqueous solutions, at 10 °C, all resonance signals of the two blocks are clearly visible indicating BCP dissolution in water. Upon heating, the peaks of the P(MEO_2MA-*co*-THPMA) block become less prominent at certain temperatures as a result of chain aggregation, thus displaying reduced intensities and broadened peaks. For the solution before the HIFU exposure, these spectral changes become clearly noticeable at 40 °C, while they are only observed in the spectrum recorded at 55 °C for the solution after the ultrasound treatment. These results confirm that 1) the decrease in solution transmittance on heating does come from chain aggregation of the

P(MEO$_2$MA-*co*-THPMA) block, and 2) this occurs at higher temperatures following the ultrasound treatment of the polymer solution. This is clearer in Figure 2-2c by plotting the change of the integral of the E resonance (magnified in Figure 2-2b) as a function of solution temperature. The sharp decrease in the peak integral, associated with chain aggregation of the P(MEO$_2$MA-*co*-THPMA) block, is visible at about 25 °C for the solution before applying ultrasounds, but around 45 °C for the solution after ultrasound treatment. The change in the LCST induced by HIFU, as revealed by ^{1}H NMR, is basically in agreement with the transmittance measurement results. Similar results are observed with other resonance peaks, e.g. the peak C assigned to the methyl group at the end of the side chain of PMEO$_2$MA. It is worth mentioning that the HIFU-induced LCST shift under the same conditions was also measured for another BCP sample containing a smaller amount of THPMA units (5 mol%), PEO$_{112}$-*b*-P(MEO$_2$MA$_{133}$-*co*-THPMA$_7$). As expected, a smaller increase in LCST of about 9 °C after the ultrasound treatment was observed.

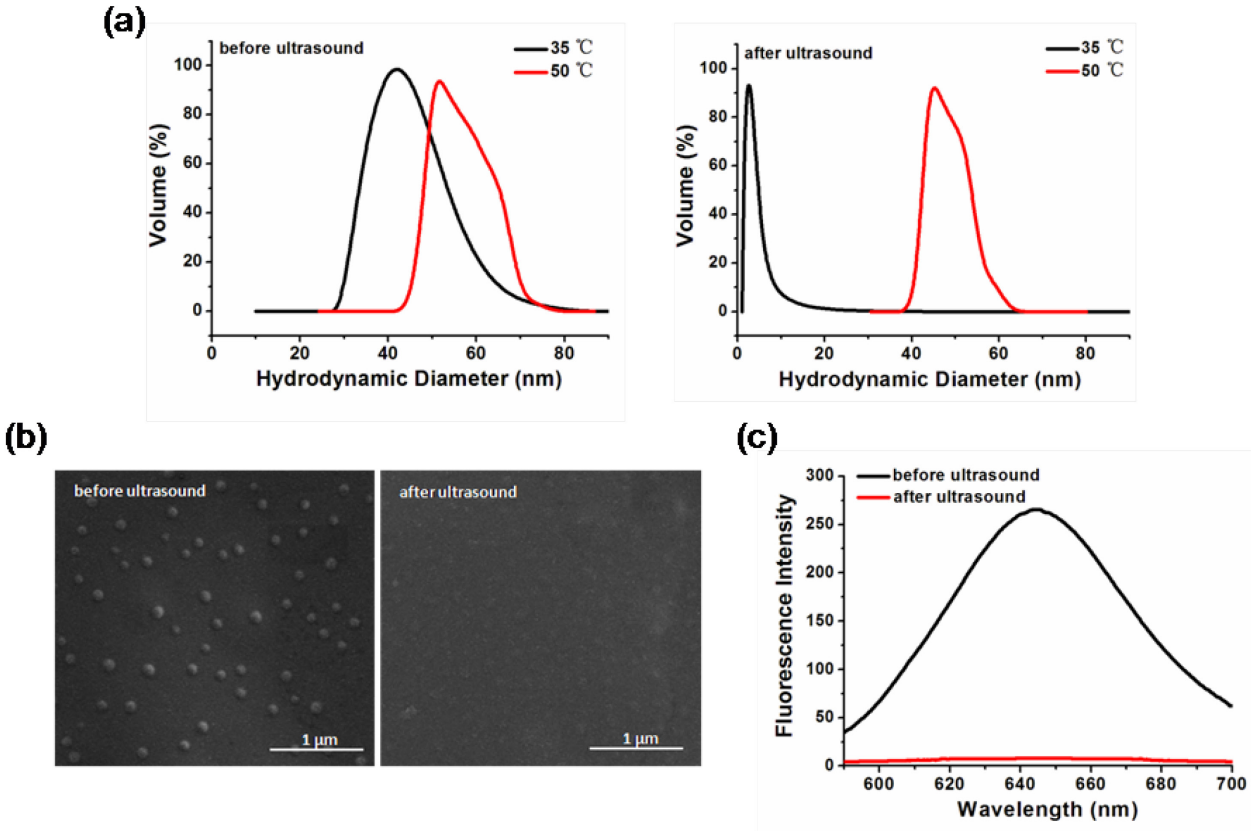

Figure 2-3. (a) DLS results showing the changes in the size distribution of the micellar aggregates

of PEO-*b*-P(MEO_2MA-*co*-THPMA) in aqueous solution before and after ultrasound exposure (1.1 MHz, 100 W, 20 min) at 35 and 50 °C. (b) SEM images obtained from the micellar solution at 35 °C before and after ultrasound irradiation. (c) Fluorescence emission spectra (λ_{ex}=540 nm) of a Nile Red-loaded micellar solution at 35 °C before and after ultrasound irradiation.

The ultrasound-induced rise in the LCST suggests the possibility of obtaining BCP micelles that can be disassembled at certain temperatures. Based on the results in Figure 2-2, we performed DLS measurements on a BCP solution at 35 and 50 °C, for each temperature both before and after HIFU exposure of the solution. The resulting changes in the size distribution of the micellar aggregates are shown in Figure 2-3a. At 35 °C, before the ultrasound treatment, micelles with an average hydrodynamic diameter of about 40 nm are observable; after ultrasound exposure, there are essentially dissolved polymer chains due to the displacement of the LCST of the P(MEO_2MA-*co*-THPMA) block to temperatures higher than 35 °C (Fig.2-3). By contrast, it is no surprise to see that at 50 °C, micellar aggregates remain after ultrasound exposure, since the increased LCST is still below the solution temperature. As shown in Figure 2-3b, the ultrasound-induced disassembly of BCP micelles at 35 °C was also confirmed by SEM observations. Micelles observed by casting the polymer solution at 35 °C disappear after HIFU irradiation. Figure 2-3c shows the result of another experiment suggesting the ultrasound-induced disassembly of BCP micelles and release of loaded substances. A model hydrophobic compound, Nile Red, was loaded into the micelles and it fluoresces when well-solubilized in the micelle core. After HIFU irradiation, the fluorescence intensity is largely quenched indicating that the dye molecules are brought into an aqueous medium, as a result of the ultrasound-induced micellar disruption.

The above results clearly support the proposed amplification mechanism for ultrasound-responsive BCP micelles that is based on a LCST shift for the micelle core- forming thermosensitive block as a result of the increased polarity of the ultrasound-labile co-monomer units (Fig.2-1). HIFU-induced hydrolysis of THP groups leads to the enhanced polarity by converting hydrophobic THPMA onto hydrophilic MAA groups. In order to obtain more evidence for the

occurrence of ultrasound-induced hydrolysis, ^{13}C NMR spectra of a BCP D_2O solution were recorded before and after HIFU exposure, and are shown in Figure 2-4. Since the most prominent peak at ~68 ppm corresponding to the CH_2 groups of the PEO block, cannot be modified by ultrasound, its intensity is used as a reference to calibrate the intensities of the remaining signals. The singlet at 176 ppm is characteristic of an ester; after ultrasound treatment, its intensity sharply decreases and the new peak appearing at 181 ppm is consistent with the formation of a carboxylic acid.[28] This spectral change indicates that hydrolysis takes place during the ultrasound treatment. Unfortunately, due to the very low peak intensities, assessing the percentage of cleaved ester groups is not possible in this case. The rest of the spectra also provides information about which of the two esters in the P(MEO_2MA-*co*-THPMA) block undergoes HIFU-induced hydrolysis.

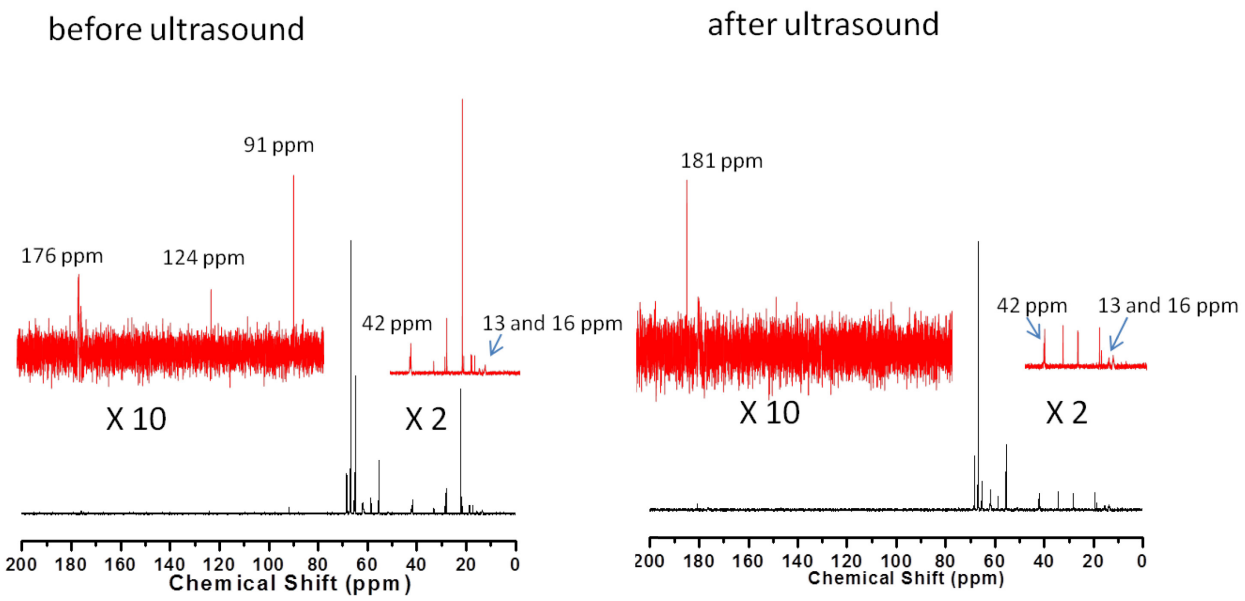

Figure 2-4. ^{13}C NMR spectra (in D_2O) of PEO-*b*-P(MEO_2MA-*co*-THPMA) before and after ultrasound irradiation.

On the one hand, as detailed in the Experimental Section below, to record the ^{13}C NMR spectrum of the BCP after ultrasound treatment, a solution was subjected to HIFU irradiation in the reactor; afterwards, the polymer was dried in a vacuum in order to remove all residual liquids before the

sample was re-dissolved in D_2O for acquiring the spectrum. Among the removed liquids, there were the solvent and also the alcohols that could be produced by the hydrolysis of both esters, i.e., oxan-2-ol for THPMA and 2-(2-methoxyethoxy) ethanol for $PMEO_2MA$. After the HIFU irradiation, the resonances which disappeared include one at 91 ppm characteristic of an O-C-O association that only exists in the THPMA, another at 124 ppm, assigned to the other carbon bounded to the oxygen in the ring of THPMA, and the peak at ~22 ppm which corresponds to the other carbons not bounded to oxygen inside the ring. The disappearance of all these peaks of the side chain of THPMA following ultrasound treatment is further strong evidence of HIFU-induced hydrolysis of THPMA side groups. The two other resonances of THPMA at 18 ppm for the CH_2 and at 34 ppm for the carbon without any hydrogen displays only a small shift of about 1 ppm after the ultrasound treatment. On the other hand, the broad peaks, with about the same widths, at 13, 16, 42, 62 and 69 ppm belong to PEO_2MA and are bound to each other. All of them are enhanced after ultrasound treatment. Generally, broad NMR resonances exist for three reasons. The first one arises from a dispersion of several peaks which creates a larger one (i.e., scattering of chemical shifts); the second one is due to the presence of a rigid environment different than in other mobile groups; and the last one is observed for atoms involved in chemical exchange between different conformations. For BCP, the second possibility is more likely, meaning that ultrasounds increase the mobility of these carbon atoms belonging to the same moiety of the molecule. For these corresponding resonances, the one at 42 ppm typically corresponds to a carbon without hydrogen in the main chain, the signals at 62 and 69 ppm belong to the CH_2 and CH_3 of the $PMEO_2MA$, respectively, while those at 13 and 16 ppm can be assigned to different methylenes of the main chain of the P(MEO_2MA-*co*-THPMA) block. These spectral changes are evidence that, in contrast to THPMA, the $PMEO_2MA$ units cannot be hydrolyzed by HIFU and their environment becomes more mobile due to the hydrolysis of THPMA. Therefore, the ^{13}C NMR spectra clearly indicate that THPMA is almost completely hydrolyzed, if not completely, by HIFU irradiation, in contrast with PEO_2MA which remains unaffected by ultrasound.

2.2.4. Experimental

Materials: Unless otherwise stated, all chemicals were purchased from Aldrich. The monomer of

tetrahydropyranyl methacrylate (THPMA, 99%) was provided by St-Jean-Photochemicals (Quebec, Canada) and passed through a column of basic alumina silica before use. 2-(2-Methoxyethoxy)ethyl methacrylate (MEO_2MA) was treated in the same way as for THPMA before polymerization. Cu(I)Br and N, N, N', N' N''-pentamethyldiethylenetriamine (PMDETA) were used without further purification. Poly(ethylene oxide) (PEO) macroinitiator (PEO_{112}-Br) was prepared according to the literature method.[27]

Synthesis of the diblock copolymer: The BCP was prepared using ATRP. A macroinitiator PEO_{112}-Br was used to grow the ultrasound-responsive, thermosensitive random copolymer block of P(MEO_2MA-*co*-THPMA). An example of the reactions is as follows. PEO_{112}-Br (0.35 g, 0.07 mmol), MEO_2MA (2.37 g, 12.6 mmol), THPMA(0.17 g, 1.4 mmol), CuBr (0.0101 g, 0.07 mmol), PMDETA (0.0121 ml, 0.07 mmol) and anisole (2 mL) were added into a 10 mL single-neck flask under N_2. The reaction mixture was degassed by three freeze-pump-thaw cycles and then purged with N_2. The flask was placed in a preheated oil bath at 60 °C for 60 min. Then, the reaction mixture was cooled to room temperature and diluted with THF. The catalyst was removed by passing the mixture through a neutral alumina column. The solution was collected, then concentrated and precipitated three times in a mixture of pentane and diethyl ether (1:1, v/v). The sample was filtered and dried at 40 °C for 24 h. From the GPC measurements using polystyrene standards and THF as the eluent, the obtained block copolymer has a number average molecular weight of 44300 with a polydispersity index of 1.17. From the ^{1}H NMR spectrum of the BCP, its composition was determined to be PEO_{112}-*b*-P($MEOMA_{189}$-*co*-$THPMA_{21}$).

Characterizations: The solution transmittance measurements (at 600 nm) were carried out using a UV-vis spectrophotometer (UV2300, Shanghai Tianmei). ^{1}H NMR spectra for the general characterizations in the synthesis were obtained with a Bruker AVANCE 400 MHz NMR spectrometer using tetramethylsilane as an internal standard. The variable-temperature ^{1}H and ^{13}C NMR measurements were performed on a Varian 600 MHz NMR spectrometer. Prior to acquiring the spectra, the polymer solution of D_2O was filtered in order to remove any solid residues. The variable-temperature ^{1}H NMR spectra were recorded on heating the solution from 10 to 70 °C at an interval of three degrees. At each chosen temperature, the sample was allowed to thermally

equilibrate for 5 minutes before the measurements. Each of the ^{13}C NMR spectrums in Figure 2-4 was recorded at 20 °C over 6 days of signal averaging in order to increase the signal to noise ratio. Dynamic light scattering (DLS) measurements were performed on a Brookhaven BI-200 goniometer with vertically polarized incident light of wavelength λ=532nm supplied by an argon laser operating at 400 mW, and a Brookhaven BI-9000 digital autocorrelator. All measurements were carried out at 25 °C at a scattering angle of 90°, with the autocorrelation functions analyzed by using a non-negatively constrained least square algorithm. Prior to ultrasound irradiation, the BCP solution was filtered through a 0.22 μm membrane. Scanning electron microscopy (SEM, Inspect F, Philips) was used to observe the micellar aggregates in dried state, cast from BCP solution before and after the ultrasound irradiation. A fluorescence spectrometer (970 CRT, Shanghai Precision & Scientific Instruments) was used to record the steady-state emission spectra, with the excitation wavelength set at 540 nm, with excitation and emission slits set to 5 and 10 nm, respectively.

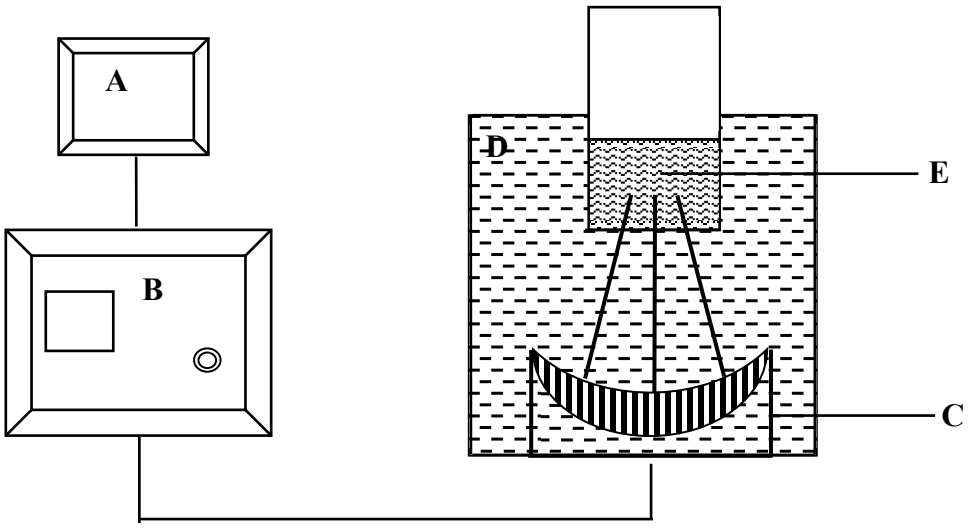

Figure 2-5. Schematic diagram of the setup used for HIFU irradiation of block copolymer micellar solution: arbitrary waveform generator (A), radio-frequency power amplifier (B), acoustic lens transducer (C), water bath (D) and polymer solution (E).

HIFU experiments: Figure 2-5 illustrates the setup used for the ultrasound irradiation of the BCP micellar solutions. HIFU was generated by a commercially available ultrasound apparatus that is comprised of three main components: an arbitrary waveform generator (33220A, Agilent), a RF power amplifier (A150, Electronics & Innovation) and an acoustic lens transducer (H-101, Sonic Concept, USA). The acoustic lens transducer could generate focused ultrasound beams of adjustable power (up to 100 W) at a high frequency of 1.1 MHz. The focal spot has a circular diameter of ~ 1.26 mm and a height of ~ 11 mm, and the focal length is about 63 mm. In all ultrasound irradiation experiments, the focal spot of the beams were positioned at the center of the micellar solution (4 mL) in a tube reactor immersed in a water tank. After the ultrasound irradiation, the tube reactor was removed from the water tank and the polymer solution was used for characterization.

2.2.5. Conclusion

In this work, we demonstrated a novel approach that amplifies the effect of HIFU on the disassembly of BCP micelles in aqueous solution. By introducing a small amount of ultrasound-labile co-monomer units into the micelle core-forming thermosensitive polymer, the ultrasound-induced reaction of the co-monomer increased the LCST of the thermosensitive polymer due to a polarity enhancement. Thus, the BCP becomes soluble in water and results in the disassembly of BCP micelles without any changes in the solution temperature. The validity of this new mechanism was shown by synthesizing and investigating a diblock copolymer of PEO_{112}-*b*-P(MEO_2MA_{189}-*co*-$THPMA_{21}$). A ^{13}C NMR spectral analysis provided critical evidence to show that the hydrolysis of THPMA groups occurs under HIFU irradiation and that the micellar disassembly originates from an increase in the LCST due to the ultrasound-induced conversion of hydrophobic co-monomer units of THPMA onto hydrophilic MAA. This approach of modulating the LCST by ultrasound is obviously general and can be applied by further exploring other ultrasound-labile moieties in the BCP design. This study thus established a new methodology to develop ultrasound-responsive BCP micelles.

Acknowledgement

YZ greately acknowledges the financial support from the Natural Sciences and Engineering Research Council of Canada (NSERC) and le Fonds québécois de la recherche sur la nature et les technologies of Québec (FQRNT). HX acknowledges financial support from the National Natural Science Foundation of China (51073100) and the Program for Changjiang Scholars and Innovative Research Team in University (IRT1163). JX thanks China Scholarship Council (CSC) for a scholarship allowing him to study in Canada. YZ is a member of the FQRNT-funded Center for Self-Assembled Chemical Structures and Centre québécois sur les matériaux fonctionnels (CQMF).

References

(1) Su, J.; Chen, F.; Cryns, V. L.; Messersmith, P. B. Catechol Polymers for pH-Responsive, Targeted Drug Delivery to Cancer Cells. *J. Am. Chem. Soc.* **2011**, *133*, 11850-11853.

(2) Zhou, K.; Wang, Y.; Huang, X.; Luby-Phelps, K.; Sumer, B. D.; Gao, J. Tunable, Ultrasensitive pH-Responsive Nanoparticles Targeting Specific Endocytic Organelles in Living Cells. *Angew. Chem. Int. Ed.* **2011**, *50*, 6109-6114.

(3) Eissa, A. M.; Khosravi, E. Synthesis of a New Smart Temperature Responsive Glycopolymer via Click-Polymerisation. *Eur. Polym. J.* **2011**, *47*, 61-69.

(4) Liu, X.; Zhou, T.; Du, Z.; Wei, Z.; Zhang, J. Recognition Ability of Temperature Responsive Molecularly Imprinted Polymer Hydrogels. *Soft Matter* **2011**, *7*, 1986-1993.

(5) Knezevic, N. Z.; Trewyn, B. G.; Lin, V. S. Y. Functionalized Mesoporous Silica Nanoparticle-Based Visible Light Responsive Controlled Release Delivery System. *Chem. Commun.* **2011**, *47*, 2817-2819.

(6) Yan, B.; Boyer, J.-C.; Branda, N. R.; Zhao, Y. Near-Infrared Light-Triggered Dissociation of Block Copolymer Micelles Using Upconverting Nanoparticles. *J. Am. Chem. Soc.* **2011**, *133*, 19714-19717.

(7) Coll, C.; Mondragón, L.; Martínez-Máñez, R.; Sancenón, F.; Marcos, M. D.; Soto, J.; Amorós, P.; Pérez-Payá, E. Enzyme-Mediated Controlled Release Systems by Anchoring Peptide Sequences on Mesoporous Silica Supports. *Angew. Chem. Int. Ed.* **2011**, *50*, 2138-2140.

(8) Pritchard, E. M.; Valentin, T.; Boison, D.; Kaplan, D. L. Incorporation of Proteinase Inhibitors into Silk-Based Delivery Devices for Enhanced Control of Degradation and Grug Release. *Biomaterials* **2011**, *32*, 909-918.

(9) Marin, A.; Sun, H.; Husseini, G. A.; Pitt, W. G.; Christensen, D. A.; Rapoport, N. Y. Drug Delivery in Pluronic Micelles: Effect of High-Frequency Ultrasound on Drug Release From Micelles and Intracellular Uptake. *J. Controlled Release* **2002**, *84*, 39-47.

(10) Rapoport, N. Combined Cancer Therapy by Micellar-Encapsulated Drug and Ultrasound. *Int. J. Pharm.* **2004**, *277*, 155-162.

(11) Rapoport, N.; Pitt, W. G.; Sun, H.; Nelson, J. L. Drug Delivery in Polymeric Micelles: from in vitro to in vivo. *J. Controlled Release* **2003**, *91*, 85-95.

(12) Li, Y.; Tong, R.; Xia, H.; Zhang, H.; Xuan, J. High Intensity Focused Ultrasound and Redox Dual Responsive Polymer Micelles. *Chem. Commun.* **2010**, *46*, 7739-7741.

(13) Zhang, H.; Xia, H.; Wang, J.; Li, Y. High Intensity Focused Ultrasound-Responsive Release Behavior of PLA-b-PEG Copolymer Micelles. *J. Controlled Release* **2009**, *139*, 31-39.

(14) Chen, D.; Wu, J. An in vitro Feasibility Study of Controlled Drug Release from Encapsulated Nanometer Liposomes Using High Intensity Focused Ultrasound. *Ultrasonics* **2010**, *50*, 744-749.

(15) Li, W.; Cai, X.; Kim, C.; Sun, G.; Zhang, Y.; Deng, R.; Yang, M.; Chen, J.; Achilefu, S.; Wang, L. V.; Xia, Y. Gold Nanocages Covered with Thermally-Responsive Polymers for Controlled Release by High-Intensity Focused Ultrasound. *Nanoscale* **2011**, *3*, 1724-1730.

(16) Moon, G. D.; Choi, S.-W.; Cai, X.; Li, W.; Cho, E. C.; Jeong, U.; Wang, L. V.; Xia, Y. A New Theranostic System Based on Gold Nanocages and Phase-Change Materials with Unique Features for Photoacoustic Imaging and Controlled Release. *J. Am. Chem. Soc.* **2011**, *133*,

4762-4765.

(17) Black Ramirez, A. L.; Ogle, J. W.; Schmitt, A. L.; Lenhardt, J. M.; Cashion, M. P.; Mahanthappa, M. K.; Craig, S. L. Microstructure of Copolymers Formed by the Reagentless, Mechanochemical Remodeling of Homopolymers via Pulsed Ultrasound. *ACS Macro Letters* **2011**, *1*, 23-27.

(18) Brantley, J. N.; Wiggins, K. M.; Bielawski, C. W. Unclicking the Click: Mechanically Facilitated 1,3-Dipolar Cycloreversions. *Science* **2011**, *333*, 1606-1608.

(19) Hickenboth, C. R.; Moore, J. S.; White, S. R.; Sottos, N. R.; Baudry, J.; Wilson, S. R. Biasing Reaction Pathways with Mechanical Force. *Nature* **2007**, *446*, 423-427.

(20) Han, D.; Tong, X.; Zhao, Y. Block Copolymer Micelles with a Dual-Stimuli-Responsive Core for Fast or Slow Degradation. *Langmuir* **2012**, *28*, 2327-2331.

(21) Wang, J.; Pelletier, M.; Zhang, H.; Xia, H.; Zhao, Y. High-Frequency Ultrasound-Responsive Block Copolymer Micelle. *Langmuir* **2009**, *25*, 13201-13205.

(22) Xuan, J.; Pelletier, M.; Xia, H.; Zhao, Y. Ultrasound-Induced Disruption of Amphiphilic Block Copolymer Micelles. *Macromol. Chem. Phy.* **2011**, *212*, 498-506.

(23) Magnusson, J. P.; Khan, A.; Pasparakis, G.; Saeed, A. O.; Wang, W.; Alexander, C. Ion-Sensitive "Isothermal" Responsive Polymers Prepared in Water. *J. Am. Chem. Soc.* **2008**, *130*, 10852-10853.

(24) Sagle, L. B.; Zhang, Y.; Litosh, V. A.; Chen, X.; Cho, Y.; Cremer, P. S. Investigating the Hydrogen-Bonding Model of Urea Denaturation. *J. Am. Chem. Soc.* **2009**, *131*, 9304-9310.

(25) Yamamoto, S.-i.; Pietrasik, J.; Matyjaszewski, K. Temperature- and pH-Responsive Dense Copolymer Brushes Prepared by ATRP. *Macromolecules* **2008**, *41*, 7013-7020.

(26) Zhao, Y.; Tremblay, L.; Zhao, Y. Phototunable LCST of Water-Soluble Polymers: Exploring a Topological Effect. *Macromolecules* **2011**, *44*, 4007-4011.

(27) Tian, Y.; Watanabe, K.; Kong, X.; Abe, J.; Iyoda, T. Synthesis, Nanostructures, and Functionality of Amphiphilic Liquid Crystalline Block Copolymers with Azobenzene Moieties.

Macromolecules **2002**, *35*, 3739-3747.

(28) H. Friebolin; *Basic one- and two-dimensional NMR spectroscopy, 5th edition, p68*.

2.3 Conclusion of the Project

In this work, we have demonstrated a novel approach that allows for amplification of the effect of HIFU irradiation on the disassembly of BCP micelles in aqueous solution. By introducing a small amount of ultrasound-labile co-monomer units into the thermosensitive polymer that forms the micelle core at a solution temperature above the LCST, ultrasound-induced reaction of the co-monomer units could increase the phase transition temperature of the thermosensitive polymer above the solution temperature due to a polarity enhancement. As a result, the BCP became soluble in water and its micelles could be disassembled without changing the solution temperature. The validity of this new mechanism was shown by using a thermo- and ultrasound- responsive diblock copolymer of PEO-*b*-P(MEO_2MA-*co*-THPMA). A ^{13}C NMR spectral analysis provided critical evidence for the hydrolysis of THPMA groups occurring under HIFU irradiation, showing that the micellar disassembly originates from an increase in the LCST due to the ultrasound-induced conversion of hydrophobic co-monomer units of THPMA onto hydrophilic MAA. This study thus established a new methodology based on modulating the LCST of the micelle core-forming polymer, which contributes to developing sensitive ultrasound-responsive BCP micelles.

CHAPTER 3. DUAL-STIMULI-RESPONSIVE MICELLE OF AN ABC TRIBLOCK COPOLYMER BEARING A REDOX-CLEAVABLE UNIT AND A PHOTO-CLEAVABLE UNIT AT TWO BLOCK JUNCTIONS

3.1. About the Project

Although BCP micelles reacting to the various stimuli have been extensively studied in recent years, making their disruption under the action of stimuli in a more efficient, more controllable or more predictable way is still a main challenge. For whatever the stimuli, the concentrations of stimuli-reactive moieties in the BCP structures are generally high, which may be problematic. For instance, the incorporation of a large amount of moieties in a BCP structure for the sensitivity to a given stimulus may alter other useful properties of the polymer or cause cytotoxicity that hinders biomedical applications of the BCP micelles. Therefore, it is of interest to develop approaches that can limit the number of stimuli-reactive groups in BCP structures while preserving the responsiveness of the micelles to the stimuli. This is not only for addressing the possible concerns but also interesting from the fundamental research point of view. For these reasons, in the present study, we designed, synthesized and investigated a novel amphiphilic ABC-type triblock copolymer system that contains a redox-cleavable disulfide function between the A and B blocks as well as a photocleavable *o*-nitrobenzyl (ONB) linkage between the B and C blocks. We show that this BCP design allows the BCP micelles to preserve the dual photo- and redox- responsive feature while requiring the use of the minimum number of stimuli-reactive moieties (two per polymer chain).

This work was published in *Langmuir* **2014**, *30*, 410−417, being authored by Juan Xuan, Dehui Han, Hesheng Xia, and Yue Zhao. This research work was conducted in the Université de Sherbrooke under the supervision of Prof. Zhao and co-supervision of Prof. Xia. The used block copolymer sample was synthesized by Dr. Han. I performed the rest of the experiments described in this publication. I wrote the first draft of the manuscript. Prof. Zhao finalized the manuscript with revision contributions from Prof. Xia.

3.2. Paper Published in Langmuir 2014, 30, 410

Dual-Stimuli-Responsive Micelle of an ABC Triblock Copolymer Bearing a Redox-Cleavable Unit and a Photo-Cleavable Unit at Two Block Junctions

Juan Xuan[1,2], Dehui Han[1], Hesheng Xia[2,*] and Yue Zhao[1,*]

xiahs@scu.edu.cn; yue.zhao@usherbrooke.ca

[1]Département de Chimie, Université de Sherbrooke, Sherbrooke, Québec, J1K 2R1, Canada

[2]State Key Laboratory State Key Laboratory of Polymer Materials Engineering, Polymer Research Institute, Sichuan University, Chengdu 610065, China

3.2.1. Abstract

The design, synthesis and study of a new dual-stimuli-responsible ABC-type triblock copolymer are reported. Using ATRP and click coupling reaction, the prepared copolymer is composed of poly(ethylene oxide) (PEO), polystyrene (PS) and poly[2-(dimethylamino)ethylmethacrylate] (PDMAEMA), and features a redox-cleavable disulfide junction between the PEO and PS blocks as well as a photocleavable *o*-nitrobenzyl linkage between the PS and PDMAEMA blocks. This design allows the triblock copolymer to respond to both a reducing agent like dithiothreitol (DTT) and UV light, while having the minimum number of stimuli-reactive moieties in the copolymer structure (two per chain). The disruption of the triblock copolymer micelles in aqueous solution was examined under the action of either UV light or DTT alone or combined use of the two stimuli. It was found that the removal of one type of hydrophilic polymer chains from the water-soluble corona of the micelles with a hydrophobic PS core, i.e., either redox-cleaved PEO or photocleaved PDMAEMA, could only result in a limited destabilization effect on the dispersion of the micelles. Severe aggregation of the polymer was observed only by applying the two stimuli converting the triblock copolymer onto three homopolymers. By monitoring the quenching by aqueous medium of the fluorescence of a hydrophobic dye (Nile Red) loaded in the triblock copolymer micelles, the effect on the payload release was also investigated of the different ways in which the micelles can be disrupted by the stimuli.

3.2.2. Introduction

Self-assembled block copolymer (BCP) micelles reacting to stimuli have been extensively studied due to their potential applications.[1-14] In recent years, a subject of interest in this area has been the development of BCP micelles that can be disrupted by two or more stimuli, which raises the level and complexity of control. Generally, such dual- or even multi-stimuli-responsiveness can readily be achieved by incorporating one or more stimuli-reactive moieties into the BCP structure, either as pendent groups or in the chain backbone.[15-24] What is more challenging, however, is to make BCP micelles undergo more efficient and more controllable disruption in response to stimuli. For this purpose, fundamental studies on rational structural design of BCPs remain a necessity.

In a previous study,[15] we reported the design and investigation of an amphiphilic ABA-type triblock copolymer of which the hydrophobic middle block contains a photocleavable *o*-nitrobenzyl (ONB) moiety and a redox-cleavable disulfide linkage in *each* of the repeating unit. With this high level of content for the two types of stimuli-reactive moieties, micelles of this BCP can be degraded either quickly by UV light or relatively slowly by a reducing agent. While a high concentration of stimuli-responsive groups in the BCP structure may be required for a number of possible applications, such as fast micellar degradation for "burst" release of payloads,[25] it may be desirable to limit their contents in other circumstances in order to, for example, reduce the possible cytotoxicity caused by the presence of a high concentration of photochromic moieties. Therefore, it is of fundamental interest to develop strategies in designing BCP structures that require the incorporation of low-content stimuli-reactive groups. To this regard, a nicely demonstrated approach consists in using a stimuli-breakable unit that links the hydrophilic and hydrophobic blocks constituting a diblock copolymer.[26-38] Since there is only one stimuli-breakable unit per chain and the cleavage basically destroys the amphiphilic BCP by breaking it onto two homopolymers, this strategy arguably is the most effective in using the minimum amount of stimuli-reactive groups to provoke the maximum disruption effect on the BCP structure and its assemblies in solution. A number of studies based on this strategy with a given type of cleavable linkage, including ONB[26-32] and disulfide,[33-39] have been reported in recent years.

Considering the above issues and being motivated by the challenge, in this paper, we report on the design, synthesis and investigation of a novel amphiphilic ABC-type triblock copolymer that contains a redox-cleavable disulfide function between the A and B blocks as well as a photocleavable ONB linkage between the B and C blocks. This design allows one to preserve the dual-stimuli-responsive feature while making use of the cleavable-block-junction approach to minimize the contents of ONB and disulfide groups. Therefore, the resulting BCP micelles differ from either those having only one type of cleavable linkage between the hydrophilic and hydrophobic blocks,[26,28,31,36,38] or those having a high content for the two types of cleavable moieties.[15] To the best of our knowledge, our study is the first demonstration of this type of BCPs. In addition to the BCP synthesis, we report the results on the disruption of the BCP micelles and the release of payloads under either the selective stimulation using one stimulus

(light or redox) or combined application of the two stimuli.

3.2.3. Experimental

Design of the Triblock Copolymer

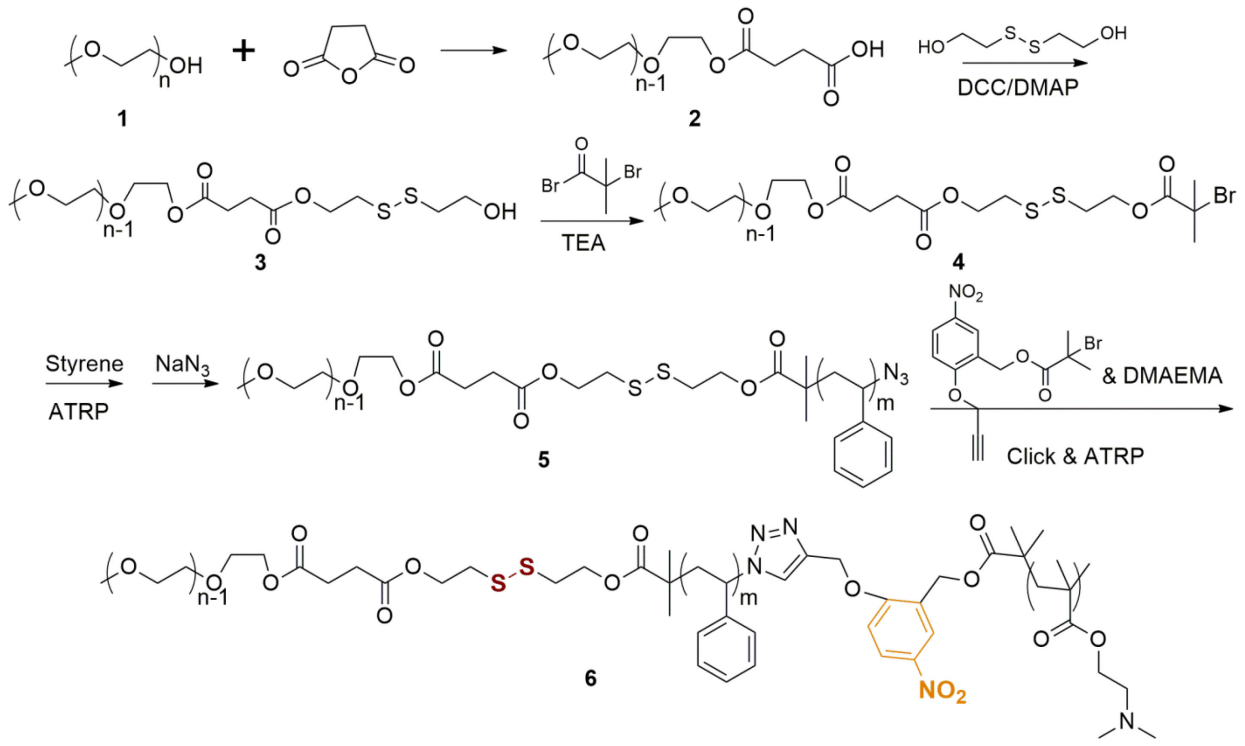

Scheme 3-1. Synthesis of the amphiphilic ABC-type triblock copolymer with a redox-cleavable disulfide and a photocleavable *o*-nitrobenzyl (ONB) group at the two junctions of the three blocks.

The synthetic route to the new ABC-type triblock copolymer PEO-*S*-*S*-PS-*ONB*-PDMAEMA is shown in Scheme 3-1. Its structure is designed to have the middle hydrophobic polystyrene (PS) block linked to two hydrophilic polymers, i.e., poly(ethylene oxide) (PEO) and poly[2-(dimethylamino)ethylmethacrylate] (PDMAEMA), by a disulfide and an ONB moiety, respectively. With this structure, self-assembled micellar aggregates in aqueous solution are expected due to the amphiphilic nature of the BCP, while UV light and reducing agents can be used to cleave the two block junctions. Atom transfer radical polymerization (ATRP) and click

coupling reaction were utilized in the synthesis. Synthetic details are reported below.

Polymer Synthesis

Materials. Prior to use, tetrahydrofuran (THF, 99%) was refluxed with sodium and a small amount of benzophenone and distilled; triethylamine (TEA) (Aldrich, ≥99) was refluxed with *p*-toluenesulfonyl chloride (Fluka, ≥99%) and distilled; dichloromethane (DCM) was distilled from CaH_2; *N,N*-dimethylforamide (DMF, 99.8%) was dried with anhydrous magnesium sulphate and distilled under reduced pressure. Succinic anhydride (≥99%), 2-hydroxyethyl disulfide, *N*,*N*′-dicyclohexylcarbodiimide (DCC, 99%), α-bromoisobutyryl bromide (98%), 4-(dimethylamino)pyridine (DMAP, ≥99%), CuCl (≥99.995%), *N,N,N',N',N''*-pentamethyldiethylenetriamine (PMDETA, 99%) and ethanol (95%) were used without purification. Styrene (99.9%) and 2-(dimethylamino)ethyl methacrylate (DMAEMA, 99%) were purchased from Aldrich and passed through a basic aluminum oxide column prior to use. Poly(ethylene glycol) methyl ethers, MPEG2000 (M_n=2000 g/mol, Aldrich) was dried by azeotropic distillation using anhydrous toluene before use. The ONB compound functionalized with ATRP initiator and alkyne for clik reaction, namely, 5-propargylether-2-nitrobenzyl bromoisobutyrate (PNB), was synthesized according to a reported literature method.[31]

Synthesis of MPEO-OC(=O)CH_2CH_2COOH. PEO with one methyl terminal group and one chain end functionalized with carboxylic acid (***2*** in Scheme 3-1) was prepared by esterification reaction between MPEO and succinic anhydride. MPEO (M_n=2000 g/mol, 4.0 g) was dissolved in dried toluene (20 mL), and then succinic anhydride (2.0 g, 20 mmol) was added. The mixture was stirred at 60 ^oC for 20 h. Toluene was removed, and the residue was dissolved in CH_2Cl_2. This polymer solution was poured into petroleum ether to afford precipitate. The precipitation treatment was repeated three times for complete removal of excess succinic anhydride. The ^1H NMR spectrum of ***2*** is shown in Supporting Information (Fig.3-S1).

Synthesis of MPEO-OC(=O)CH_2CH_2CC(=O)OCH_2CH_2S-SCH_2CH_2OH. PEO containing a disulfide unit (***3*** in Scheme 3-1) was then synthesized by using esterification reaction between ***2*** and 2-hydroxyethyl disulfide in the presence of DCC/DMAP. ***2*** (3.6 g, 1.8 mmol) and

2-hydroxyethyl disulfide (2.8 g, 18.2 mmol) were dissolved in 100 mL of anhydrous DCM. DCC (0.38 g, 1.8 mmol) and DMAP (0.02 g, 0.18 mmol) were added to the solution in presence of argon. The mixture was stirred at room temperature for 48 h. During this period, the reaction mixture slowly turned yellow and insoluble DCC urea precipitated. After filtration to remove the solid, the polymer was precipitated in diethyl ether to remove excess 2-hydroxyethyl disulfide. After being redissolved in THF, the polymer was precipitated again in hexane to remove DCC and DCC urea. This purification procedure was repeated three times, and the polymer collected by filtration was dried in a vacuum oven for 24 h at room temperature, yielding a white powder (2.6 g, 85%). The polymer structure was confirmed by ^{1}H NMR analysis (Fig.3-S2). For this reaction, in order to avoid the possible coupling reaction of acid-terminated PEG (***2*** in Scheme 1) with hydroxyl-terminated PEG (***3*** in Scheme 1), ten-time excess of 2-hydroxyethyl disulfide was used to ensure that the terminal acid group of PEG could easily react with the small molecule of 2-hydroxyethyl disulfide while rendering the coupling reaction between acid- and hydroxyl-terminated PEG unlikely. ^{1}H NMR and GPC measurements confirmed the absence of the coupling side-reaction.

Synthesis of Disulfide-Containing PEO ATRP Macroinitiator. PEO ATRP macroinitiator bearing a disulfide unit (***4*** in Scheme 3-1) was synthesized by reaction of ***3*** with α-bromoisobutyryl bromide in the presence of TEA. Into a 100 mL round-bottom flask with a magnetic stirrer, ***3*** (2.8 g, 1.4 mmol), TEA (0.5 mL, 3.6 mmol), and CH_2Cl_2 (30 mL) were added. After the mixture was cooled to 0 ^oC, α-bromoisobutyryl bromide (0.20 mL, 1.6 mmol) was added dropwise over a period of 10 min. The reaction mixture was then brought back to room temperature and stirred for 24 h. The salt formed was removed by filtration, and the filtrate was washed with NaCl solution several times. The organic phase was then dried over $MgSO_4$. After concentrating the filtrate under reduced pressure, the product was obtained by precipitation into diethyl ether. It was further dissolved in CH_2Cl_2 for precipitation purification in diethyl ether. The polymer structure was characterized by using ^{1}H NMR (Fig.3-S3).

Synthesis of PEO-*S*-*S*-PS-N_3. To obtain the triblock copolymer PEO-*S*-*S*-PS-*ONB*-PDMAEMA, the PEO-*S*-*S*-PS diblock of PEO and PS was first prepared by using the PEO macroinitiator to

grow the PS block. For this reaction: PEO_{45}-S-S-C(=O)$OC(CH_3)_2$-Br (0.26 g, 0.13 mmol), CuCl (16.0 mg, 0.16 mmol), styrene (8.0 g, 76.8 mmol), PMDETA (27.60 mg, 0.16 mmol) and anisole (4.0 mL) were added successively into a 10-mL flask. The reaction mixture was degassed by three-pump-thaw cycles, back-filled with N_2 and placed in an oil bath thermostated at 100 °C for 12 h. It was then diluted with THF and passed through a column of neutral alumina to remove the metal salt. After precipitation by adding the polymer solution of THF into methanol, the white diblock copolymer was collected by filtration and then dried under vacuum overnight (5.6 g, yield: 67.8 %). The ^{1}H NMR spectroscopic analysis found the diblock composition to be PEO_{45}-*S*-*S*-PS_{430}-Cl. Afterwards, azide group-ended diblock copolymer PEO_{45}-*S*-*S*-PS_{430}-N_3 (***5*** in Scheme 3-1) was obtained as follows: PEO_{45}-*S*-*S*-PS_{430}-Cl (2.80 g, 0.06 mmol), NaN_3 (0.039 g, 0.6 mmol), and DMF (6.0 mL) were added into a 10-mL round bottle flask with a magnetic stirrer, and the reaction mixture was stirred for 24 h at room temperature. After purification by precipitation of the polymer solution into methanol twice, PEO_{45}-*S*-*S*-PS_{430}-N_3 was obtained (white solid, 2.3 g, yield 82 %). The ^{1}H NMR spectrum of the diblock copolymer is given in Figure 3-S4.

Synthesis of PEO-*S*-*S*-PS-*ONB*-PDMAEMA. As shown in Scheme 3-1, the targeted triblock copolymer PEO-*S*-*S*-PS-*ONB*-PDMAEMA was synthesized by simultaneous ATRP and click reaction in one pot following the literature method.[31] In this step, an ONB compound substituted with both an alkyne and a bromine group, namely, 5-propargylether-2-nitrobenzyl bromoisobutyrate (PNB), was used to polymerize DMAEMA and in the same time, link the PDMAEMA block to the PEO-*S*-*S*-PS diblock via the ONB linkage. A typical synthesis was as follows. PEO_{45}-*S*-*S*-PSt_{430}-N_3 (0.68g, 0.012 mmol), CuCl (2.2 mg, 0.022 mmol), PNB (4.8 mg, 0.013 mmol), DMAEMA (0.36 g, 2.3 mmol), PMDETA (3.8 mg, 0.022 mmol) and THF (4.0 mL) were added successively into a 10-mL flask. The reaction mixture was degassed by three-pump-thaw cycles, back-filled with N_2 and placed in an oil bath thermostated at 60 °C for 22 h. The polymerization was quenched quickly by cooling the mixture with iced-water. It was then diluted with THF and passed through a column of neutral alumina to remove the metal salt. After precipitation by adding the polymer solution of THF into ether, the light yellow-colored triblock copolymer was collected and then dried under vacuum overnight (0.76 g, yield: 73.0 %). ^{1}H NMR

analysis determined the triblock copolymer composition to be PEO_{45}-*S*-*S*-PS_{430}-*ONB*-$PDMAEMA_{80}$. Its ^1H NMR spectrum is given in Figure 3-S5.

Preparation of Dye-Loaded Micelles and Characterization Techniques

Triblock copolymer micelles loaded with the Nile Red (NR) dye were prepared in the following way. PEO_{45}-*S*-*S*-PS_{430}-*ONB*-$PDMAEMA_{80}$ (2 mg) and NR (0.25 mg) were first dissolved in THF (1 mL) that is a good solvent for the three blocks and the dye. Then the solution was added quickly to pure water (10 mL) under ultrasonic agitation using an ultrasonic cleaner (50 Hz). The whole solution was stirred at room temperature overnight to completely remove THF by evaporation. The obtained aqueous solution was the filtered through a filter paper (0.45 μm pore size) to remove NR not solubilzed by the micelles. The final dye-loaded micellar solution was adjusted to reach a BCP concentration of 0.2 mg/mL and stored in dark before use. Triblock copolymer micelles without loaded NR were prepared using the same procedure.

Changes in the absorption spectrum with the irradiation time and the optical transmittance (measured at 600 nm) of a given polymer solution were monitored using a Varian 50 Bio UV-Vis spectrophotometer. Fluorescence emission spectra were recorded on a Varian Cary Eclipse Fluorescence spectrophotometer. DLS measurements were performed on a Malvern Zetasizer Nano ZS ZEN3600 dynamic light scattering particle sizer with a helium-neon laser (wavelength, λ= 633 nm). All measurements were carried out at a scattering angle of 173°. The morphologies of the polymer micelles were examined using a Hitachi H-7500 transmission electron microscope (TEM) operating at 60 kV. Samples for TEM observations were prepared by casting a drop of a given micelle solution on a TEM copper grid with formvar/carbon support film (200 mesh, from Electron Microscopy Sciences), with the excess solution removed by using a filter paper and the sample dried at room temperature overnight. ^1H NMR spectra were recorded on a Bruker 300MHz spectrometer using deuterated chloroform as the solvent and tetramethylsilane as the internal standard. Size exclusion chromatograph (SEC) measurements were performed on a Waters system equipped with a photodiode array detector (PDA 996) and a refractive index detector (RI 410). THF was used as the eluent at an elution rate of 1 mL/min, while PS standards were used for

calibration. For photoinduced cleavage of the triblock copolymer, UV light from a Novacure spot-curing system (300-390 nm filter with maximum around 360 nm, 200 mW/cm^2) was utilized.

3.2.4. Results and Discussion

Photo- and Redox-Cleavage of Block Junctions

The obtained PEO_{45}-*S*-*S*-PS_{430}-*ONB*-$PDMAEMA_{80}$ triblock copolymer was expected to undergo two controlled block junction cleavages under the effect of UV light and a reducing agent. Scheme 3-2 shows the two-step cleavage reactions of the triblock into three homopolymers when UV light is applied to and dithiothreitol (DTT) is introduced in the polymer solution in a sequential way. A complete photocleavage of the ONB junction should result in a mixture of the PEO-*S*-*S*-PS diblock and PDMAEMA, while the subsequent redox-induced cleavage of the disulfide linkage should further break the diblock into PEO and PS.

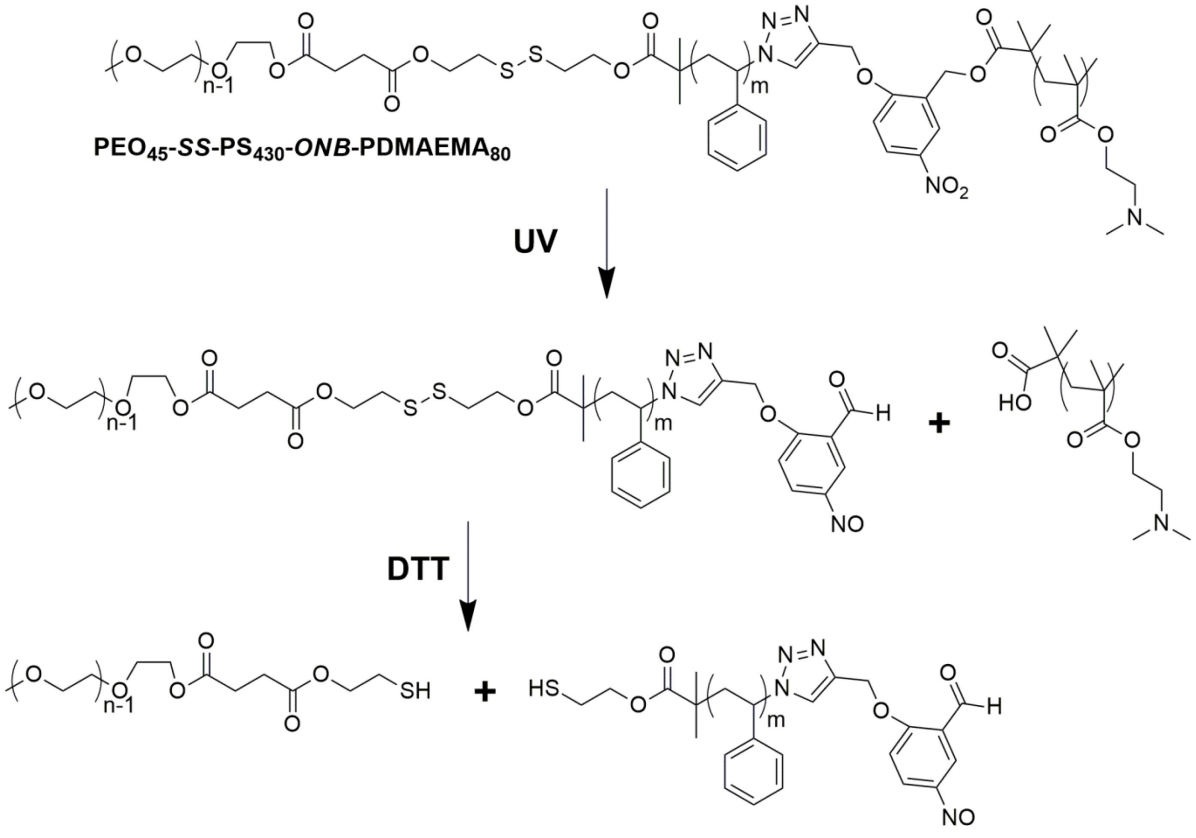

Scheme 3-2. Expected photo- and redox-induced cleavage reactions at the junctions of the PEO_{45}-*S*-*S*-PS_{430}-*ONB*-$PDMAEMA_{80}$ triblock copolymer under subsequent UV light exposure and

reduction by dithiothreitol (DTT).

Experiments were first carried out to investigate the cleavage reactions triggered by the two stimuli. Figure 3-1 shows the SEC and UV-vis spectroscopic results. After 1 h UV irradiation of the triblock copolymer in CH_2Cl_2 (2 mg/mL, 1.5 mL solution), the elution peak appears at longer times indicating reduced molecular weights. However, there are no two distinct peaks (Figure 3-1a). Assuming that the ONB block junction is cleaved by UV light, the results suggest that the PEO-*S*-*S*-PS diblock and the PDMAEMA have similar hydrodynamic volume so that their elution peaks are mostly superimposed. The occurrence of the photocleavage was confirmed by the UV-vis spectra of the same triblock copolymer solution expose to UV light (Figure 3-1b). As

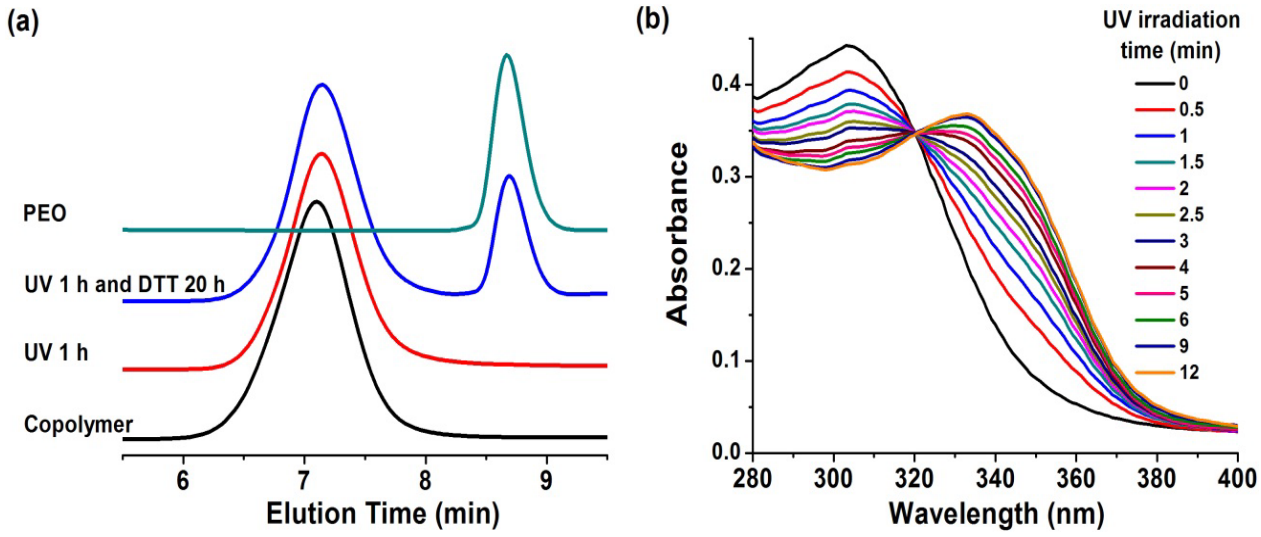

Figure 3-1. (a) Size exclusion chromatograph (SEC) traces of the triblock copolymer PEO-*S*-*S*-PS-*ONB*-PDMAEMA, up from the bottom: before UV exposure, after 1 h UV exposure, after 20 h reaction with DTT and, for comparison, the PEO block (M_n=2000 g/mol). The UV irradiation was performed on the triblock copolymer in CH_2Cl_2 (2 mg/mL) and DTT was added in THF solution of the triblock copolymer (7.5 mg/mL, the weight ratio of DTT to the polymer was 3.75:1). (b) UV-vis absorption spectra of the triblock copolymer in CH_2Cl_2 (2 mg/mL, 1.5 mL)

recorded at various UV irradiation times.

the UV irradiation time increased, the characteristic absorption band of ONB near 303 nm decreased, which was accompanied by the rise of the absorption band of the resulting nitroso compound (Scheme 3-2) at around 340 nm. By contrast, the DTT-induced cleavage of the disulfide block junction was visible from the SEC results. After 1 h UV irradiation, the CH_2Cl_2 solvent was removed and the remaining polymer was re-dissolved in THF with DTT added (DTT/polymer=3.75/1, w/w). After 20 h reaction, the SEC measurement displays a new elution peak at longer times that correspond to that of the PEO block used to prepare the triblock copolymer. Therefore, the results in Figure 3-1 confirm that the photoinduced cleavage of the ONB linkage and the redox-induced breaking of the disulfide junction take place under the action of UV light and DTT, respectively.

Effect of Photo- or Redox-Cleavage alone on Triblock Copolymer Micelles

Due to the amphiphilic nature of PEO-*S*-*S*-PS-*ONB*-PDMAEMA, with the two hydrophilic end blocks of PEO and PDMAEMA and the hydrophobic middle block of PS, the copolymer can form stable micelles in aqueous solution, being composed of a PS core and a mixed PEO and PDMAEMA corona. Firstly, by means of DLS, we investigated how the cleavage of one end block, either PEO by using DTT or PDMAEMA by UV light, could disrupt the micelles. For the UV irradiation experiments (Fig.3-2a), micelles of the triblock copolymer having two different average D_H of 24 and 38 nm were obtained by changing the preparation conditions (smaller micelles were obtained by increasing the volume of water while keeping the polymer concentration in the added THF solution and other conditions the same). In both cases, exposing the UV light to the micelle solution, the apparent micellar size increased quickly within the first 5 min, reaching about 46 and 54 nm, respectively. However, prolonged UV irradiation time resulted in no further increase in D_H. This result suggests that removal of the PDMAEMA chains from the corona have limited effect on the micelle. Similar results were obtained by cleaving the PEO chains using DTT from the micellar corona (Fig.3-2b): the redox reaction induced an increase in

the apparent size of micelles. With the small DTT/polymer ratio of 0.25, no significant effect was observable. When the ratio increased to 1.25, the increase in D_H became more prominent. With the ratio further increased to 3.75, an effect on the micelles similar to the UV irradiation was observed. Likewise, longer DTT reaction time, up to 20 h (Fig.3-2c), had little effect on D_H. The DLS results indicate that 1) as designed, the micelles of PEO-*S*-*S*-PS-*ONB*-PDMAEMA are responsive to both UV light and a reducing agent like DTT, and 2) however, the removal from the micelle corona of either the PDMAEMA chains by the block junction photocleavage or the PEO chains with the block junction redox-cleavage cannot impose a severe disruption of the micelles, inducing instead a limited increase in the apparent sizes of the micelles.

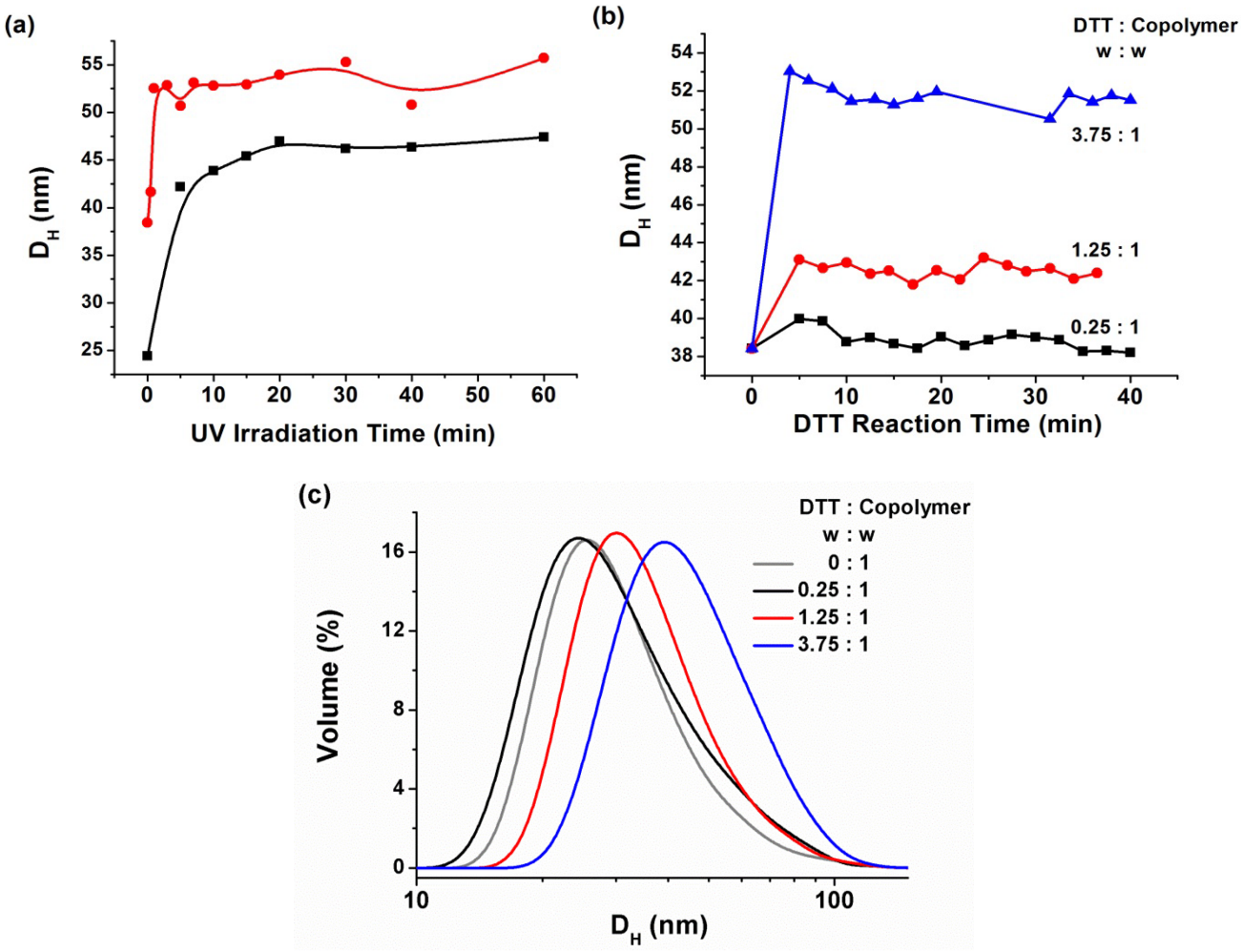

Figure 3-2. Dynamic light scattering (DLS) results showing the apparent changes in the size (hydrodynamic diameter D_H) of the micellar aggregates of PEO-*S*-*S*-PS-*ONB*-PDMAEMA in response to UV exposure (200 mW/cm^2) or the presence of DTT: (a) D_H vs. UV irradiation time

for two sets of micelles of different initial sizes; (b) D_H vs. reduction reaction time for the same micelle solution with different amounts of DTT; and (c) size distribution of the micelles for the solutions in (b) after 20 h reaction as compared to the solution before adding DTT. All solutions had a block copolymer concentration of 0.2 mg/mL and the solution volume was 2 mL for the measurements.

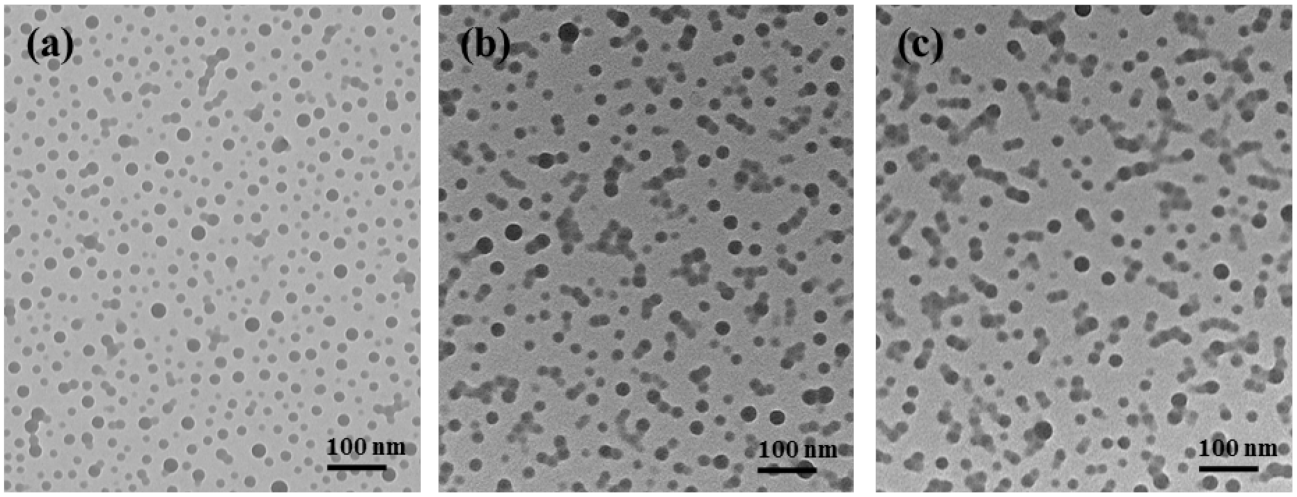

Figure 3-3. TEM images of (a) micelle solution without any treatment; (b) after UV irradiation for 1 h (200 mW/cm^2); and (c) after DTT treatment for 20 h (DTT:polymer=3.75:1).

The TEM images in Figure 3-3 provided us with more insight into the effect of photocleavage or redox-cleavage alone on the micelles of PEO-*S*-*S*-PS-*ONB*-PDMAEMA. With all samples prepared under the same conditions, it is seen that after either UV irradiation (image b) or redox reaction with DTT (image c), micelles essentially remained intact with good dispersion. However, as compared to the micelle solution without UV or DTT treatment (image a), more aggregates of a few micelles appear, which could account for the increase in the apparent average size of micelles (Fig.3-2). Combining the results of DLS and TEM, what follows seems to be a plausible explanation. The removal of either PDMAEMA or PEO chains, which converts the triblock PEO-*S*-*S*-PS-*ONB*-PDMAEMA onto the diblock PEO-*S*-*S*-PS and PS-*ONB*-PDMAEMA, respectively, could change the polymer's hydrophilic-hydrophobic balance. This changing amphiphilicity could give rise to a destabilization effect for the micelles, which results in a limited

aggregation between a few micelles in solution. However, good dispersion of the micelles remains because the destabilization effect is not strong enough to induce, for example, coalescence and precipitation of the aggregates. Indeed, the micelle solution after either UV irradiation or DTT reaction (Fig.3-2) displayed only a small decease in transmittance (Fig.3-4).

Effect of Combined Photo- and Redox-Cleavage on Triblock Copolymer Micelles

According to the design of PEO-*S*-*S*-PS-*ONB*-PDMAEMA, if both the photocleavage and the redox-cleavage at the two block junctions occur, the triblock copolymer is degraded into three homopolymers and, consequently, any self-assembled structures due to the amphiphilicity should be severely disrupted. This indeed was found to be the case when the polymer micelle solution was exposed to the two stimuli of UV light and redox agent subsequently, in either order of DTT-first and UV-second or vice versa. Figure 3-4 shows the change in transmittance of the polymer micelle solution as a function of the reaction time with DTT, for micelles with two different initial sizes (average D_H=24 and 38 nm respectively). Without UV irradiation, the transmittance for both micelle solutions decreased slightly over time indicating limited

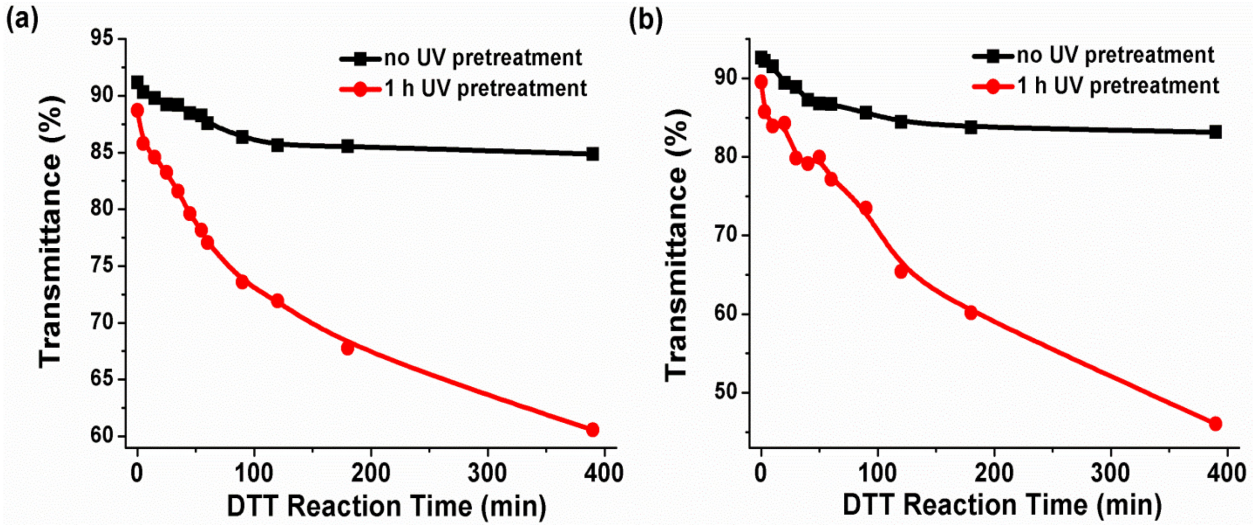

Figure 3-4. Transmittance (at 600 nm) vs DTT reaction time for a triblock copolymer micelle solution (DTT:polymer=3.75:1) without (black line) and with (red line) a UV pretreatment of 1 h before adding DTT. The experiments were carried out on micelles of two different average sizes:

D_H=24 nm (a) and 38 nm (b).

aggregation, which is consistent with the results in Figures 3-2 and 3-3. By contrast, when the two solutions were pretreated with UV irradiation for 1 h, which in itself also resulted in slight transmittance decrease, subsequent reaction with DTT gave rise to a much greater reduction of the solution transmittance, which indicates the occurrence of more important aggregation of the micellar aggregates by applying the two stimuli-induced junction cleavages of the triblock copolymer.

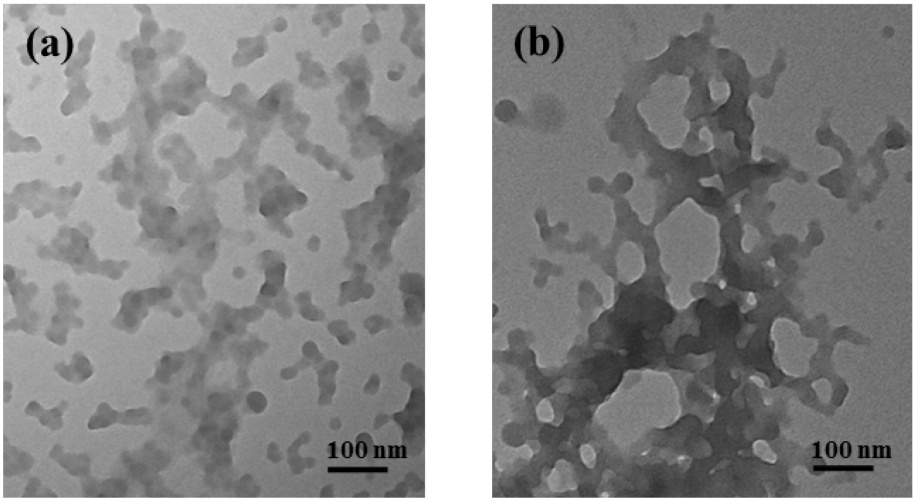

Figure 3-5. TEM images of (a) micelle solution exposed to UV light for 1 h (200 mW/cm^2) before addition of DTT for 20 h (DTT:polymer=3.75:1); and (b) the same solution treated in the reversed order, DTT for 20 h followed by 1 h UV irradiation, under otherwise the same conditions.

This was further confirmed by TEM observations as shown in Figure 3-5. For the same micelle solution (micelle size: D_H=38 nm), when it was exposed to UV light for 1 h, followed by 20 h reaction with DTT (image a), or treated in the reversed order, i.e., reaction with DTT followed by UV irradiation (image b), large and irregularly-shaped aggregates were found from the TEM images, with only a few discernible micelles. These results indicate that the triblock copolymer

micelles can be severely disrupted by sequential application of the two stimuli for photo- and redox-cleavage. We mention that in the UV-first and redox-second order, the reaction with DTT took place with the UV light turned off. By contrast, in the redox-first and UV-second order, UV light was exposed to the solution containing DTT. In other words, in the former the two stimuli were applied sequentially, while in the latter case, they acted simultaneously when UV light was applied. The results indicate that either way activating the two block junction cleavages can exert basically the same disruption effect on the micelles.

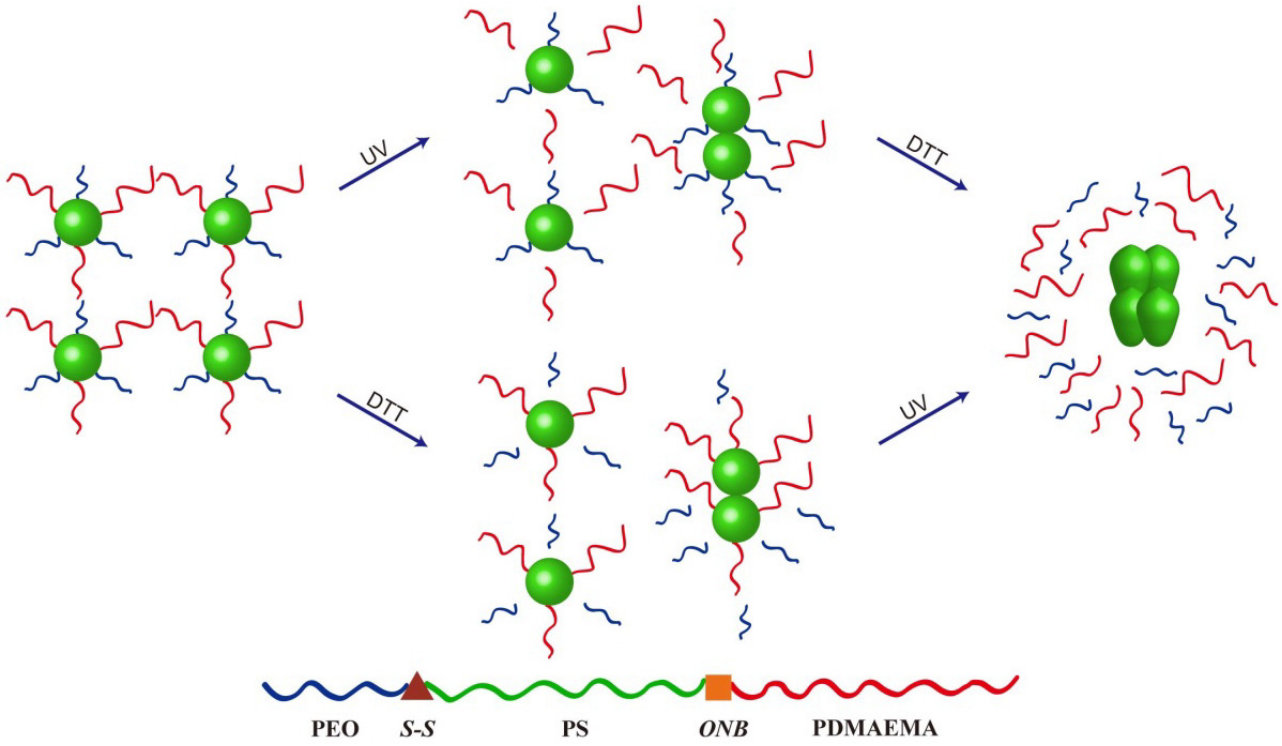

Figure 3-6. Schematic recapitulation of the photo- and redox-responsive behaviors of PEO-*S*-*S*-PS-*ONB*-PDMAEMA micelles in aqueous solution.

Figure 3-6 presents a schematic recapitulation of how the micelles of PEO-*S*-*S*-PS-*ONB*-PDMAEMA can respond to the optical and redox stimuli in different ways. When one of the stimuli is applied to cleave one of the two hydrophilic blocks, part of the micelle corona is removed, which perturbs the hydrophilic-hydrophobic balance and results in a slight destabilization effect. The consequence is a limited aggregation between a few micelles, while the

whole micellar dispersion remains stable. Following either UV irradiation or reaction with DTT, if the second stimulus is applied to cleave the remaining hydrophilic block in the micelle corona, hydrophobic cores can no longer be stabilized, which results in severe aggregation, and the initial spherical micelles are transformed on aggregates of irregular shapes.

Release of Loaded Dye Molecules upon Photo- and Redox-Stimulation

At last, we wanted to know how the different disruption behaviors of the triblock copolymer micelles could be related to stimuli-controlled release of hydrophobic compounds loaded in the micelles. The Nile Red dye was used for the purpose because it is a model compound often used for such investigations.[25,40-41] It fluoresces when solubilized by the hydrophobic micelle core, but the fluorescence emission intensity deceases when the micelle is disrupted brining the dye molecules in contact with water. Figure 3-7 summarizes representative results.

On the one hand, when only DTT was added in the micelle solution or only UV light was applied to irradiate the solution (Fig.3-7a), the fluorescence intensity of Nile Red decreased over the used reaction time of 1 h. Under the used experimental conditions, the decrease is more important with UV light than with DTT. This result suggests that even under a limited disruption of the micelles, as a result of either photocleavage or redox-cleavage alone, the micelle-encapsulated dye molecules undergo partial fluorescence quenching due to contact with, or, in a more general sense, release into an aqueous medium. It seems that the photocleavage imposes an effect that is more important than the redox reaction. On the other hand, when the two stimuli were used to disrupt the micelles more severely due to the photo- and redox-cleavage of the two hydrophilic blocks (Figs. 7b and 7c), the fluorescence quenching became more prominent, as expected. The kinetics of the decrease can easily be varied by reversing the order in which the two stimuli are applied. When the micelle solution was exposed to UV light first for 1 h and subsequently underwent the redox reaction with added DTT for another hour (Fig.3-7b), it is seen that most part of the fluorescence quenching was achieved during the UV irradiation. The subsequent DTT reaction only further quenched the fluorescence slowly. By contrast, when the micelle solution was first subjected to reaction with DTT before being exposed to the UV light (Fig.3-7c), the fluorescence

quenching developed quite slowly over even 4 h of redox reaction. The subsequent application of the UV light gave rise to a sharp decrease in the fluorescence intensity over the period of 1 h. The results in Figure 3-7 show that it is possible to use only either stimulus or combine the two stimuli in different ways to obtain various dye release kinetics or profiles. In principle, this flexibility in using stimuli to impart controlled release of micelle payloads is of interest.

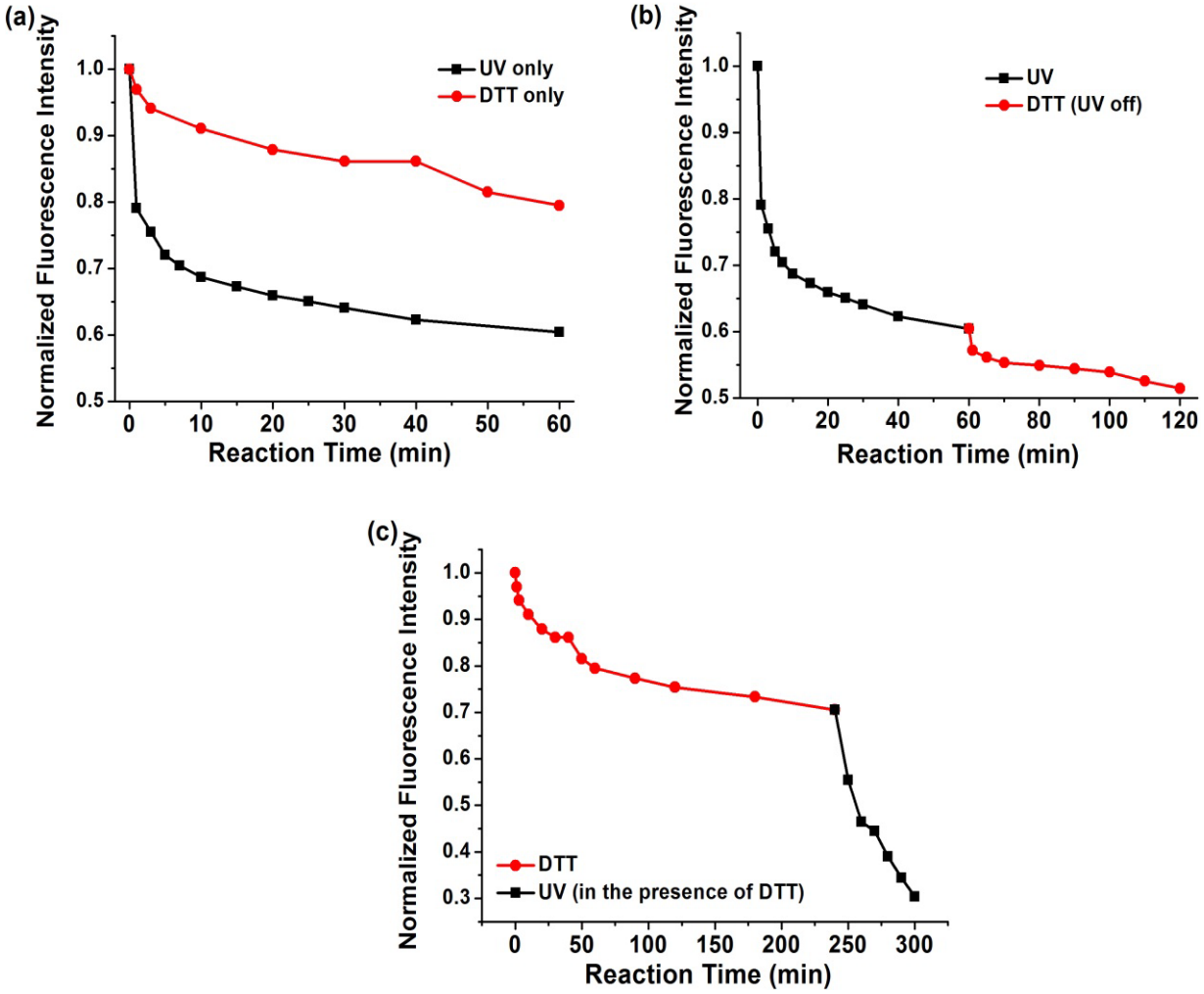

Figure 3-7. Change in the fluorescence emission intensity of Nile Red loaded in the micelles of PEO-*S*-*S*-PS-*ONB*-PDMAEMA in aqueous solution over photo- or redox reaction time (λ_{ex}= 520 nm): (a) only with DTT or only under UV irradiation; (b) under UV irradiation followed by reaction with DTT, and (c) with DTT followed by UV irradiation. All other experimental conditions were the same: polymer concentration of 0.2 mg/mL, micelle solution volume of 2 mL,

UV light intensity of 200 mW/cm^2 and DTT:polymer (weight ratio)=3.75:1. The fluorescence intensity of Nile Red measured over time was normalized with respect to the emission intensity of the initial solution before application of any stimulus.

3.2.5. Conclusion

We have designed and synthesized a new amphiphilic ABC-type triblock copolymer of PEO-*S*-*S*-PS-*ONB*-PDMAEMA, which features a redox-cleavable disulfide and a photocleavable ONB group at the two junctions of the three blocks. We showed that this design is a useful strategy to allow a triblock copolymer and its self-assembled micelles to respond to both a reducing agent like DTT in solution and exposure to UV light while having the *minimum* number of stimuli-reactive moieties in the block copolymer structure (two units per chain). Our investigations found that the micelles of this triblock copolymer could be disrupted in different ways. When only one stimulus is applied, the removal of one type of hydrophilic polymer chains from the micelle corona, either PEO by redox-cleavage or PDMAEMA by photocleavage, results in a limited destabilization effect on the dispersion of the micelles. The agglomeration between a few micelles appears but the dispersion remains essentially stable. By contrast, under combined use of the two stimuli that cleaves both PEO and PDMAEMA, severe polymer aggregation occurs as a result of elimination of the polymer amphiphilicity. Moreover, by loading the hydrophobic Nile Red in the micelles, the fluorescence quenching of the dye by aqueous medium under the different uses of the two stimuli appeared to correlate with the different extents of the micellar disruption.

3.2.6. Supporting Information

^{1}H NMR spectra. This material is available free of charge via the Internet at http://pubs.acs. org.

1. ^{1}H NMR Spectra

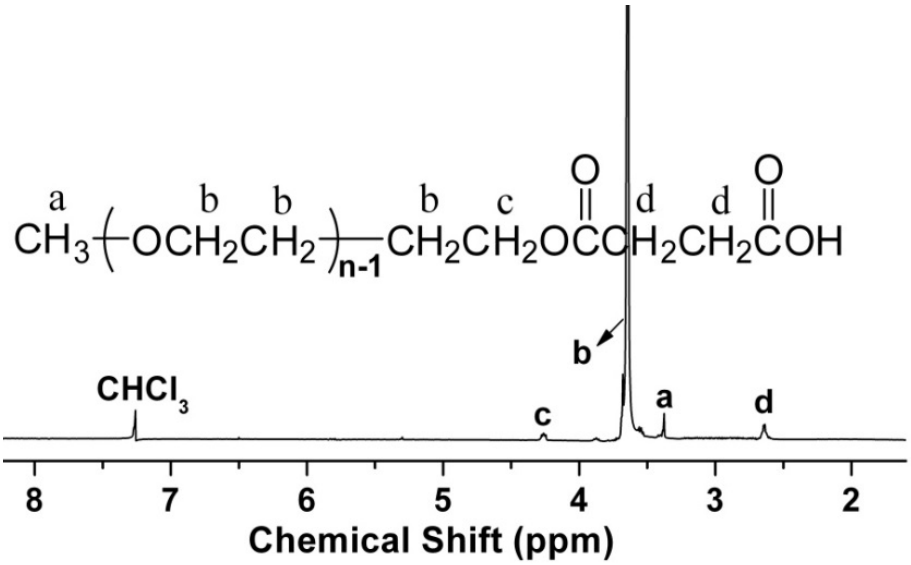

Figure 3-S1. ^{1}H NMR spectrum of MPEO-OC(=O)CH_2CH_2COOH in $CDCl_3$ (***2*** in Scheme 3-1).

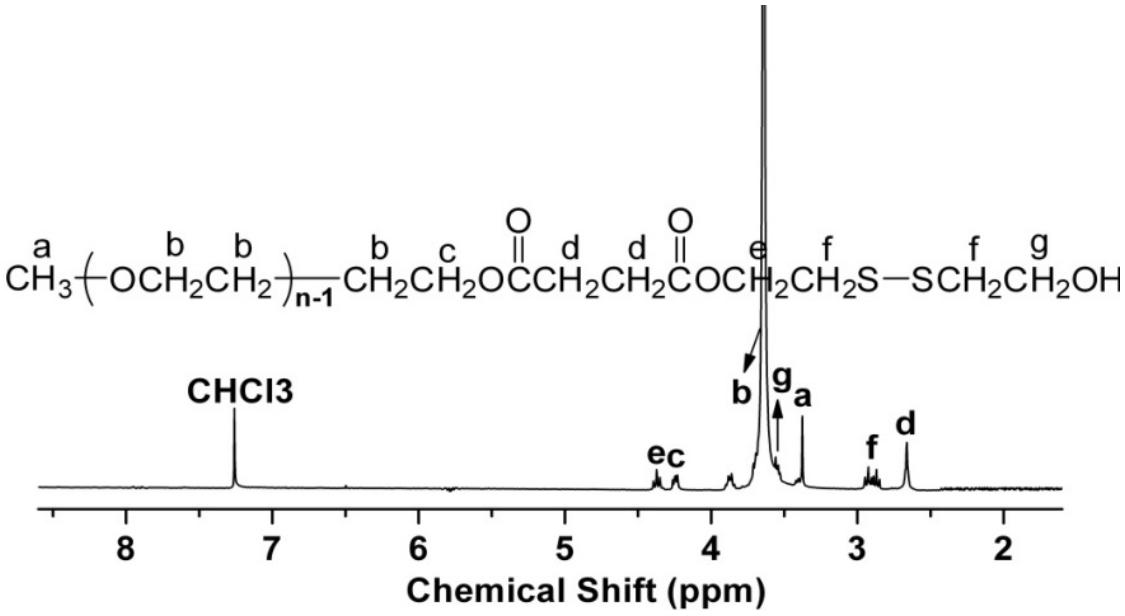

Figure 3-S2. ^{1}H NMR spectrum of MPEO-OC(=O)CH_2CH_2CC(=O)OCH_2CH_2S-SCH_2CH_2OH in $CDCl_3$ (***3*** in Scheme 3-1).

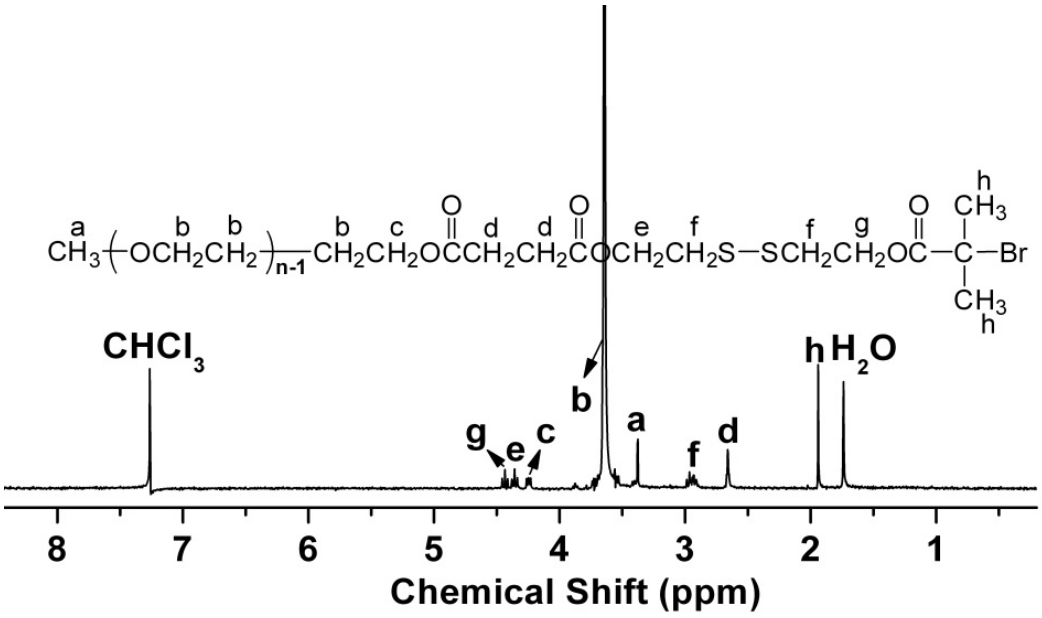

Figure 3-S3. ^{1}H NMR spectrum of the disulfide-containing PEO ATRP macroinitiator in $CDCl_3$ (*4* in Scheme 3-1).

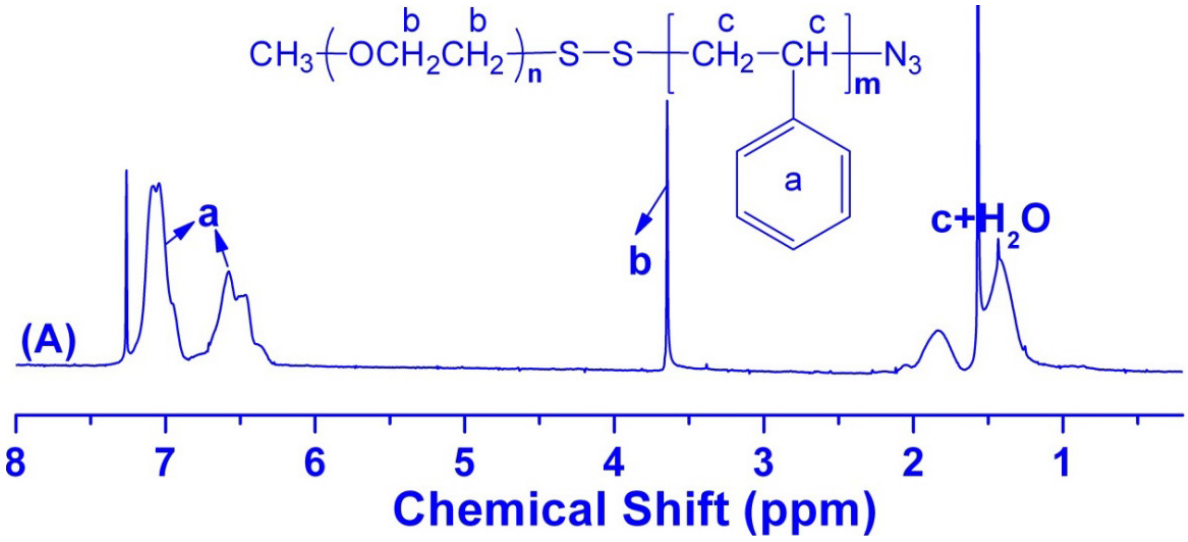

Figure 3-S4. ^{1}H NMR spectrum of the diblock copolymer PEO-*S*-*S*-PS-N_3 in $CDCl_3$.

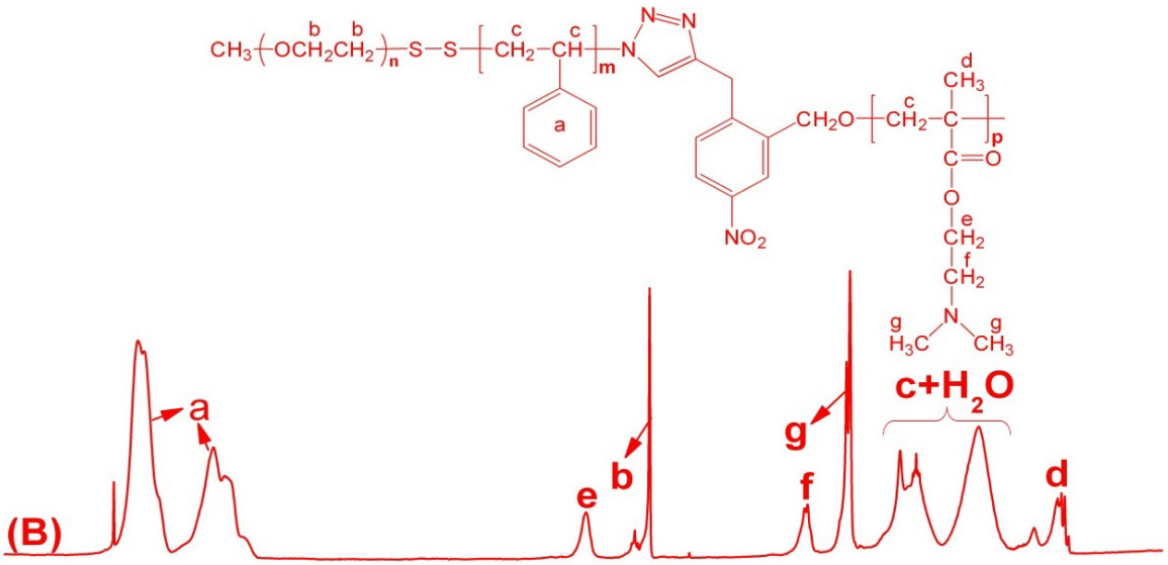

Figure 3-S5. ^{1}H NMR spectrum of the triblock copolymer PEO-*S*-*S*-PS-*ONB*-PDMAEMA in $CDCl_3$.

2. Critical Micelle Concentration

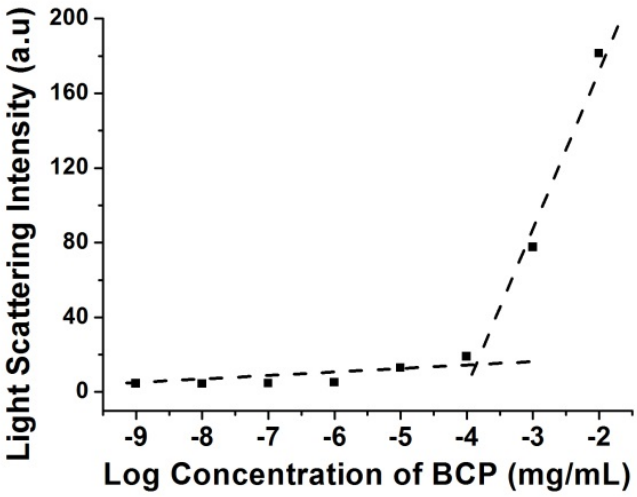

Figure 3-S6. Light scattering intensity (at 90^{o}) vs. logarithmic concentration of the triblock copolymer in aqueous solution. The critical micelle concentration, determined at the intersection of the two lines, is about 1.5x10^{-4} mg/mL.

The critical micelle concentration (CMC) of the used triblock copolymer sample was measured by using light scattering measurements (at 90^{o}). The result in Figure S6 shows a CMC of about $1.5x10^{-4}$ mg/mL. For this experiment, aqueous solution of the polymer at different dilute concentrations were prepared by adding a small volume of THF solution in a large volume of water, with THF removed by evaporation at room temperature (solution under rigorous stirring).

Acknowledgements

YZ acknowledges the financial support from the Natural Sciences and Engineering Research Council of Canada (NSERC) and le Fonds québécois de la recherche sur la nature et les technologies of Québec (FQRNT). JX thanks the support of China Scholarship Council (CSC). HX acknowledges the financial support of the major project of Ministry of Education of China (313036). YZ is a member of the FQRNT-funded Center for Self-Assembled Chemical Structures (CSACS) and the Centre québécois sur les matériaux fonctionnels (CQMF).

References

(1) Zhao, Y. Light-Responsive Block Copolymer Micelles. *Macromolecules* **2012**, *45*, 3647-3657.

(2) Yan, Q.; Yuan, J.; Cai, Z.; Xin, Y.; Kang, Y.; Yin, Y. Voltage-Responsive Vesicles Based on Orthogonal Assembly of Two Homopolymers. *J. Am. Chem. Soc.* **2010**, *132*, 9268-9270.

(3) Li, M.-H.; Keller, P. Stimuli-Responsive Polymer Vesicles. *Soft Matter* **2009**, *5*, 927-937.

(4) Thevenot, J.; Oliveira, H.; Sandre, O.; Lecommandoux, S. Magnetic Responsive Polymer Composite Materials. *Chem. Soc. Rev.* **2013**, *42*, 7047-7054.

(5) Gohy, J.-F.; Zhao, Y. Photo-Responsive Block Copolymer Micelles: Design and Behavior. *Chem. Soc. Rev.* **2013**, *42*, 7117-7129.

(6) Felber, A. E.; Dufresne, M.-H.; Leroux, J.-C. pH-Sensitive Vesicles, Polymeric Micelles, and Nanospheres Prepared with Polycarboxylates. *Adv. Drug Delivery Rev.* **2012**, *64*, 979-992.

(7) Hu, J.; Zhang, G.; Liu, S. Enzyme-Responsive Polymeric Assemblies, Nanoparticles and

Hydrogels. *Chem. Soc. Rev.* **2012**, *41*, 5933-5949.

(8) Pergushov, D. V.; Muller, A. H. E.; Schacher, F. H. Micellar Interpolyelectrolyte Complexes. *Chem. Soc. Rev.* **2012**, *41*, 6888-6901.

(9) Rapoport, N. Physical Stimuli-Responsive Polymeric Micelles for Anti-cancer Drug Delivery. *Prog. Polym. Sci.* **2007**, *32*, 962-990.

(10) Liu, Y.; Wang, Z.; Zhang, X. Characterization of Supramolecular Polymers. *Chem. Soc. Rev.* **2012**, *41*, 5922-5932.

(11) Liu, K.; Kang, Y.; Wang, Z.; Zhang, X. Reversible and Adaptive Functional Supramolecular Materials: "Noncovalent Interaction" Matters. *Adv. Mater.* **2013**, *25*, 5530-5548.

(12) Zhang, Q.; Re Ko, N.; Kwon Oh, J. Recent Advances in Stimuli-Responsive Degradable Block Copolymer Micelles: Synthesis and Controlled Drug Delivery Applications. *Chem. Commun.* **2012**, *48*, 7542-7552.

(13) Morachis, J. M.; Mahmoud, E. A.; Almutairi, A. Physical and Chemical Strategies for Therapeutic Delivery by Using Polymeric Nanoparticles. *Pharmacol. Rev.* **2012**, *64*, 505-519.

(14) Jochum, F. D.; Theato, P. Temperature- and Light- Responsive Smart Polymer Materials. *Chem. Soc. Rev.* **2013**, *42*, 7468-7483.

(15) Han, D.; Tong, X.; Zhao, Y. Block Copolymer Micelles with a Dual-Stimuli-Responsive Core for Fast or Slow Degradation. *Langmuir* **2012**, *28*, 2327-2331.

(16) Klaikherd, A.; Nagamani, C.; Thayumanavan, S. Multi-Stimuli Sensitive Amphiphilic Block Copolymer Assemblies. *J. Am. Chem. Soc.* **2009**, *131*, 4830-4838.

(17) Li, Y.; Tong, R.; Xia, H.; Zhang, H.; Xuan, J. High Intensity Focused Ultrasound and Redox Dual Responsive Polymer Micelles. *Chem. Commun.* **2010**, *46*, 7739-7741.

(18) Chan, N.; Khorsand, B.; Aleksanian, S.; Oh, J. K. A Dual Location Stimuli-Responsive Degradation Strategy of Block Copolymer Nanocarriers for Accelerated Release. *Chem. Commun.* **2013**, *49*, 7534-7536.

(19) Schattling, P.; Jochum, F. D.; Theato, P. Multi-Stimuli Responsive Polymers - the all-in-one Talents *Polym. Chem.* **2014**.

(20) Schilli, C. M.; Zhang, M.; Rizzardo, E.; Thang, S. H.; Chong, Y. K.; Edwards, K.; Karlsson, G.; Müller, A. H. E. A New Double-Responsive Block Copolymer Synthesized via RAFT Polymerization: Poly(N-isopropylacrylamide)-*block*-poly(acrylic acid). *Macromolecules* **2004**, *37*, 7861-7866.

(21) Schmidt, B. V. K. J.; Hetzer, M.; Ritter, H.; Barner-Kowollik, C. UV Light and Temperature Responsive Supramolecular ABA Triblock Copolymers via Reversible Cyclodextrin Complexation. *Macromolecules* **2013**, *46*, 1054-1065.

(22) Ma, N.; Li, Y.; Xu, H.; Wang, Z.; Zhang, X. Dual Redox Responsive Assemblies Formed from Diselenide Block Copolymers. *J. Am. Chem. Soc.* **2009**, *132*, 442-443.

(23) Chen, J.; Qiu, X.; Ouyang, J.; Kong, J.; Zhong, W.; Xing, M. M. Q. pH and Reduction Dual-Sensitive Copolymeric Micelles for Intracellular Doxorubicin Delivery. *Biomacromolecules* **2011**, *12*, 3601-3611.

(24) Dai, J.; Lin, S.; Cheng, D.; Zou, S.; Shuai, X. Interlayer-Crosslinked Micelle with Partially Hydrated Core Showing Reduction and pH Dual Sensitivity for Pinpointed Intracellular Drug Release. *Angew. Chem. Int. Ed.* **2011**, *50*, 9404-9408.

(25) Han, D.; Tong, X.; Zhao, Y. Fast Photodegradable Block Copolymer Micelles for Burst Release. *Macromolecules* **2011**, *44*, 437-439.

(26) Zhao, H.; Sterner, E. S.; Coughlin, E. B.; Theato, P. *o*-Nitrobenzyl Alcohol Derivatives: Opportunities in Polymer and Materials Science. *Macromolecules* **2012**, *45*, 1723-1736.

(27) Cabane, E.; Malinova, V.; Menon, S.; Palivan, C. G.; Meier, W. Photoresponsive Polymersomes as Smart, Triggerable Nanocarriers. *Soft Matter* **2011**, *7*, 9167-9176.

(28) Zhao, H.; Gu, W.; Sterner, E.; Russell, T. P.; Coughlin, E. B.; Theato, P. Highly Ordered Nanoporous Thin Films from Photocleavable Block Copolymers. *Macromolecules* **2011**, *44*, 6433-6440.

(29) Kang, M.; Moon, B. Synthesis of Photocleavable Poly(styrene-*block*-ethylene oxide) and Its Self-Assembly into Nanoporous Thin Films. *Macromolecules* **2008**, *42*, 455-458.

(30) Rabnawaz, M.; Liu, G. Preparation and Application of a Dual Light-Responsive Triblock Terpolymer. *Macromolecules* **2012**, *45*, 5586-5595.

(31) Schumers, J.-M.; Gohy, J.-F.; Fustin, C.-A. A Versatile Strategy for the Synthesis of Block Copolymers Bearing a Photocleavable Junction. *Polym. Chem.* **2010**, *1*, 161-163.

(32) Theato, P. One is Enough: Influencing Polymer Properties with a Single Chromophoric Unit. *Angew. Chem. Int. Ed.* **2011**, *50*, 5804-5806.

(33) Takae, S.; Miyata, K.; Oba, M.; Ishii, T.; Nishiyama, N.; Itaka, K.; Yamasaki, Y.; Koyama, H.; Kataoka, K. PEG-Detachable Polyplex Micelles Based on Disulfide-Linked Block Catiomers as Bioresponsive Nonviral Gene Vectors. *J. Am. Chem. Soc.* **2008**, *130*, 6001-6009.

(34) Li, C.; Madsen, J.; Armes, S. P.; Lewis, A. L. A New Class of Biochemically Degradable, Stimulus-Responsive Triblock Copolymer Gelators. *Angew. Chem. Int. Ed.* **2006**, *45*, 3510-3513.

(35) Nelson-Mendez, A.; Aleksanian, S.; Oh, M.; Lim, H.-S.; Oh, J. K. Reductively Degradable Polyester-Based Block Copolymers Prepared by Facile Polycondensation and ATRP: Synthesis, Degradation, and Aqueous Micellization. *Soft Matter* **2011**, *7*, 7441-7452.

(36) Klaikherd, A.; Ghosh, S.; Thayumanavan, S. A Facile Method for the Synthesis of Cleavable Block Copolymers from ATRP-Based Homopolymers. *Macromolecules* **2007**, *40*, 8518-8520.

(37) Cerritelli, S.; Velluto, D.; Hubbell, J. A. PEG-SS-PPS: Reduction-Sensitive Disulfide Block Copolymer Vesicles for Intracellular Drug Delivery. *Biomacromolecules* **2007**, *8*, 1966-1972.

(38) Ko, N. R.; Yao, K.; Tang, C.; Oh, J. K. Synthesis and Thiol-Responsive Degradation of Polylactide-Based Block Copolymers Having Disulfide Junctions Using ATRP and ROP. *J. Polym. Sci., Part A: Polym. Chem.* **2013**, *51*, 3071-3080.

(39) Lee, M.H.; Yang, Z.; Lim, C.W.; Lee, Y.H.; Sun, D.; Kang, C.; Kim, J.S. Disulfide-Cleavage-Triggered Chemosensors and Their Biological Applications. *Chem. Rev.* **2013**, *113*, 5071-5109.

(40) Goodwin, A. P.; Mynar, J. L.; Ma, Y.; Fleming, G. R.; Frechet, J. M. J. Synthetic Micelle Sensitive to IR Light via a Two-Photon Process. *J. Am. Chem. Soc.* **2005**, *127*, 9952-9953.

(41) Jiang, J.; Tong, X.; Morris, D.; Zhao, Y. Toward Photocontrolled Release Using Light-Dissociable Block Copolymer Micelles. *Macromolecules* **2006**, *39*, 4633-4640.

(42) Dong, J.; Wang, Y.; Zhang, J.; Zhan, X.; Zhu, S.; Yang, H.; Wang, G. Multiple Stimuli-Responsive Polymeric Micelles for Controlled Release. *Soft Matter* **2013**, *9*, 370-373.

3.3. Conclusion of the Project

As part of our effort for developing efficient dual-stimuli-responsive BCP micelles, in this project, we have designed and synthesized a new amphiphilic ABC-type triblock copolymer of PEO-*S*-*S*-PS-*ONB*-PDMAEMA. The particular feature of this BCP is simultaneous presence of a redox-cleavable disulfide and a photocleavable ONB group at the two junctions of the three blocks. We showed that this design is a useful strategy to allow BCP micelles to respond to both a reducing agent like DTT in solution and to exposure to UV light while having the minimum number of stimuli-reactive moieties in the polymer structure (two units per chain). The results revealed that the micelles of this triblock copolymer could be disrupted in different ways, by either of the stimuli or both of them. When only one stimulus is applied, the removal of one type of hydrophilic polymer chains from the micelle corona, either PEO chains by redox-cleavage or PDMAEMA by photocleavage, gives rise to a limited destabilization effect on the dispersion of the micelles. The agglomeration between a few micelles appears to occur but the whole dispersion remains essentially stable. By contrast, under combined use of DTT and UV light that cleaves both PEO and PDMAEMA, severe polymer aggregation occurs as a result of elimination of the BCP amphiphilicity. We also investigated the release behavior of loaded Nile Red dye under the various uses of the two stimuli. The main significance of this study is the generality of the demonstrated BCP design, which can easily be extended to other dual-stimuli-responsive BCP micelles with different stimuli combinations, such as pH-light, pH-redox, light-gas, ultrasound-light, etc.

CHAPTER 4. DISCUSSION AND PERSPECTIVES

The research work presented in this thesis aimed at developing new BCP micelles that can respond to two stimuli and investigating their potential applications as drug delivery systems. The thesis can be divided into two parts according to the stimuli methods. The first part was focused on the design of an ultrasound-responsive BCP structure using the thermosensitivity in order to amplify the effect of ultrasound. The second part concerned a BCP design that allows the micelles to react to both redox and light stimuli while bearing the minimum number of stimuli-reactive moieties in the polymer structure.

In the first part, two projects on ultrasound-responsive BCP micelles have been completed, leading to publication of the two papers presented in Chapters 1-2 of the thesis. In the first project, in order to find possible polymer structures that are susceptible to be affected by ultrasound, a comparative study on the disruption of the micelles formed by various BCPs and the concomitant release of an encapsulated hydrophobic dye (Nile Red) by HIFU was conducted. Combining the characterization results, we found that of the four BCPs investigated, the micelles of PEO-*b*-PIBMA and PEO-*b*-PTHPMA, especially the latter system, appeared to be more sensitive to ultrasound irradiation resulting in a more severe micellar disruption. IR spectra showed evidence of ultrasound-induced chemical reactions, most likely hydrolysis. This study provided us an interesting prospect of using ultrasound-responsive BCP micelles for controlled delivery applications.

In the second project, based on the finding of the previous study,, we proposed a way to couple the ultrasound sensitivity and thermosensitivity in BCPs., We investigated a new approach for amplifying the effect of HIFU in disassembling BCP micelles in aqueous solution, using a diblock copolymer comprised of a water-soluble PEO and a thermosensitive $PMEO_2MA$ block containing a small amount of HIFU-labile THPMA co-monomer units. Upon ultrasound exposure, the removal of THPMA groups results in an increase in polarity and, consequently, an increase in the LCST of the $PMEO_2MA$ to above the solution temperature; when this happens, micelle core forming block becomes soluble in water and the micelles are dissolved.

Always in the pursuit of unveiling BCP designs that could amplify the effects of stimuli or improve the sensitivity with which BCP micelles react to the stimuli, the second part of the research, presented in Chapter 3, had a specific objective. We studied the design of a new dual-stimuli-responsible ABC-type triblock copolymer whose micelles can be disrupted by either light or redox while having the minimum number of stimuli-reactive moieties in the polymer structure. The amphiphilic triblock copolymer of PEO-*S*-*S*-PS-*ONB*-PDMAEMA features a redox-cleavable disulfide linkage between the PEO and PS blocks as well as a photocleavable ONB group as the junction of the PS and PDMAEMA blocks. With this design, the triblock copolymer micelles could indeed respond to both a reducing agent like dithiothreitol (DTT) in solution and exposure to UV light while bearing only two stimuli-reactive moieties per chain.

4.1 General Discussion

4.1.1 Ultrasound-Responsive BCP Micelles

Amphiphilic BCPs can form micelles in aqueous solution. An effective way to disrupt the micelles by stimuli is to allow a BCP structural change to occur under the effect of the stimuli, which shifts the hydrophilic-hydrophobic balance toward the destabilization of the micelles. In our research, we investigated new approaches combining two stimuli that can make this situation happen. More specifically, we studied the use of HIFU as a novel stimulating method, considering the many advantages such as remote activation, deep penetration through tissues as well as enhanced spatial and temporal control over micelle disruption and thus drug release. Following previous reports from our groups[1] showing that HIFU irradiation can disrupt BCP micelles, in this thesis, we took a more rational approach. We started with a comparative investigation on a series of four amphiphilic BCPs composed of the same hydrophilic block of PEO and a hydrophobic block of polymethacrylate with, however, different ester groups. Under the same conditions (pH 7, same ultrasound power, micellar solution volume and irradiation time), combined characterization results of fluorescence, DLS, AFM, SEM and FTIR show that those micelles, differing in the chemical structure of the micelle-core-forming polymethacrylate, could be disrupted by HIFU to different extents. For PEO-*b*-PIBMA and PEO-*b*-PTHPMA, the polymethacrylates bear a labile acetal unit; their micelles appeare to be more sensitive to ultrasound irradiation resulting in a more

severe micellar disruption as compared to those with a more stable polymethacrylate micelle core, particularly, micelles of PEO-*b*-PMMA. Infrared spectra recorded after HIFU irradiation of the micellar solutions show evidence of ultrasound-induced chemical reactions, most likely hydrolysis. This first study allowed us to identify THPMA as the ester group most labile to HIFU irradiation, setting the basis for the following studies making use of combined ultrasound-sensitivity and thermosensitivity..

Using the results obtained in the first project (Chapter 1), we made a rational design of a diblock copolymer and investigated a new approach that allows for amplifying the effect of HIFU on disassembling BCP micelles in aqueous solution (Chapter 2). Our idea consists in introducing a small amount of ultrasound-labile co-monomer units into the hydrophobic micelle core-forming thermosensitive polymer. Upon HIFU exposure of the micelle solution, ultrasound-induced hydrolysis reaction of THPMA could increase the polarity of the thermosensitive polymer and, as a result, shifts its LCST above the solution temperature. When this condition is fulfilled, the hydrophobic block turns hydrophilic and BCP micelles will be disassembled in water without changing the solution temperature. This concept based on combining the ultrasound and thermosensitivity has been validated by our study. We chose $PMEO_2MA$ as a thermosensitive block, which is hydrophobic at T>LCST, and THPMA as the ultrasound-labile co-monomer due to its higher reactivity under HIFU than other methacrylate structures investigated in the Chapter 1. We synthesized a diblock copolymer of PEO-*b*-P(MEO_2MA-*co*-THPMA) and found that indeed the BCP micelles, formed at a solution temperature above the LCST, could be disrupted under HIFU. Characterization using various techniques, including ^{13}C NMR, confirmed the hydrolysis of THPMA groups converting the initial hydrophobic THPMA co-monomer units into hydrophilic methacrylic acid groups, which results in increase of the LCST above the solution temperature.

These studies have contributed to our understanding of how ultrasound-controllable BCP micelles can be designed with the requirement of incorporating a small amount of certain ultrasound-labile moieties. This approach of tuning the LCST by ultrasound can be applied for further exploring other ultrasound-labile moieties in the BCP design. This study thus demonstrated a new methodology to amplify the effect of HIFU on possible drug delivery systems.

4.1.2 Dual-Stimuli-Responsive Micelles Requiring Few Stimuli-Reactive Moieties

Although self-assembled BCP micelles have been extensively studied, raising the level and complexity of their control still has much interest, not only from fundamental research point of view, but also as a requirement for practical applications. Therefore, making BCP micelles undergo more efficient and more controllable disruption by stimuli remains a main challenge in this area. To this regard, new and innovative BCP design may hold the key to resolving many problems. In the third project, we tried to tackle one of the important issues. Generally, stimuli-responsive BCP micelles require a high concentration of stimuli-reactive groups to be sensitive to stimuli. This can be problematic. For instance, the presence of a high concentration of photochromic moieties in BCP micelles can cause cytotoxicity that prevents their use as safe drug carriers. We demonstrated a new approach to show how this problem can be overcome for dual-stimuli-responsive BCP micelles.

In our study presented in Chapter 3, we designed and synthesized a novel amphiphilic ABC-type triblock copolymer of PEO-*S*-*S*-PS-*ONB*-PDMAEMA, which contains a redox-cleavable disulfide linkage between the A and B blocks as well as a photocleavable ONB junction between the B and C blocks. With this design, we showed that the BCP micelles could be disrupted by both stimuli of UV light and reducing agents like DTT while having the minimum number of stimuli-reactive moieties (two per chain). Our investigation found that the micelles of this triblock copolymer could be disrupted in different ways. When one stimulus is applied, only a limited number of micelles destabilized, due to only one type of hydrophilic polymer chains removal from the micelle corona, either PEO chains by the redox-cleavage or PDMAEMA chains by the photocleavage. By contrast, by combining two stimuli to cleave both PEO and PDMAEMA chains, severe polymer aggregation occurs as a result of the removal of the micelle corona and elimination of the polymer amphiphilicity.

This work is important for its scientific significance. The method actually may be the most effective way using the minimum amount of stimuli-reactive groups to prepare BCP micelles that can be disrupted by two types of stimuli. Moreover, the method is obviously general and can be applied to many BCP systems with block junctions that can be cleaved by a variety of other

stimuli such as temperature change, pH change, gas and enzyme.

4.2 Possible Future Studies of Dual-Stimuli-Responsive Polymers

4.2.1. Crosslinked Block Copolymer Micelles

Owning to the continuously growing interest in drug delivery systems, stimuli-responsive BCP micelles will continue to represent an active research area for the next decade, exploring the feature that. The hydrophobic inner core can act as a depot for poorly water-soluble, drugs and the hydrophilic outer shell as a protective interface between the micelle core and the external aqueous milieu.[2,3] Some inherent properties of BCP micelles, including nano-scaled sizes, stability in plasma, prolonged time for circulation in the blood and preferential accumulation via the enhanced permeability and retention effect, make them possess distinct advantages for drug delivery. However, one practical challenge remaining in developing stimuli-responsive BCP micelles is their low stability in vivo, because of the large dilution volume once introduced into the body and/or the interactions with cells and biomolecules presented in the blood, which often lead to premature payload release, aggregation, and a diminished ability to release the payload on the target.[4] In order to overcome this obstacle, cross-linking of the polymer chains constituting the micelles has been proved to be an effective way to improve the BCP micellar stability by providing the structural integrity of the micelles, since the crosslinking prevents polymer chains from being dissociated. Generally, crosslinking only part of the micelles will be sufficient for the structural integrity such as cross-linking of the hydrophilic shell, within the hydrophobic core, or at the core-shell interface. However, it should be noted that although these crosslinking approaches can improve the stability of micelles, these overly stable nanoparticles are also far from optimal for drug delivery applications, because the chain crosslinking may slow down the rate or reduce the efficiency of drug release. Therefore, in order to minimize the conflicting effect, it is important to develop crosslinked BCP micelles that can be effectively disintegrated or “opened” upon exposure to stimuli after arrival on the target site. The approaches developed in this thesis about the use of two stimuli offer possible ways for making dual-stimuli-responsive crosslinked BCP micelles.

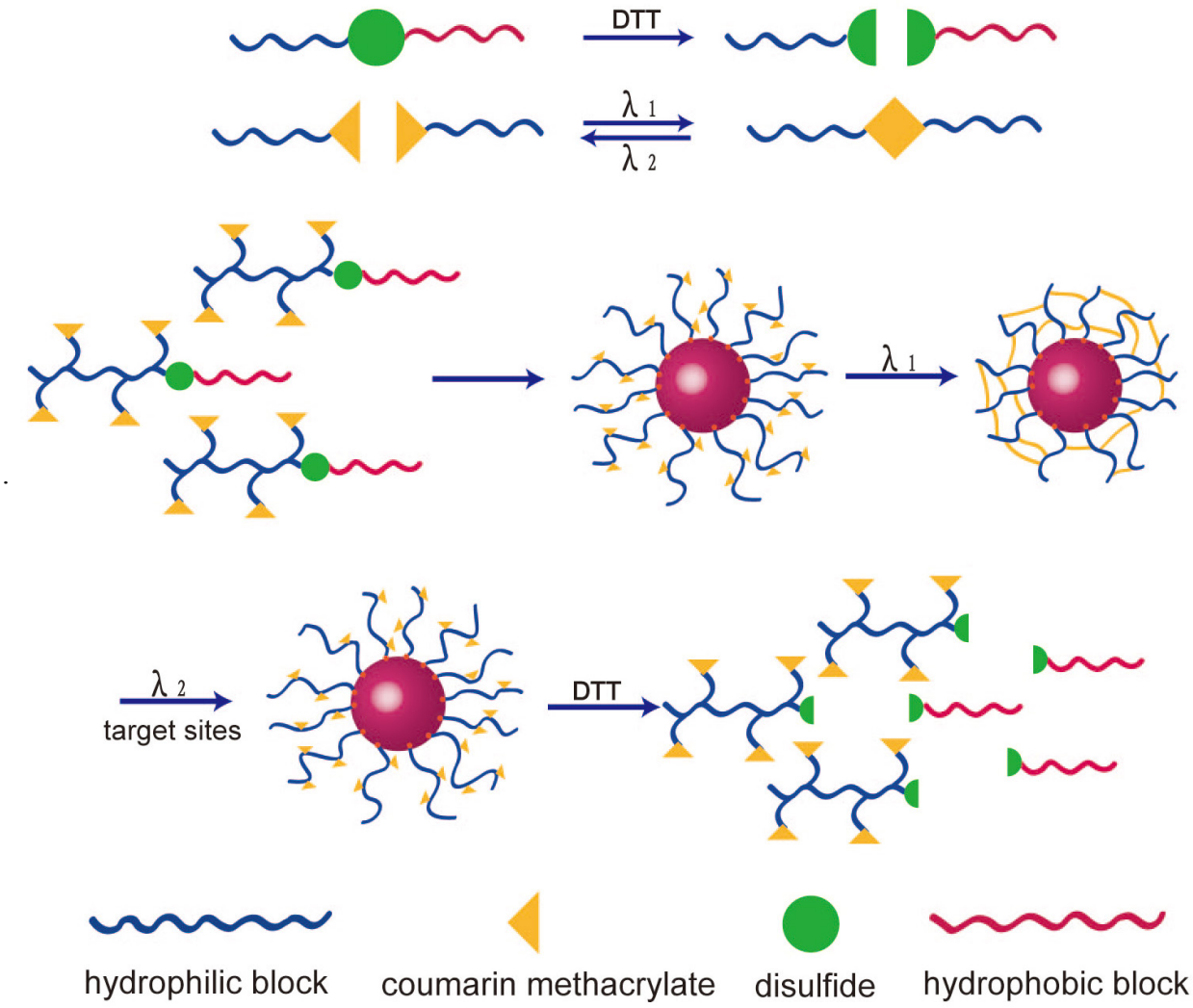

Figure 4-1. Schematic illustration of BCP micelles with photo-crosslinkable shell for stability and subsequent photo-de-crosslinkable and/or redox-removable shell for destability.

An example of BCP design to afford crosslinked dual-stimuli-responsive micelles is schematically illustrated in Figure 4-1. On the one hand, the hydrophilic block contains a number of photochromic co-monomer units that can undergo the reversible photodimerization and cleavage upon absorption of light at two different wavelengths (e.g. methacrylates bearing a coumarin ester group). On the other hand, a redox-cleavable linkage (e.g. disulfide) is positioned at the junction of the hydrophilic and hydrophobic blocks. Using this design, the BCP can self-assemble into micelles whose shell can be photo-crosslinked to ensure the micellar stability. Subsequently, the

disruption of the micelles can be achieved by either de-crosslinking the shell using light at a different wavelength or simply by removal of the shell through redox-induced cleavage of the block junction. It has been shown in the literature that there exists a large difference in the redox potential between the mildly oxidizing extracellular milieu and the reducing intracellular fluids, which renders reduction-sensitive polymers particularly appealing for biomedical applications.[5-8] This design of crosslinked BCP micelles responsive to redox and light is worth to be investigated in future studies.

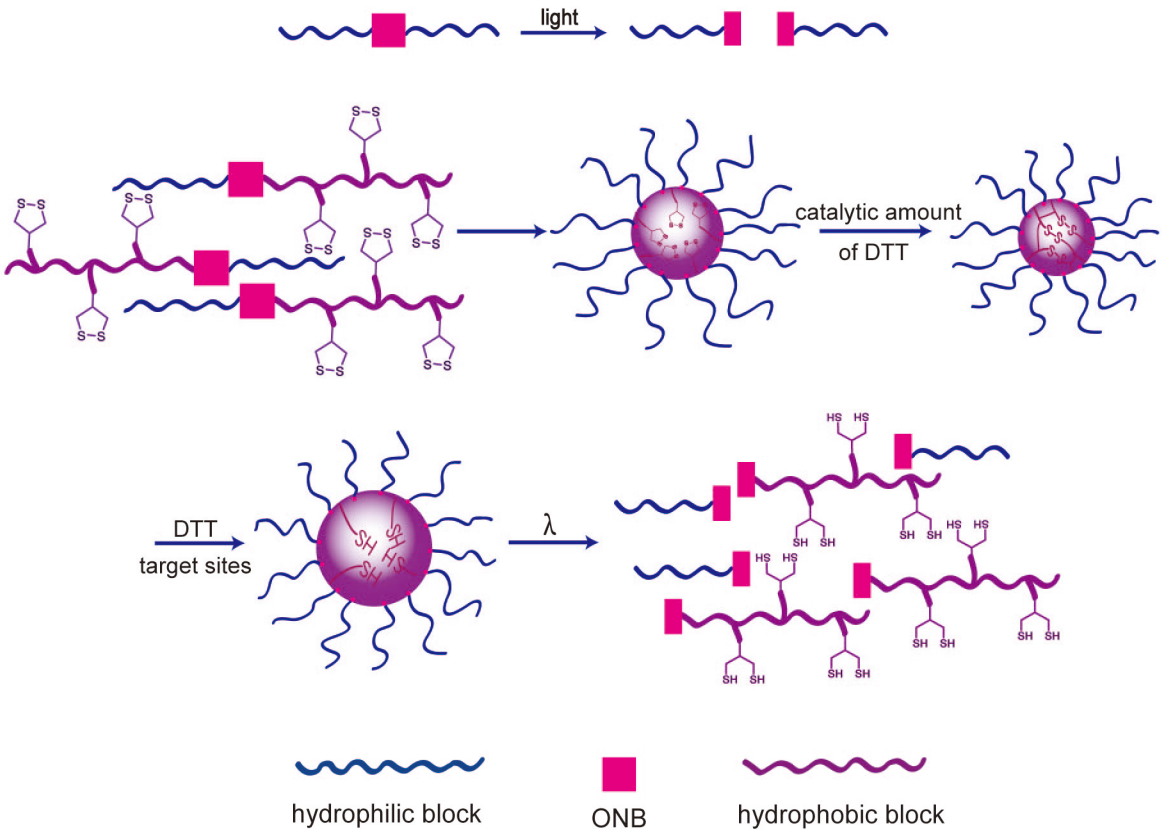

Figure 4-2. Schematic illustration of BCP micelles with crosslinkable core for stability and subsequent redox-de-crosslinkable core and photo-removable shell for destability.

To demonstrate the many possibilities, Figure 4-2 shows another BCP design for photo- and redox-responsive micelles. In this case, the micelle core can be crosslinked, while the junction of the two blocks is photocleavable. The design can easily be tested by synthesizing a diblock

copolymer of which the hydrophobic block contains a number of lipoyl units for crosslinking and the block junction is an ONB group. With this BCP design, after the micelles are formed, the micelle core can be crosslinked based on thiol-disulfide exchange under catalysis by DTT,[9,10] wherein lipoyl rings are opened to form preferentially linear disulfide bonds between different lipoyl units.[11]

When the micelles reach the target sites, such as cancer cells, the linear disulfide bonds will be cleaved, because the intracellular concentration of GSH, a thiol-containing tripeptide that cleaves disulfide bonds by a redox reaction, is substantially higher than the level in the extracellular environment. Taking advantage of this difference in the GSH concentration, the reversible disulfide crosslinked micelles in the design is interesting for targeting intracellular release of anticancer drugs. Furthermore, it is possible that the size of the crosslinked micelles could increase gradually in the presence of reductive GSH, due to the cleavage of the disulfide bond in the micellar core. Simultaneously, the decrease in the core crosslinking density caused by the cleavage of disulfide bonds will allow the drug release from the micelles to occur. Moreover, upon light exposure, due to the cleavage of photo-sensitive block junction, the amphiphilic diblock copolymer converts to hydrophilic or hydrophobic block inducing the disruption of micelle systems and could achieve drug burst release. Therefore, the micelles formed by this polymer possess a photo-sensitive block junction and a cross-linking hydrophobic core that can be disintegrated either rapidly via photocleavage of block junction or slowly through cleavage of disulfide groups by a reducing agent in the micellar solution. Thus, it could achieve fast drug release for some therapies, a slow and sustained release in other cases, or combined use of the two stimuli for more possibilities. This feature makes this photo and redox dual-stimuli micelle system attractive for potential drug delivery applications.

4.2.2. Hydrogels

The interest of the research works in this thesis is not limited to BCP micelles. What has been learned can also be applied to other BCP-based materials, such as hydrogels. Hydrogels are a class of soft three-dimensional polymer networks, and capable of absorbing large amounts of

water or biological fluids into their cross-linked architectures. Since they were introduced as possible biomaterials in the 1960s,[12] the research on hydrogels has become a fast-developing and exciting topic in chemistry. The softness and hydrophilicity feature makes the hydrogels particularly appealing for practical biomedical or pharmaceutical applications, such as the low molecular weight drug solubilization, controlled release, labile biomacromolecule delivery, cell immobilization, and tissue engineering.[13-16] To prepare hydrogels, it is necessary to have chemically or physically cross-linked junctions such as chemical bonds and chain entanglements, which allow them to swell in water instead of dissolution. Like BCP micelles, stimuli-responsive hydrogels have attracted much attention in rcent years. Thanks to our knowledge and understanding, dual-stimuli-responsive hydrogels can be developed from BCPs for future studies.

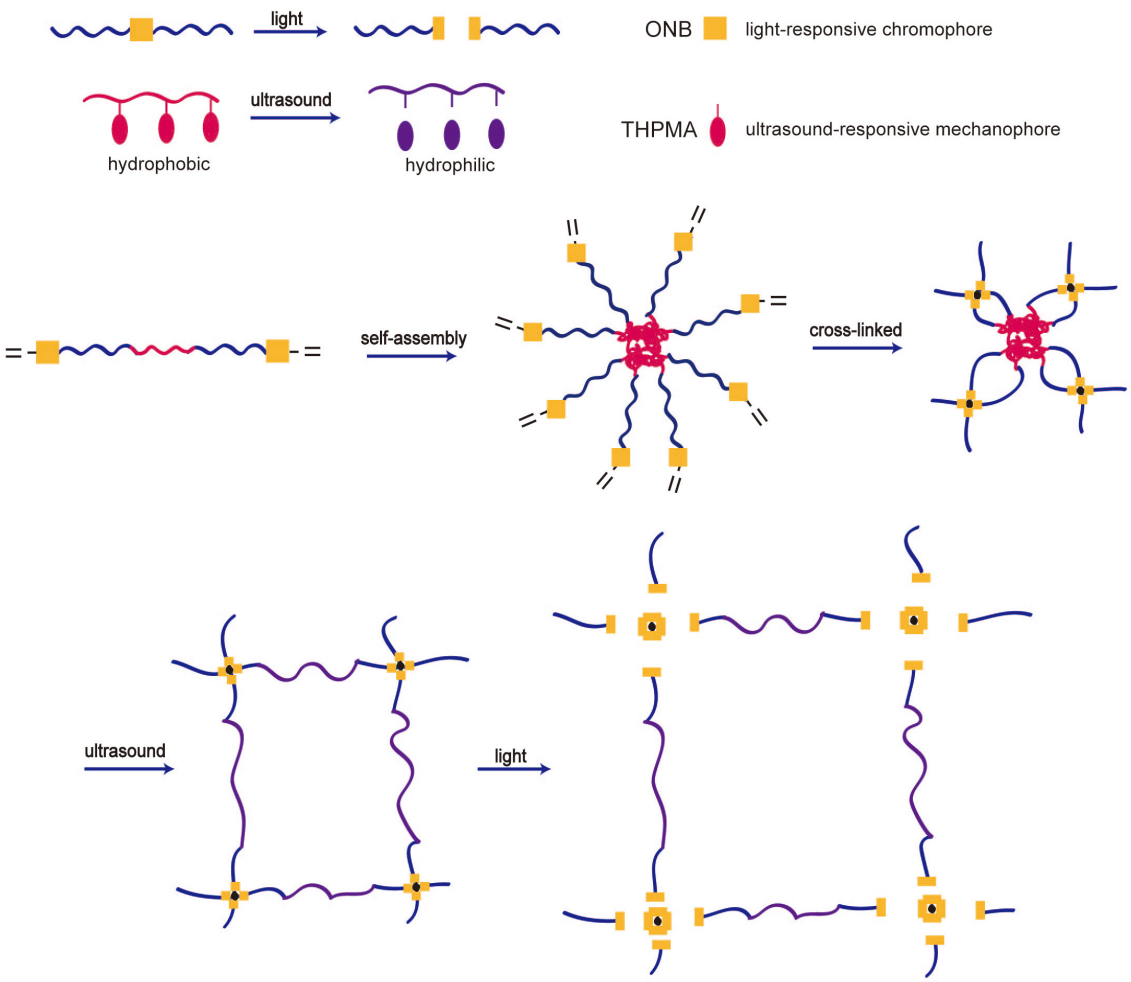

Figure 4-3. Schematic illustration of a triblock copolymer-based hydrogel responsive to ultrasound and light.

Figure 4-3 illustrates a physically and chemically cross-linked hydrogel that may respond to ultrasound and light. It is an ABA-type triblock copolymer of which the middle B block is hydrophobic and sensitive to HIFU (e.g., PTHPMA with labile side groups removable under ultrasound that turns the block to be hydrophilic), while the two A blocks are water-soluble and have a reactive (e.g., vinyl) chain end group functionalized a photocleavable ONB unit. With this BCP design, the triblock copolymer will self-assemble into core-shell micelles in aqueous solution, and a subsequent reaction will result in hydrogel with both physical and chemical crosslinks. As sketched, on the one hand, upon HIFU irradiation, the physical crosslinking (hydrophobic micelle core) could be dissolved inducing the crosslinking density. This ultrasound-induced change will increase the swelling degree of the hydrogel and allows payloads to be released slowly. On the other hand, since the chemical crosslinking is formed by photocleavable ONB, when the hydrogel is exposed to UV light, the gel-to-sol transition will take place as a result of disappearance of the network structure. In the latter case, the release of any payloads should be fast. Of course, the order in which the two stimuli are applied can be reversed to light first and ultrasound afterwards. This could result in different hydrogel structural evolution, leading to different release profiles.

This triblock copolymer design for dual-stimuli-responsive hydrogels is general, suggesting many possibilities. For instance, by replacing the ONB linkage with disulfide, the resulting hydrogel will be sensitive to ultrasound and redox. Using the disulfide linkage while replacing HIFU-removable THPMA by photocleavable ONB side groups, the hydrogel should respond to redox and light. Another interesting feature of this type of hydrogels is that both hydrophilic and hydrophobic drugs or bioagents can be loaded due to the presence of hydrophobic micelle cores in addition to the fluid aqueous medium.

Although hydrogels can be formed by covalent crosslinking of water-soluble polymers, the reaction used in the hydrogel preparation generally involves chemical reagents such as initiators, which is not desired for biomedical applications.[17-19] Therefore, hydrogels based on physical crosslinks are emerging as materials more suitable for biomedical applications. The aforementioned ABA-type triblock copolymer self-assembly is a convenient way to prepare

physically crosslinked hydrogels. As compared with the chemical crosslinks, the physical interactions, especially hydrophobic interactions, may also be more sensitive to specific physiological stimuli. Therefore, it is of interest to develop stimuli-responsive hydrogels that can be spontaneously formed in human body *in-situ* after injection of the polymer.

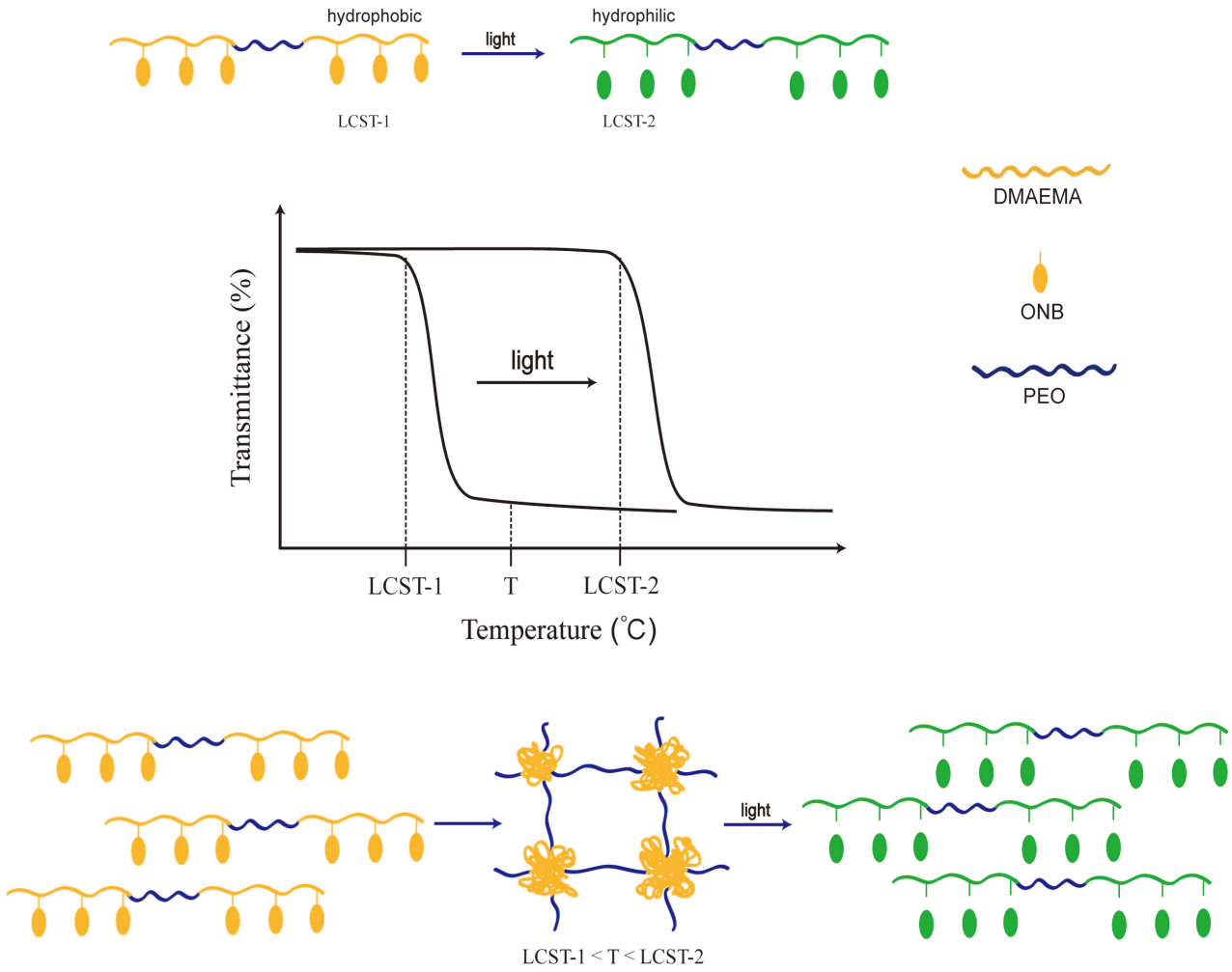

Figure 4-4. Schematic illustration of a photosensitive injectable hydrogel formation using ABA-type triblock copolymers.

Figure 4-4 illustrates the design of a physically crosslinked hydrogel formed by self-assembly of a thermo- and photosensitive ABA triblock copolymer. Similar to the BCP in Figure 4-3, the B

block is a “permanent” hydrophilic polymer (e.g. PEG) and the two flank blocks are a LCST polymer (e.g. PNIPAM or $PMEO_2MA$) containing a number of photo-sensitive co-monomer units whose cleavage upon light irradiation will shift the LCST to a higher temperature. The thermosensitive A blocks should be chosen to possess an initial LCST-1 between the room and body temperatures, i.e., soluble in aqueous solution at room temperature but insoluble at the body temperature. Under this condition, when the BCP solution is injected into the body, at appropriate concentrations, hydrogel can be formed upon dehydration of the B blocks. The temperature-dependent sol–gel transition of the hydrogel is reversible in water, which makes it more biocompatible for the human body and much easier to realize the control release. Moreover, the polymer sol-gel transition point can be readily dictated by the block copolymer composition, specifically by the ratio of hydrophilic and hydrophobic blocks. As a result, when guest molecules are encapsulated into such injectable hydrogels, cargo release can be adjusted by tuning these parameters. Moreover, with this BCP design, the gel-sol transition can also be achieved by light, since the photo-removal of the photochromic groups could increase the LCST of the B block to LCST-2 above the body temperature. In other words, the photoreaction makes the B block soluble in water at the body temperature and, consequently, the gel is dissolved.

Reference

(1) Wang, J.; Pelletier, M.; Zhang, H.; Xia, H.; Zhao, Y. *Langmuir* **2009**, *25*, 13201.

(2) Riess, G. *Prog. Polym. Sci.* **2003**, *28*, 1107.

(3) Min, K. H.; Lee, H. J.; Kim, K.; Kwon, I. C.; Jeong, S. Y.; Lee, S. C. *Biomaterials* **2012**, *33*, 5788.

(4) Bae, Y. H.; Yin, H. *J. Controlled Release.* **2008**, *131*, 2.

(5) Kim, T.-i.; Kim, S. W. *React. Funct. Polym.* **2011**, *71*, 344.

(6) Carelli, S.; Ceriotti, A.; Cabibbo, A.; Fassina, G.; Ruvo, M.; Sitia, R. *Science* **1997**, *277*, 1681.

(7) Jones, D. P.; Carlson, J. L.; Samiec, P. S.; Sternberg Jr, P.; Mody Jr, V. C.; Reed, R. L.;

Brown, L. A. S. *Clin. Chim. Acta.* **1998**, *275*, 175.

(8) Saeed, A. O.; Magnusson, J. P.; Moradi, E.; Soliman, M.; Wang, W.; Stolnik, S.; Thurecht, K. J.; Howdle, S. M.; Alexander, C. *Bioconjugate Chem.* **2011**, *22*, 156.

(9) Li, Y.-L.; Zhu, L.; Liu, Z.; Cheng, R.; Meng, F.; Cui, J.-H.; Ji, S.-J.; Zhong, Z. *Angew. Chem. Int. Ed.* **2009**, *48*, 9914.

(10) Zhang, A.; Zhang, Z.; Shi, F.; Ding, J.; Xiao, C.; Zhuang, X.; He, C.; Chen, L.; Chen, X. *Soft Matter* **2013**, *9*, 2224.

(11) Sadownik, A.; Stefely, J.; Regen, S. L. *J. Am. Chem. Soc.* **1986**, *108*, 7789.

(12) Wichterle, O.; Lim, D. *Nature* **1960**, *185*, 117.

(13) Lim, F.; Sun, A. *Science* **1980**, *210*, 908.

(14) Nguyen, K. T.; West, J. L. *Biomaterials* **2002**, *23*, 4307.

(15) Hoffman, A. S. *Adv Drug Deliv Rev.* **2012**, *64, Supplement*, 18.

(16) Seif-Naraghi, S. B.; Singelyn, J. M.; Salvatore, M. A.; Osborn, K. G.; Wang, J. J.; Sampat, U.; Kwan, O. L.; Strachan, G. M.; Wong, J.; Schup-Magoffin, P. J.; Braden, R. L.; Bartels, K.; DeQuach, J. A.; Preul, M.; Kinsey, A. M.; DeMaria, A. N.; Dib, N.; Christman, K. L. *Sci Transl Med.* **2013**, *5*, 173ra25.

(17) Qiu, B.; Stefanos, S.; Ma, J.; Lalloo, A.; Perry, B. A.; Leibowitz, M. J.; Sinko, P. J.; Stein, S. *Biomaterials* **2003**, *24*, 11.

(18) Jin, R.; Hiemstra, C.; Zhong, Z.; Feijen, J. *Biomaterials* **2007**, *28*, 2791.

(19) Tae, G.; Kim, Y.-J.; Choi, W.-I.; Kim, M.; Stayton, P. S.; Hoffman, A. S. *Biomacromolecules* **2007**, *8*, 1979.

CONCLUSIONS

The three completed projects presented in this thesis were focused on the design, synthesis and study of novel amphiphilic dual-stimuli-responsive block copolymers (BCPs) that can self-assemble into core-shell micelles in aqueous solution. The first two projects dealt with BCP micelles that can be disrupted by high-intensity focused ultrasound (HIFU). Our approach to improve the sensibility of the micelles to ultrasound beam is based on using LCST-exhibiting thermosensitive polymers for the micelle core-forming hydrophobic block, and relies on the idea that an ultrasound-induced reaction may shift the LCST above the solution temperature to result in dissolution of the micelles. To this end, we first investigated the effect of chemical structure of the hydrophobic block on the disruption of micelles and the concomitant release of encapsulated dye molecules under HIFU irradiation. This comparative study, described in Chapter 1, using four different BCPs allowed us to identify an ultrasound-labile methacrylate monomer structure, i.e., THPMA, that undergoes HIFU-induced hydrolysis reaction.

In the follow-up study, presented in Chapter 2, we were able to test the validity of a new approach designed to amplify the effect of HIFU on the disassembly of BCP micelles in aqueous solution. Using a diblock copolymer of PEO-*b*-P(MEO_2MA-*co*-THPMA), in which a small amount of ultrasound-labile THPMA co-monomer units are introduced into the micelle core-forming $PMEO_2MA$, we found that the ultrasound-induced reaction of THPMA could raise the LCST of the thermosensitive polymer above the solution temperature due to a polarity increase, resulting in the disassembly of BCP micelles without changing the solution temperature.

The second part of the thesis work is about a new BCP structural design for dual-stimuli-responsive micelles while having the minimum number of stimuli-reactive moieties in the polymer structure. In Chapter 3, we described the design and synthesis of an amphiphilic ABC-type triblock copolymer of PEO-*S*-*S*-PS-*ONB*-PDMAEMA, as well as the disruption of the micelles by either UV light or a reducing agent like DTT. The novelty about this BCP design is the simultaneous use of redox-cleavable disulfide functionality between the A and B blocks and a photocleavable ONB group at the B and C blocks. In contrast with having a large number of

stimuli-reactive moieties as side groups or in the main chain, placing just a few stimuli-cleavable groups at the block junctions, which probably are the most strategically important positions, may be sufficient for inducing a significant disrupting effect on the BCP micelles.

In conclusion, the research work described in this thesis made significant contributions to our fundamental knowledge and understanding on designing dual-stimuli-responsive BCP micelles. The two approaches, i.e., using a stimulus-induced reaction to change the thermal LCST phase transition and using two different stimuli-cleavable linkages at two block junctions, hold promise for developing effective stimuli-responsive BCP micelles. For the first approach, future studies need to discover stimuli-labile co-monomer units "ideal" for LCST increase. The key requirement is that the stimuli-induced reaction of only a few co-monomer units can induce a large increase in the polarity of the thermosensitive block and shift its LCST to higher temperatures. The basic idea demonstrated in the second approach has great potential to be extended to BCPs of various architectures using a variety of stimuli.

BIBLIOGRAPHY

1 Ganta, S.; Devalapally, H.; Shahiwala, A.; Amiji, M. *J. Controlled Release* **2008**, *126*, 187.

2 Roy, D.; Cambre, J. N.; Sumerlin, B. S. *Prog. Polym. Sci.* **2010**, *35*, 278.

3 Stuart, M. A. C.; Huck, W. T. S.; Genzer, J.; Muller, M.; Ober, C.; Stamm, M.; Sukhorukov, G. B.; Szleifer, I.; Tsukruk, V. V.; Urban, M.; Winnik, F.; Zauscher, S.; Luzinov, I.; Minko, S. *Nat Mater* **2010**, *9*, 101.

4 Lee, H.-i.; Pietrasik, J.; Sheiko, S. S.; Matyjaszewski, K. *Prog. Polym. Sci.* **2010**, *35*, 24.

5 Mendes, P. M. *Chem. Soc. Rev.* **2008**,*37*, 2512.

6 Motornov, M.; Roiter, Y.; Tokarev, I.; Minko, S. *Prog. Polym. Sci.* **2010**, *35*, 174 .

7 Jeong, B.; Gutowska, A. *Trends Biotechnol.* **2002**,*20*, 305.

8 Stayton, P. S.; Shimoboji, T.; Long, C.; Chilkoti, A.; Ghen, G.; Harris, J. M.; Hoffman, A. S. *Nature* **1995**, *378*, 472.

9 Liu, F.; Urban, M. W. *Prog. Polym. Sci.* **2010**, *35*, 3.

10 Mano, J. F. *Adv. Eng. Mater.* **2008**, *10*, 515.

11 Alarcon, C. d. l. H.; Pennadam, S.; Alexander, C. *Chem. Soc. Rev.* **2005**, *34*, 276.

12 Theato, P.; Sumerlin, B. S.; O'Reilly, R. K.; Epps, III. T. H. *Chem. Soc. Rev.* **2013**, *42*, 7055.

13 Hoffman, A. S. *Adv Drug Deliver Rev.* **2013**, *65*, 10.

14 Fleige, E.; Quadir, M. A.; Haag, R. *Adv Drug Deliver Rev.* **2012**,*64*, 866.

15 Qiu, Y.; Park, K. *Adv Drug Deliver Rev.* **2012**, *64*, 49.

16 Rodríguez-Hernández, J.; Lecommandoux, S. *J. Am. Chem. Soc.* **2005**, *127*, 2026.

17 Rijcken, C. J. F.; Soga, O.; Hennink, W. E.; Nostrum, C. F. v. *J. Controlled Release.* **2007**, *120*, 131.

18 Meng, F.; Zhong, Z.; Feijen, J. *Biomacromolecules* **2009**,*10*, 197.

19 Yin, Q.; Shen, J.; Zhang, Z.; Yu, H.; Li, Y. *Adv Drug Deliver Rev.* **2013**,*34*, 11.

20 Shim, M. S.; Kwon, Y. J. *Adv Drug Deliver Rev.* **2012**, *64*, 1046.

21 Langer, R. *Nature* **1998**,*392*, 5.

22 Mano, M. P. J. F. *Drug Delivery.* **2004**, *12*, 41.

23 Jeong, B.; Bae, Y. H.; Lee, D. S.; Kim, S. W. *Nature* **1997**, *388*, 860.

24 Allen, T. M.; Cullis, P. R. *Science* **2004**, *303*, 1818.

25 Kataoka, K.; Harada, A.; Nagasaki, Y. *Adv Drug Deliver Rev.* **2012**, *64*, 37.

26 Duncan, R. *Nat Rev Drug Discov.* **2003**, *2*, 347.

27 Prime, K. L.; Whitesides, G. M. *J. Am. Chem. Soc.* **1993**, *115*, 10714.

28 Stolnik, S.; Illum, L.; Davis, S. S. *Adv Drug Deliver Rev.* **1995**, *16*, 195.

29 Su, J.; Chen, F.; Cryns, V. L.; Messersmith, P. B. *J. Am. Chem. Soc.* **2011**, *133*, 11850.

30 Zhou, K.; Wang, Y.; Huang, X.; Luby-Phelps, K.; Sumer, B. D.; Gao, J. *Angew. Chem. Int. Ed.* **2011**, *50*, 6109.

31 Eissa, A. M.; Khosravi, E. *Eur. Polym. J.* **2011**, *47*, 61.

32 Liu, X.; Zhou, T.; Du, Z.; Wei, Z.; Zhang, J. *Soft Matter* **2011**, *7*, 1986.

33 Yan, B.; Boyer, J.-C.; Habault, D.; Branda, N. R.; Zhao, Y. *J. Am. Chem. Soc.* **2012**, *134*, 16558.

34 Yan, Q.; Han, D.; Zhao, Y. *Polym. Chem.* **2013**, *4*, 5026.

35 Coll, C.; Mondragón, L.; Martínez-Máñez, R.; Sancenón, F.; Marcos, M. D.; Soto, J.; Amorós, P.; Pérez-Payá, E. *Angew. Chem. Int. Ed.* **2011**, *50*, 2138.

36 Pritchard, E. M.; Valentin, T.; Boison, D.; Kaplan, D. L. *Biomaterials* **2011**, *32*, 909.

37 Marin, A.; Sun, H.; Husseini, G. A.; Pitt, W. G.; Christensen, D. A.; Rapoport, N. Y. *J. Controlled Release.* **2002**, *84*, 39.

38 Rapoport, N. *Int. J. Pharm.* **2004**, *277*, 155.

39 Rapoport, N.; Pitt, W. G.; Sun, H.; Nelson, J. L. *J. Controlled Release.* **2003**, *91*, 85.

40 Li, Y.; Tong, R.; Xia, H.; Zhang, H.; Xuan, J. *Chem. Commun.* **2010**, *46*, 7739.

41 Zhang, H.; Xia, H.; Wang, J.; Li, Y. *J. Controlled Release.* **2009**, ***139***, 31.

42 Rapoport, N. *Prog. Polym. Sci.* **2007**, *32*, 962.

43 Kheirolomoom, A.; Lai, C.-Y.; Tam, S. M.; Mahakian, L. M.; Ingham, E. S.; Watson, K. D.; Ferrara, K. W. *J. Controlled Release.* **2013**, *172*, 266.

44 Rapoport, N. Y.; Kennedy, A. M.; Shea, J. E.; Scaife, C. L.; Nam, K.-H. *J. Controlled Release.* **2009**, *138*, 268.

45 Chen, D.; Wu, J. *Ultrasonics* **2010**, *50*, 744.

46 Grüll, H.; Langereis, S. *J. Controlled Release.* **2012**, *161*, 317.

47 Mitragotri, S. *Nat Rev Drug Discov.* **2005**, *4*, 255.

48 Liu, Y.; Yang, H.; Sakanishi, A. *Biotechnol. Adv.* **2006**, *24*, 1.

49 Bommannan, D.; Menon, G.; Okuyama, H.; Elias, P.; Guy, R. *Pharm Res.* **1992**, *9*, 1043.

50 Riesz, P.; Kondo, T. *Free Radical Biol. Med.* **1992**, *13*, 247.

51 Wood, R. W.; Loomis, A. L. *Philos. Mag.Ser. 7.* **1927**, *4*, 417.

52 Fry, W. J.; Fry, F. J. *Medical Electronics, IRE Transactions on.* **1960**, *7*, 166.

53 Dogra, V. S.; Zhang, M.; Bhatt, S. *Ultrasound Clinics.* **2009**, *4*, 307.

54 Int. J. *Hyperthermia* **2007**, *23*, 89.

55 Lin, H.-Y.; Thomas, J. L. *Langmuir* **2003**, *19*, 1098.

56 Shchukin, D. G.; Gorin, D. A.; Möhwald, H. *Langmuir* **2006**, *22*, 7400.

57 Skirtach, A. G.; De Geest, B. G.; Mamedov, A.; Antipov, A. A.; Kotov, N. A.; Sukhorukov, G. B. *J. Mater. Chem.* **2007**, *17*, 1050.

58 Lee, M.-H.; Lin, H.-Y.; Chen, H.-C.; Thomas, J. L. *Langmuir* **2008**, *24*, 1707.

59 Husseini, G. A.; Myrup, G. D.; Pitt, W. G.; Christensen, D. A.; Rapoport, N. Y. *J. Controlled Release.* **2000**, *69*, 43.

60 Rapoport, N. *Colloids Surf., B: Biointerfaces* **1999**, *16*, 93.

61 Wang, J.; Pelletier, M.; Zhang, H.; Xia, H.; Zhao, Y. *Langmuir* **2009**, *25*, 13201.

62 Wei, H.; Cheng, S.-X.; Zhang, X.-Z.; Zhuo, R.-X. *Prog. Polym. Sci.* **2009**, *34*, 893.

63 Rejinold, N. S.; Chennazhi, K. P.; Nair, S. V.; Tamura, H.; Jayakumar, R. *Carbohydr. Polym.* **2011**, *83*, 776.

64 Pelton, R. *Adv. Colloid Interface Sci.* **2000**, *85*, 1.

65 Bittrich, E.; Burkert, S.; Müller, M.; Eichhorn, K.-J.; Stamm, M.; Uhlmann, P. *Langmuir* **2012**, *28*, 3439.

66 Jiang, L.; Zhou, Q.; Mu, K.; Xie, H.; Zhu, Y.; Zhu, W.; Zhao, Y.; Xu, H.; Yang, X. *Biomaterials* **2013**, *34*, 7418.

67 Dimitrov, I.; Trzebicka, B.; Müller, A. H. E.; Dworak, A.; Tsvetanov, C. B. *Prog. Polym. Sci.* **2007**, *32*, 1275 .

68 Schild, H. G. *Prog. Polym. Sci.* **1992**, *17*, 163.

69 Wang, X.; Qiu, X.; Wu, C. *Macromolecules* **1998**, *31*, 2972.

70 Lutz, J.-F.; Akdemir, Ö.; Hoth, A. *J. Am. Chem. Soc.* **2006**, *128*, 13046 .

71 Lutz, J.-F. J. *Polym. Sci., Part A: Polym. Chem.* **2008**, *46*, 3459.

72 Han, S.; Hagiwara, M.; Ishizone, T. *Macromolecules* **2003**, *36*, 8312.

73 Mertoglu, M.; Garnier, S.; Laschewsky, A.; Skrabania, K.; Storsberg, J. *Polymer*, **2005**, *46*, 7726.

74 Lutz, J.-F.; Hoth, A. *Macromolecules* **2005**, *39*, 893.

75 Tao, L.; Mantovani, G.; Lecolley, F.; Haddleton, D. M. *J. Am. Chem. Soc.* **2004**, *126*, 13220.

76 Popescu, D. C.; Lems, R.; Rossi, N. A. A.; Yeoh, C. T.; Loos, J.; Holder, S. J.; Bouten, C. V. C.; Sommerdijk, N. A. J. M. *Adv. Mater.* **2005**, *17*, 2324.

77 Oyane, A.; Ishizone, T.; Uchida, M.; Furukawa, K.; Ushida, T.; Yokoyama, H. *Adv. Mater.* **2005**, *17*, 2329.

78 Plamper, F. A.; Ruppel, M.; Schmalz, A.; Borisov, O.; Ballauff, M.; Müller, A. H. E. *Macromolecules* **2007**, *40*, 8361.

79 Bütün, V.; Armes, S. P.; Billingham, N. C. *Polymer* **2001**, *42*, 5993.

80 Liu, Q.; Yu, Z.; Ni, P. *Colloid Polym Sci.* **2004**, *282*, 387.

81 Lowe, A. B.; Billingham, N. C.; Armes, S. P. *Macromolecules* **1998**, *31*, 5991.

82 McCormick, C. L.; Blackmon, K. P.; Elliott, D. L. *Polymer* **1986**, *27*, 1976.

83 Lee, A. S.; Bütün, V.; Vamvakaki, M.; Armes, S. P.; Pople, J. A.; Gast, A. P. *Macromolecules* **2002**, *35*, 8540.

84 Yamamoto, S.-i.; Pietrasik, J.; Matyjaszewski, K. *Macromolecules* **2008**, *41*, 7013.

85 Fournier, D.; Hoogenboom, R.; Thijs, H. M. L.; Paulus, R. M.; Schubert, U. S. *Macromolecules* **2007**, *40*, 915.

86 Zhao, Y.; Tremblay, L.; Zhao, Y. *Macromolecules* **2011**, *44*, 4007.

87 Cho, S. H.; Jhon, M. S.; Yuk, S. H.; Lee, H. B. J. *Polym. Sci., Part B: Polym. Phys.* **1997**, *35*, 595.

88 Schmaljohann, D. *Adv Drug Deliver Rev.* **2006**, *58*, 1655.

89 Ruel-Gariépy, E.; Leroux, J.-C. *Eur. J. Pharm. Biopharm.* **2004**, *58*, 409.

90 Kono, K. *Adv Drug Deliver Rev.* **2001**, *53*, 307.

91 Chilkoti, A.; Dreher, M. R.; Meyer, D. E.; Raucher, D. *Adv Drug Deliver Rev.* **2002**, *54*, 613.

92 Roy, D.; Brooks, W. L. A.; Sumerlin, B. S. *Chem. Soc. Rev.* **2013**, *42*, 7214.

93 Boissiere, O.; Han, D.; Tremblay, L.; Zhao, Y. *Soft Matter* **2011**, *7*, 9410.

94 Jin, Q.; Liu, G.; Ji, J. *J. Polym. Sci., Part A: Polym. Chem.* **2010**, *48*, 2855.

95 Jin, Q.; Liu, X.; Liu, G.; Ji, J. *Polymer* **2010**, *51*, 1311.

96 Liu, Y.-J.; Pallier, A.; Sun, J.; Rudiuk, S.; Baigl, D.; Piel, M.; Marie, E.; Tribet, C. *Soft Matter* **2012**, *8*, 8446.

97 Feng, Z.; Lin, L.; Yan, Z.; Yu, Y. Macromol. Rapid Commun. , **2010**, 31, 640.

98 Diehl, C.; Schlaad, H. *Macromol Biosci.* **2009**, *9*, 157.

99 Ueki, T.; Yamaguchi, A.; Ito, N.; Kodama, K.; Sakamoto, J.; Ueno, K.; Kokubo, H.; Watanabe, M. *Langmuir* **2009**, *25*, 8845.

100 Gohy, J.-F.; Zhao, Y. *Chem. Soc. Rev.* **2013**, *42*, 7117.

101 Fomina, N.; McFearin, C. L.; Sermsakdi, M.; Morachis, J. M.; Almutairi, A. *Macromolecules* **2011**, *44*, 8590.

102 Yang, Y.; Yue, L.; Li, H.; Maher, E.; Li, Y.; Wang, Y.; Wu, L.; Yam, V. W.-W. *Small* **2012**, *8*, 3105.

103 Schumers, J.-M.; Fustin, C.-A.; Gohy, J.-F. Macromol. *Rapid Commun.* **2010**, *31*, 1588.

104 Wang, G.; Tong, X.; Zhao, Y. *Macromolecules* **2004**, *37*, 8911.

105 Patchornik, A.; Amit, B.; Woodward, R. B. *J. Am. Chem. Soc.* **1970**, *92*, 6333.

106 Zhao, Y.; Zheng, Q.; Dakin, K.; Xu, K.; Martinez, M. L.; Li, W.-H. *J. Am. Chem. Soc.* **2004**, *126*, 4653.

107 Il'ichev, Y. V.; Schwörer, M. A.; Wirz, J. *J. Am. Chem. Soc.* **2004**, *126*, 4581.

108 Zhao, H.; Sterner, E. S.; Coughlin, E. B.; Theato, P. *Macromolecules* **2012**, *45*, 1723.

109 Kloxin, A. M.; Kasko, A. M.; Salinas, C. N.; Anseth, K. S. *Science* **2009**, *324*, 59.

110 Holmes, C. P. *J. Org. Chem.* **1997**, *62*, 2370.

111 San Miguel, V. n.; Bochet, C. G.; del Campo, A. n. *J. Am. Chem. Soc.* **2011**, *133*, 5380.

112 Hagen, V.; Dekowski, B.; Nache, V.; Schmidt, R.; Geißler, D.; Lorenz, D.; Eichhorst, J.; Keller, S.; Kaneko, H.; Benndorf, K.; Wiesner, B. *Angew. Chem. Int. Ed.* **2005**, *44*, 7887.

113 Babin, J.; Pelletier, M.; Lepage, M.; Allard, J.-F.; Morris, D.; Zhao, Y. *Angew. Chem. Int. Ed.* **2009**, *48*, 3329.

114 Furuta, T.; Wang, S. S.-H.; Dantzker, J. L.; Dore, T. M.; Bybee, W. J.; Callaway, E. M.; Denk, W.; Tsien, R. Y. *Proc. Natl. Acad. Sci. USA.***1999**, *96*, 1193.

115 Dugave, C.; Demange, L. *Chem. Rev.* **2003**, *103*, 2475.

116 Natansohn, A.; Rochon, P. *Chem. Rev.* **2002**, *102*, 4139.

117 Ikeda, T.; Tsutsumi, O. *SCIENCE-NEW YORK THEN WASHINGTON* **1995**, 1873.

118 Berkovic, G.; Krongauz, V.; Weiss, V. *Chem. Rev.* **2000**, *100*, 1741.

119 Paramonov, S. V.; Lokshin, V.; Fedorova, O. A. *J. Photoch. Photobio. C.* **2011**, *12*, 209.

120 Irie, M. *Chem. Rev.* **2000**, *100*, 1685.

121 Chen, Y.; Jean, C.-S. *J. Appl. Polym. Sci.* **1997**, *64*, 1759.

122 Chen, Y.; Chou, C.-F. *J. Polym. Sci., Part A: Polym. Chem.* **1995**, *33*, 2705.

123 Guo, Z.; Jiao, T.; Liu, M. *Langmuir* **2007**, *23*, 1824.

124 Jiang, J.; Tong, X.; Zhao, Y. *J. Am. Chem. Soc.* **2005**, *127*, 8290.

125 Jiang, J.; Tong, X.; Morris, D.; Zhao, Y. *Macromolecules* **2006**, *39*, 4633.

126 Kumar, S.; Allard, J.-F.; Morris, D.; Dory, Y. L.; Lepage, M.; Zhao, Y. *J. Mater. Chem.* **2012**, *22*, 7252.

127 Discher, D. E.; Eisenberg, A. *Science* **2002**, *297*, 967.

128 Haag, R. *Angew. Chem. Int. Ed.* **2004**, *43*, 278.

129 Torchilin, V. P.; Trubetskoy, V. S. *Adv Drug Deliver Rev.* **1995**, *16*, 141.

130 Yan, B.; Boyer, J.-C.; Branda, N. R.; Zhao, Y. *J. Am. Chem. Soc.* **2011**, *133*, 19714.

131 Ma, N.; Li, Y.; Xu, H.; Wang, Z.; Zhang, X. *J. Am. Chem. Soc.* **2009**, *132*, 442.

132 Eloi, J.-C.; Rider, D. A.; Cambridge, G.; Whittell, G. R.; Winnik, M. A.; Manners, I. *J. Am. Chem. Soc.* **2011**, *133*, 8903.

133 Ryu, J.-H.; Jiwpanich, S.; Chacko, R.; Bickerton, S.; Thayumanavan, S. *J. Am. Chem. Soc.* **2010**, *132*, 8246.

134 Johnston, A. P. R.; Such, G. K.; Caruso, F. *Angew. Chem. Int. Ed.* **2010**, *49*, 2664.

135 Petros, R. A.; Ropp, P. A.; DeSimone, J. M. *J. Am. Chem. Soc.* **2008**, *130*, 5008.

136 Oh, J. K.; Tang, C.; Gao, H.; Tsarevsky, N. V.; Matyjaszewski, K. *J. Am. Chem. Soc.* **2006**, *128*, 5578.

137 Tsarevsky, N. V.; Matyjaszewski, K. *Macromolecules* **2005**, *38*, 3087.

138 Zhang, L.; Liu, W.; Lin, L.; Chen, D.; Stenzel, M. H. *Biomacromolecules* **2008**, *9*, 3321.

139 Tsarevsky, N. V.; Matyjaszewski, K. *Macromolecules* **2002**, *35*, 9009.

140 Takae, S.; Miyata, K.; Oba, M.; Ishii, T.; Nishiyama, N.; Itaka, K.; Yamasaki, Y.; Koyama, H.; Kataoka, K. *J. Am. Chem. Soc* **2008**, *130*, 6001.

141 Li, C.; Madsen, J.; Armes, S. P.; Lewis, A. L. *Angew. Chem. Int. Ed.* **2006**, *45*, 3510.

142 Hong, R.; Han, G.; Fernández, J. M.; Kim, B.-j.; Forbes, N. S.; Rotello, V. M. *J. Am. Chem. Soc.* **2006**, *128*, 1078.

143 Oh, J. K.; Siegwart, D. J.; Lee, H.-i.; Sherwood, G.; Peteanu, L.; Hollinger, J. O.; Kataoka, K.; Matyjaszewski, K. *J. Am. Chem. Soc.* **2007**, *129*, 5939.

144 Bulmus, V.; Woodward, M.; Lin, L.; Murthy, N.; Stayton, P.; Hoffman, A. *J. Controlled Release.* **2003**, *93*, 105.

145 Kim, T.-i.; Kim, S. W. *React. Funct. Polym.* **2011**, *71*, 344.

146 Carelli, S.; Ceriotti, A.; Cabibbo, A.; Fassina, G.; Ruvo, M.; Sitia, R. *Science* **1997**, *277*, 1681.

147 Jones, D. P.; Carlson, J. L.; Samiec, P. S.; Sternberg Jr, P.; Mody Jr, V. C.; Reed, R. L.; Brown, L. A. S. *Clin. Chim. Acta.* **1998**, *275*, 175.

148 Saeed, A. O.; Magnusson, J. P.; Moradi, E.; Soliman, M.; Wang, W.; Stolnik, S.; Thurecht, K. J.; Howdle, S. M.; Alexander, C. *Bioconjugate Chem.* **2011**, *22*, 156.

149 Wong, L.; Boyer, C.; Jia, Z.; Zareie, H. M.; Davis, T. P.; Bulmus, V. *Biomacromolecules* **2008**, *9*, 1934.

150 Liu, J.; Bulmus, V.; Barner-Kowollik, C.; Stenzel, M. H.; Davis, T. P. *Macromol. Rapid Commun.* **2007**, *28*, 305.

151 Klaikherd, A.; Ghosh, S.; Thayumanavan, S. *Macromolecules* **2007**, *40*, 8518.

152 Khorsand, B.; Lapointe, G.; Brett, C.; Oh, J. K. *Biomacromolecules* **2013**, *14*, 2103.

153 Chen, W.; Shi, Y.; Feng, H.; Du, M.; Zhang, J. Z.; Hu, J.; Yang, D. *J. Phys. Chem. B.* **2012**, *116*, 9231.

154 Dong, W.-F.; Kishimura, A.; Anraku, Y.; Chuanoi, S.; Kataoka, K. *J. Am. Chem. Soc.* **2009**, *131*, 3804.

155 Ghosh, S.; Yesilyurt, V.; Savariar, E. N.; Irvin, K.; Thayumanavan, S. *J. Polym. Sci., Part A: Polym. Chem.* **2009**, *47*, 1052.

156 Liu, J.; Liu, H.; Jia, Z.; Bulmus, V.; Davis, T. P. *Chem. Commun.* **2008**, 6582.

157 Sun, H.; Guo, B.; Cheng, R.; Meng, F.; Liu, H.; Zhong, Z. *Biomaterials* **2009**, *30*, 6358.

158 Cerritelli, S.; Velluto, D.; Hubbell, J. A. *Biomacromolecules* **2007**, *8*, 1966.

159 Sun, K. H.; Sohn, Y. S.; Jeong, B. *Biomacromolecules* **2006**, *7*, 2871.

160 Read, E. S.; Armes, S. P. *Chem. Commun.* **2007**, 3021.

161 O'Reilly, R. K.; Hawker, C. J.; Wooley, K. L. *Chem. Soc. Rev.* **2006**, *35*, 1068.

162 Koo, A. N.; Lee, H. J.; Kim, S. E.; Chang, J. H.; Park, C.; Kim, C.; Park, J. H.; Lee, S. C. *Chem. Commun.* **2008**, 6570.

163 Zhang, A.; Zhang, Z.; Shi, F.; Ding, J.; Xiao, C.; Zhuang, X.; He, C.; Chen, L.; Chen, X. *Soft Matter* **2013**, *9*, 2224.

164 Schattling, P.; Jochum, F. D.; Theato, P. *Polym. Chem.* **2014**, *5*, 25.

165 Li, W.; Cai, X.; Kim, C.; Sun, G.; Zhang, Y.; Deng, R.; Yang, M.; Chen, J.; Achilefu, S.; Wang, L. V.; Xia, Y. *Nanoscale* **2011**, *3*, 1724.

166 Moon, G. D.; Choi, S.-W.; Cai, X.; Li, W.; Cho, E. C.; Jeong, U.; Wang, L. V.; Xia, Y. *J. Am. Chem. Soc.* **2011**, *133*, 4762.

167 Mondal, S. *Appl. Therm. Eng.* **2008**, *28*, 1536.

168 Choi, S.-W.; Zhang, Y.; Xia, Y. *Angew. Chem. Int. Ed.* **2010**, *49*, 7904.

169 Kungwatchakun, D.; Irie, M. Makromo. *Chem. Rapid Commun.* **1988**, *9*, 243.

170 Jochum, F. D.; zur Borg, L.; Roth, P. J.; Theato, P. *Macromolecules* **2009**, *42*, 7854.

171 Kröger, R.; Menzel, H.; Hallensleben, M. L. *Macromol. Chem. Phys.* **1994**, *195*, 2291.

172 Tao, X.; Gao, Z.; Satoh, T.; Cui, Y.; Kakuchi, T.; Duan, Q. *Polym. Chem.* **2011**, *2*, 2068.

173 Ishii, N.; Mamiya, J.-i.; Ikeda, T.; Winnik, F. M. *Chem. Commun.* **2011**, *47*, 1267.

174 Jochum, F. D.; Theato, P. *Chem. Soc. Rev.* **2013**, *42*, 7468.

175 Dirani, A.; Laloyaux, X.; Fernandes, A. E.; Mathy, B.; Schicke, O.; Riant, O.; Nysten, B.; Jonas, A. M. *Macromolecules* **2012**, *45*, 9400.

176 He, J.; Tong, X.; Zhao, Y. *Macromolecules* **2009**, *42*, 4845.

177 He, J.; Tong, X.; Tremblay, L.; Zhao, Y. *Macromolecules* **2009**, *42*, 7267.

178 Phillips, D. J.; Gibson, M. I. *Chem. Commun.* **2012**, *48*, 1054.

179 Phillips, D. J.; Gibson, M. I. *Biomacromolecules* **2012**, *13*, 3200.

180 You, Y.-Z.; Zhou, Q.-H.; Manickam, D. S.; Wan, L.; Mao, G.-Z.; Oupický, D. *Macromolecules* **2007**, *40*, 8617.

181 Morimoto, N.; Qiu, X.-P.; Winnik, F. o. M.; Akiyoshi, K. *Macromolecules* **2008**, *41*, 5985.

182 Lv, W.; Liu, S.; Feng, W.; Qi, J.; Zhang, G.; Zhang, F.; Fan, X. *Macromol. Rapid Commun.* **2011**, *32*, 1101.

183 Tan, J.; Kang, H.; Liu, R.; Wang, D.; Jin, X.; Li, Q.; Huang, Y. *Polym. Chem.* **2011**, *2*, 672.

184 You, Y.-Z.; Hong, C.-Y.; Pan, C.-Y. *Macromolecules* **2009**, *42*, 573.

185 Xu, H.; Meng, F.; Zhong, Z. *J. Mater. Chem.* **2009**, *19*, 4183.

186 Cheng, R.; Meng, F.; Ma, S.; Xu, H.; Liu, H.; Jing, X.; Zhong, Z. *J. Mater. Chem.* **2011**, *21*, 19013.

187 Kuramoto, N.; Shishido, Y.; Nagai, K. *J. Polym. Sci., Part A: Polym. Chem.* **1997**, *35*, 1967.